Laser-based Packaging of Micro-devices

Norbert Lorenz

A dissertation submitted for the degree of Doctor of Philosophy

Heriot-Watt University

School of Engineering and Physical Sciences

October 2011

Abstract

In this PhD thesis the development of laser-based processes for packaging applications in microsystems technologies is investigated. Packaging is one of the major challenges in the fabrication of micro-electro-mechanical systems (MEMS) and other micro-devices. A range of bonding processes have become established in industry, however, in many or even most cases heating of the entire package to the bonding temperature is required to effect efficient and reliable bonding. The high process temperatures of up to 1100°C involved severely limit the application areas of these techniques for packaging of temperature sensitive materials. As an alternative production method, two localised heating processes using a laser were developed where also the heat is restricted to the joining area only by active cooling.

Silicon to glass joining with a Benzocyclobutene adhesive layer was demonstrated which is a typical MEMS application. In this laser-based process the temperature in the centre of the device was kept at least 120°C lower than in the bonding area. For chip-level packaging shear forces as high as 290 N were achieved which is comparable and some cases even higher than results obtained using conventional bonding techniques. Furthermore, a considerable reduction of the bonding time from typically 20 minutes down to 8 s was achieved. A further development of this process to wafer-level packaging was demonstrated. For a simplified pattern of 5 samples the same quality of the seal could be achieved as for chip-level packaging. Packaging of a more densely packed pattern of 9 was also investigated. Successful sealing of all nine samples on the same wafer was demonstrated proving the feasibility of wafer-level packaging using this localised heating bonding process.

The development of full hermetic glass frit packaging processes of Leadless Chip Carrier (LCC) devices in both air and vacuum is presented. In these laser-based processes the temperature in the centre of the device was kept at least 230°C below the temperature in the joining region (375°C to 440°C). Testing according to MIL-STD-883G showed that hermetic seals were achieved in high yield processes (>90%) and the packages did withstand shear forces in excess of 1 kN. Residual gas analysis has shown that a moderate vacuum of around 5 mbar was achieved inside the vacuum packaged LCC devices. A localised heating glass frit packaging process was developed without any negative effect of the thermal management on the quality of the seal.

Dedication

This thesis is dedicated to

Matthias Baunack

(1953 – 2006)

Acknowledgements

Firstly, I would like to express my gratitude to Professor Duncan Hand for giving me the opportunity to work within the Applied Optics and Photonics Group and for guiding and supervising me throughout the last 3½ years; without him this work would not have been possible.

I would like to thank my colleagues of the AOP group for their support during my PhD; and Robert for proofreading the thesis. Special thanks must go to Suzanne Millar for the good collaboration and the leak testing of the packaged devices. Furthermore, I would like to thank the technical staff at Heriot-Watt University for their support; in particular Mark Stewart for engineering my bonding setup and Neil Ross for dicing sheer endless amounts of wafers.

I feel honoured that my research was so highly recognised by the Association of Laser Users (AILU). I would like to express my sincerest thanks to the committee of AILU for awarding me the AILU's Young UK Laser Engineer's Prize 2011.

I am glad that during my time at Heriot-Watt University I made such great friends with so many people, especially Brian, Dave, Jack, Jens, Stefan and Yves – I will miss you all! Finally, I must thank my family and Teresa for their continuous moral support and their endless belief in me. I couldn't have done it without you and I could always rely on you!

ACADEMIC REGISTRY
Research Thesis Submission

Name*:*	NORBERT LORENZ		
School/PGI:	School of Engineering and Physical Sciences		
Version: *(i.e. First, Resubmission, Final)*	Final	Degree Sought (Award **and** Subject area)	Doctor of Philosophy in Physics

Declaration

In accordance with the appropriate regulations I hereby submit my thesis and I declare that:

1) the thesis embodies the results of my own work and has been composed by myself
2) where appropriate, I have made acknowledgement of the work of others and have made reference to work carried out in collaboration with other persons
3) the thesis is the correct version of the thesis for submission and is the same version as any electronic versions submitted*.
4) my thesis for the award referred to, deposited in the Heriot-Watt University Library, should be made available for loan or photocopying and be available via the Institutional Repository, subject to such conditions as the Librarian may require
5) I understand that as a student of the University I am required to abide by the Regulations of the University and to conform to its discipline.

* *Please note that it is the responsibility of the candidate to ensure that the correct version of the thesis is submitted.*

Signature of Candidate*:*		Date:	

Submission

Submitted By *(name in capitals):*	
Signature of Individual Submitting:	
Date Submitted:	

For Completion in the Student Service Centre (SSC)

Received in the SSC by *(name in capitals):*			
Method of Submission *(Handed in to SSC; posted through internal/external mail):*			
*E-thesis Submitted (**mandatory for final theses)***			
Signature:		Date:	

Table of Contents

List of Tables

List of Figures

List of Symbols and Abbreviations

AGC	– Asahi Glass Company
BCB	– Benzocyclobutene
CAD	– Computer aided design
CCD	– Charge-coupled device
CMOS	– Complementary metal-oxide-semiconductor
CQFP	– Ceramic quadflatpack
CTE	– Coefficient of thermal expansion
CVD	– Chemical vapour deposition
cw	– Continuous wave
DRIE	– Deep reactive ion etching
FTIR	– Fourier transform infrared spectroscopy
IC	– Integrated circuit
IR	– Infrared
LCC	– Leadless Chip Carrier
MEMS	– Micro-electro-mechanical systems
ND	– Neutral density
OLED	– Organic light emitting diode
PMMA	– Polymethylmethacrylate
PTFE	– Polytetrafluoroethylene
RF-MEMS	– Radiofrequency MEMS
RGA	– Residual gas analysis
RoHS	– Restriction of Hazardous Substances
RTC	– Rapid thermal curing
SCAPS	– Scanner application software
UKAS	– The United Kingdom Accreditation Service
UV	– Ultraviolet
a	– Radius of a glass plate
E	– Young’s modulus
k	– Thermal conductivity
Q	– Heat flow
t	– Thickness of a glass plate
T	– Temperature
w	– Evenly distributed load

x – Thickness of a layer

δ – Maximum deflection of a glass plate

ε'' – Imaginary dielectric constant

ε_r – Relative permittivity of a material

σ – Maximum bending stress of a glass plate

λ – Wavelength

List of Publications and Awards

Journal Publications:

Wu, Q., N. Lorenz, and D.P. Hand, *Localised laser joining of glass to silicon with BCB intermediate layer*. Microsystem Technologies, 2009. **15**(7): p. 1051-1057.

Wu, Q., N. Lorenz, K.M. Cannon, and D.P. Hand, *Glass frit as a hermetic joining layer in laser based joining of miniature devices.* IEEE Transactions on Components and Packaging Technologies, 2010. **33**(2): p. 470-477.

Lorenz, N., S. Millar, M. Desmulliez, and D.P. Hand, *Hermetic glass frit packaging in air and vacuum with localized laser joining.* Journal of Micromechanics and Microengineering, 2011. **21**(4): p. 045039.

Lorenz, N., M.D. Smith, and D.P. Hand, *Wafer-level packaging of silicon to glass with a BCB intermediate layer using localised laser heating.* Microelectronics Reliability, 2011. **In Press, Corrected Proof**.

Conference Papers:

Wu, Q., S. Kloss, N. Lorenz, C.H. Wang, A.J. Moore, and D.P. Hand. *Localised laser joining of glass to silicon with nanoparticle doped BCB*. in *Proceedings of the fourth International WLT-Conference on Lasers in Manufacturing (LIM 2007)*. 2007. Munich, Germany.

Wu, Q., S. Kloss, N. Lorenz, C.H. Wang, A.J. Moore, and D.P. Hand. *Localised laser joining of glass to silicon with BCB intermediate layer*. in *3rd Pacific International Conference on Application of Lasers and Optics (PICALEO 2008)*. 2008. Beijing, China.

Wu, Q., N. Lorenz, K. Cannon, W. Changhai, A.J. Moore, and D.P. Hand. *Hermetic joining of micro-devices using a glass frit intermediate layer and a scanning laser beam*. in *2nd Electronics Systemintegration Technology Conference (ESTC 2008)*. 2008. Greenwich, UK.

Wu, Q., N. Lorenz, K. Cannon, C. Wang, A.J. Moore, and D.P. Hand. *Hermetic joining of micro-devices using a glass frit intermediate layer and a scanning laser beam*. in *27th International Congress on Applications of Lasers & Electro-Optics (ICALEO 2008)*. 2008. Temecula, CA, US.

Lorenz, N., S. Millar, and D.P. Hand. *Localised laser joining of micro-devices for hermetic packaging using a glass frit intermediate layer*. in *Proceedings of the Fifth International WLT-Conference on Lasers in Manufacturing (LIM 2009)*. 2009. Messe Munich, Germany.

Lorenz, N., M.D. Smith, S. Millar, M. Desmulliez, and D.P. Hand. *Advances in laser based joining processes of micro-devices using localised heating*. in *28th International Congress on Applications of Lasers & Electro-Optics (ICALEO 2009)*. 2009. Orlando, FL, US.

Hand, D.P., N. Lorenz, M.D. Smith, S. Millar, and M. Desmulliez. *Laser-based joining for the packaging of miniature optoelectronic devices* (invited paper). in *Laser-based Micro- and Nanopackaging and Assembly IV*. 2010. San Francisco, California, USA: SPIE.

Lorenz, N., S. Millar, M. Desmulliez, and D.P. Hand. *Laser based vacuum packaging of micro-devices using localised heating*. in *Proceedings of LPM 2010 - the 11th International Symposium on Laser Precision Microfabrication*. 2010. Stuttgart, Germany.

Lorenz, N., M.D. Smith, and D.P. Hand. *Low temperature wafer-level packaging of MEMS using selective laser bonding*. in *29th Internatinoal Congress on Applications of Lasers & Electro-Optics (ICALEO2010)*. 2010. Anaheim, CA, US.

Awards:

AILU (Association of Laser Users) Young UK Laser Engineer's Prize 2011

"Norbert Lorenz is awarded the AILU's Young UK Laser Engineer Prize 2011 in recognition of his contribution to the development of laser-based sealing processes." – AILU Website (www.ailu.org.uk)

1 Introduction

1.1 Rationale

Packaging is one of the major challenges in the production of micro-electro-mechanical systems (MEMS) and other micro-devices. In contrast to integrated circuit (IC) packaging, where convenient packaging processes already exist, MEMS packaging is often application specific and not suitable for industrial production. MEMS packaging has to meet numerous and often conflicting requirements which make it challenging and often costly (up to 90% of overall device costs).

Some typical requirements are:

- protection of the device from the often harsh external environment they operate in whilst at the same time permitting interactions with stimuli from the environment (e.g. in sensing applications);
- encapsulation whilst still maintaining optical access;
- hermetic packaging for controlled atmospheres with long-term stability to avoid device failure;
- bio-compatibility in bio-medical applications;

  and, most importantly,
- the packaging process must not destroy or influence the performance of the device to be packaged.

Numerous applications require a vacuum within the package for improved functionality. At the same time communication (e.g. via interconnects) with other devices is required; resulting in even higher demands on the packaging process.

State-of-the-art bonding techniques often are restricted to certain materials, involve elaborate pre-bonding preparation steps, and in general still require heating of the entire device to the bonding temperature and thereby restrict the use of temperature sensitive materials within the package. In addition, multi-stage packaging processes where several heating cycles are carried out in sequence generate problems. Parts joined in an earlier assembly step can disassemble in a later one.

1.2 Aims and Objectives

The main aim of this PhD is the development of laser-based encapsulation processes for packaging of temperature sensitive devices and materials. The demonstration of a MEMS wafer-level bonding process and hermetic packaging of components under vacuum are two of the main objectives. Furthermore, the heat input into the bulk of the package should be reduced to a minimum. To provide for all these requirements the design and development of a multi-purpose bonding setup and process are required.

The work presented in this thesis has been primarily driven by the interest of industrial collaborators, QinetiQ, GE Aviation and C-MAC Micro Technologies, who have a direct interest in applying these technologies in actual device manufacture. This PhD thesis describes the development of two laser-based localised heating joining processes, where also the lateral heat flow into the centre of the device is greatly reduced by active cooling.

Silicon to glass joining with an adhesive bonding layer is investigated which is a typical MEMS application. The bonding material used in this case is Benzocyclobutene (BCB). The laser-based process, using localised heating, is demonstrated with packaging on a chip-level first. This is followed by a further development of this process to wafer-level packaging.

The development of full hermetic packaging processes of Leadless Chip Carrier (LCC) devices in both air and vacuum is presented. In this technique a glass frit intermediate layer is used.

The major benefit of these laser-based processes is that by using a localised heating technique and active cooling of the component, the temperature in the centre of the device to be packaged can be greatly reduced in comparison to standard furnace-based processes.

1.3 Summary of Chapters

- Chapter 2 comprises a comprehensive review of conventional packaging technologies using global heating. This chapter also gives an introduction to the more recent development of localised heating bonding techniques including a

comparison of laser-based processes. The latter is the most promising approach which is therefore pursued in this thesis.

- Chapter 3 describes the development of a multi-purpose bonding setup and the process development of the two novel laser-based joining techniques. These are silicon to glass joining with a BCB intermediate layer and hermetic glass frit packaging in air and vacuum. The setup fulfils all the numerous requirements for these bonding processes and only minimal adaptations are required to change between the processes.

- Chapter 4 covers the experimental work conducted on laser-based silicon to glass joining with a BCB adhesive layer. The development of this bonding technique based on localised heating from single chip packaging to wafer-level packaging and the challenges involved are described. A technique to provide the bonding force individually for every single device on a wafer is presented. This is the key issue in laser-based wafer-level packaging. The investigations from this chapter are published in the Elsevier journal of Microelectronics Reliability [1].

- Chapter 5 contains the continuation of the description of the experimental bonding results examining laser-based glass frit bonding of LCC packages. Full hermetic packaging in both air and vacuum is accomplished by applying truly localised heating. The temperature in the sensitive device area is kept considerably lower than in the joining area. The main focus, in particular for the vacuum packaging process, is on tailoring the heat flow within the substrate to achieve the lowest possible temperatures whilst still realising reliable seals. The work from this chapter resulted in a publication of the IOP Journal of Micromechanics and Microengineering [2].

- Chapter 6 provides the overall conclusions of the investigations presented in this thesis. Suggestions for future research and possible benefits of these processes to industrial applications are also discussed.

2 Literature Review and Background

This chapter presents a review of conventional methods for packaging of micro-devices and micro-electro-mechanical systems, the so-called MEMS. A range of processes have been developed for packaging of micro-devices which are all well established in the market. However, these are often limited to certain materials and some are incompatible with temperature sensitive devices. In this chapter the most relevant conventional bonding techniques are reviewed and compared to the laser-based approach developed and investigated in this PhD thesis. A short introduction of the existing knowledge on the intermediate bonding layers investigated in this work and a brief review of the general state-of-the-art in MEMS packaging is also included in this chapter.

2.1 Motivation – Challenges and Issues in Packaging of Micro-devices

As mentioned in the Introduction, packaging is one of the major challenges in the production of MEMS and other micro-devices due to the plentiful and often contradicting requirements on the packaging process [3]. The main attention of the research was often focused on the development of such devices. Assembly and packaging, however, were neglected and limited to prototypes in laboratories which are unsuitable for industrial production [4, 5]. The research presented in this PhD is concentrating on the packaging process which is one of the remaining obstacles for the commercialisation of micro-devices and MEMS.

For integrated circuit (IC) devices convenient packaging processes already exist. On average they account for 20% of the entire manufacturing costs. The techniques developed for IC packaging can be used for packaging in microsystems technologies, but often these methods have to be enhanced according to the special applications of the devices. Therefore, the packaging costs are estimated to be more than 50% and can even reach 90% [6, 7].

The main challenge in microsystems packaging is that in contrast to conventional IC devices MEMS must be able to interact with their environment. In a prosaic sense, if the traditional IC is the brain, MEMS adds the eyes, nose, ears, muscles and many others senses that humans do not possess [8].

Packaging of ICs has to meet the following four major requirements: signal distribution, power distribution, heat dissipation and protection of the device from the environment. The sensitive device to be encapsulated must be protected from mechanical, chemical, electromagnetic and other environmental influences [9]. Packaging in microsystems technologies has to perform one additional, complex function. It has to ensure that the device can interact directly with certain stimuli of the environment but at the same time it has to protect it against others which are hostile for the device. As a consequence, packaging is often application specific posing another hurdle for a low-cost generic packaging process [4, 5].

As discussed above, there are several issues involved with packaging. Neither should the packaging process damage the pre-fabricated device nor should it have any influence on the performance of the device. In particular stress, induced by the heat load during packaging, may have a great influence on the performance of devices like sensors [10]. Dependent on the application, some devices require hermetic, vacuum sealing or low temperature packaging. A full hermetic seal can protect a package from moisture ingress for years. Thereby, failure of the device due to condensing water vapour inside the package is avoided. In addition, the packaging process should be applicable to different types of devices to reduce manufacturing costs [11].

Some microsystems contain moving parts. Cavity-style packages are required for those devices to ensure sufficient free space around the structures. Particle contamination must be minimized during the packaging process. Particles are one of the main reasons for device failure [4]. Another issue involved with small, moving parts on the micro- and nanometre scale is stiction. The elements in a micromechanical device can stick together because of adhesion forces (e.g. van der Waal, electrostatic), which are comparatively small in the macro world. This can require high starting forces for moving parts and it can even result in device failure [4, 8].

One of the main concerns in MEMS packaging remains the long-term stability of vacuum sealed devices. Numerous applications such as resonant and tunnelling devices, pressure sensors, infrared detectors, and vacuum displays require a vacuum within the package for improved functionality [12]. The vacuum, however, is often destroyed by out-gassing of the intermediate layer during the bonding procedure or due to a lack of hermeticity of the seal [4, 8].

State-of-the-art bonding techniques often are restricted to silicon and glass materials, involve elaborate pre-bonding preparation steps, and in general require heating of the entire device to the bonding temperature and thereby restrict the use of temperature sensitive materials within the package. In this PhD thesis the development of two laser-based localised heating joining processes is presented where the lateral heat flow into the centre of the device is greatly reduced by active cooling.

Silicon to glass joining, a typical MEMS application, using an adhesive bonding layer is investigated. The bonding material used is Benzocyclobutene (BCB). The laser-based process, using localised heating, is first demonstrated for packaging on a chip-level. This is followed by a further development of this process to wafer-level packaging.

The development of full hermetic packaging processes of Leadless Chip Carrier (LCC) devices in both air and vacuum using a glass frit intermediate layer is investigated in the second experimental part of this thesis.

The major benefit of these laser-based processes is that by localised heating and active cooling the temperature in the centre of the device to be packaged can be reduced greatly in comparison to conventional packaging processes where the heat is applied to the entire package.

2.2 Traditional Direct Bonding Techniques

In this section the most common direct bonding techniques in microsystems technologies – silicon fusion bonding and anodic bonding – are discussed. The term "direct bonding" implies that these bonding processes do not require any additional intermediate bonding layers. It has been shown that this places a high demand on the surfaces to be bonded with respect to roughness and cleanliness.

2.2.1 Silicon Fusion Bonding

Silicon fusion bonding was first reported by Lasky [13] at IBM and Shimbo et al. [14] at Toshiba almost simultaneously in 1986. Since then, extensive research has been carried out by various work groups to apply this method to packaging in microsystems technologies [9, 15-20]. Silicon fusion bonding benefits from mechanically and chemically strong seals which are achieved in high yield processes. In general,

however, these processes require immaculate bond interfaces, i.e. surface roughness in the nm-regime and very high demands on freedom from particulate contamination [15, 16]. In addition, high process temperatures of up to 1100°C are required for some processes which severely limit the application areas for these techniques. The quality of the bond strongly depends on the quality (surface finish) of the bond interfaces. For successful bonding, i.e. small non-bonded areas or voids between the bond interfaces, the experiments need to be carried out in a clean room of class 10 or better [14, 15] since even small particles can result in extended voids [15, 16]. The typical stated flatness requirements of the silicon surfaces to be bonded are micro roughness of <4 nm [9] and the curvature should not exceed 25 µm for a 4"-wafer [9, 15].

The bonding process is divided into three main steps: (i) surface pre-treatment, (ii) pre-bonding at room temperature and (iii) annealing at high temperature.

(i) The basic principle of direct silicon fusion bonding of silicon to silicon is a chemical reaction between the OH groups of the oxide layers of the bonding partners. For successful bonding, hence, an oxide layer is required on both interfaces. The oxide can either be a native oxide or a thermally oxidized layer. Prior to bonding, the silicon surfaces are treated with a series of cleaning steps to ensure the surface is particle-free and to generate hydrophilic surface which is essential for bonding [15-17].

(ii) For pre-bonding at room temperature the polished sides of the silicon wafers are brought into contact in a clean room. Usually they are pressed together starting from a small area which then spreads over the entire surface area, given there are no particles preventing intimate contact and a sufficient smoothness of the wafers. The wafer pair is hold together by van der Waal's forces [15, 17].

(iii) After room temperature bonding the wafer pair is heated up to temperatures of typically up to 1100°C to form the silicon – oxide – silicon bond. After around 2 hours annealing a sufficient area of the surface has bonded that separation of the bonded wafers results in breaking of the silicon itself [16, 19].

Using this direct bonding process strong and hermetic seals can be achieved with a high yield. Bonding strengths up to 20 MPa have been reported [9, 16, 19] which is in the

range of the fracture strength of single crystalline silicon. Due to the high process temperatures, however, temperature sensitive materials cannot be packaged using this bonding technique, e.g. the maximum temperature limit for packaging standard active electronics (IC compatibility) ranges from 420°C to 450°C [9]. In recent years silicon fusion bonding techniques have been developed where the process temperature is kept below 400°C [18, 20], however rather long annealing steps of up to 6 hours are required. The same bonding technique can also be used to bond other materials apart from silicon to silicon given sufficiently polished and properly conditioned surfaces. The choice of these materials is primarily limited by the maximum permitted mismatch of the coefficient of the thermal expansion (CTE) of the bonding partners. When bonding dissimilar materials, the differences in CTE can result in de-bonding of the interfaces at elevated temperatures during the annealing step. Successful bonding of quartz wafers, GaAs to silicon and silicon to glass, for example, has been demonstrated [9, 15].

Strong and hermetic seals can be achieved with all the techniques mentioned above. In general, the two major drawbacks are that as precondition for successful bonding the processes must be accomplished in a particle-free environment (clean room of class 10) and the micro roughness of the mirror-polished bond interfaces must be in the nm-regime. Elaborate, labour intensive pre-bonding steps and very costly equipment (clean room) are required to fulfil these requirements. The practicability of those processes in small scale production in industry or packaging applications in research laboratories is rather limited unless the required equipment is already available and used in part of the production processes of the devices to be packaged.

2.2.2 Anodic Bonding

Anodic bonding, which is also referred to as field assisted bonding, was first reported by Wallis and Pomerantz [21] in 1969. Initially developed for sealing of glass to metals, it is nowadays mostly applied to the bonding of glass to silicon for packaging applications in the production of microsystems and MEMS, e.g. encapsulation of sensors [22-24]. For bonding a silicon wafer to a glass wafer – both polished and particle free – the parts are placed into intimate contact and a typical temperature of around 400°C to 450°C and a voltage ranging from 400 V to 1200 V are applied. A strong bond (15-25 MPa) is formed between the two surfaces in an electrochemical

reaction [20, 22, 24, 25]. A typical configuration of such a bonding process is shown schematically in Figure 2.1.

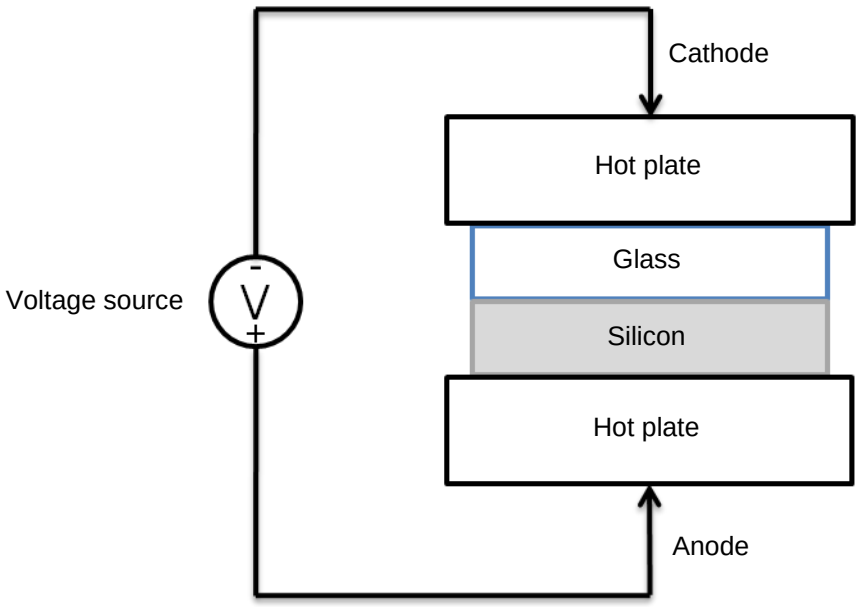

Figure 2.1: Schematic sketch of setup for anodic bonding process

For successful bonding sodium rich glasses are required. Widely used glasses are Corning #7740, Corning #7070, soda lime #0080 and K_4 glass [9, 23, 24, 26, 27] although many other glasses are suitable. A prerequisite for successful bonding is that the coefficients of thermal expansion (CTE) of the bond partners must be closely matched over the temperature range of the bonding process. Otherwise the mechanical stress inside the materials can result in splitting of the bond during cool down or in permanent warpage which might influence the performance of the device to be packaged [9, 21, 24, 26]. In comparison to silicon fusion bonding (see previous section 2.2.1) anodic bonding benefits from less stringent requirements on the surface quality of the wafers to be bonded; however clean, smooth and polished interfaces with a surface roughness <1 µm are still required for reliable seals. Similarly, the process is also sensitive to dust particles which otherwise result in extended non-bonded (non-contact) areas of the bond interfaces [9, 21, 27] but the larger surface roughness allows for a reduced requirement of freedom of particulate matter compared to silicon fusion bonding.

The anodic bonding process consists of four major steps. (i) First the bond interfaces are polished and cleaned to ensure smooth and particle-free surfaces. (ii) Then the polished sides of the wafers are placed into intimate contact and heated to the required

bonding temperature in an oven or between hot plates as shown in Figure 2.1. (iii) By application of the electrostatic field the actual bonding process is initiated. (iv) After bonding (typically 5 to 10 min [9]) the wafer stack is cooled down. The cool down rate depends on the mismatch of the CTE of the bond partners.

The most important process parameters are the bonding temperature and the applied voltage. In general, higher bonding temperatures and stronger electric fields result in higher quality bonds given the temperature is restricted to a maximum of 450°C. Above 450°C the CTE of glass and silicon differ considerably resulting in too high mechanical stress [9, 22, 25, 27].

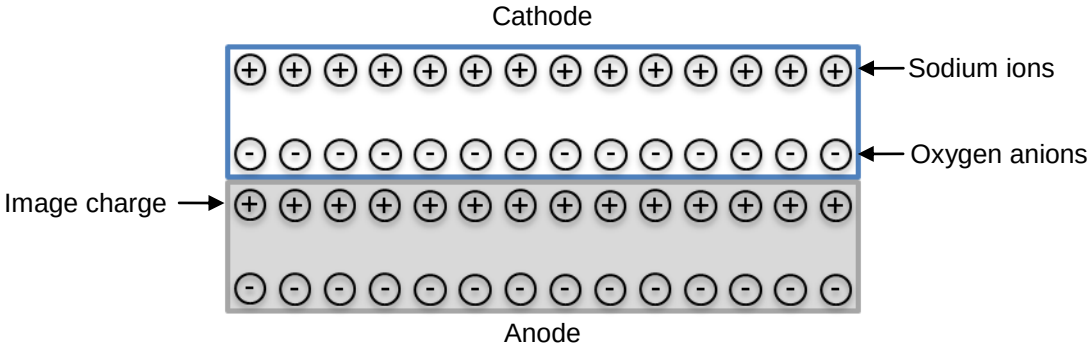

Figure 2.2: Schematic representation of charge distribution within the glass to silicon wafer pair during the anodic bonding process

The finer details of the bonding mechanism at the glass to silicon interface are presently still being debated. A generally accepted explanation [9, 22, 24, 25] is described in the following. A temperature of typically 400°C to 450°C and a voltage ranging from 400 V to 1200 V are applied to the wafers to be bonded, whereas the glass wafer acts as cathode and the silicon wafer as anode. Due to the elevated temperature the movement of the sodium ions (Na^+) is improved within the glass wafer. The positively charged Na^+ move towards the cathode, thereby creating a depletion area in the glass side of the glass to silicon interface (see Figure 2.2). The negatively charged and relatively immobile oxygen anions are left behind forming a space charge region. On the opposite side, in the silicon side of the glass to silicon interface, an equivalent positive charge (image charge) is created. This results in a strong electrostatic attraction of the bond interfaces pulling them into intimate contact. The oxygen anions drift across this interface induced by the high electric field and react with the silicon due to the elevated

bonding temperature. The applied temperature and electric field (i.e. voltage), hence, are the most important process parameters as mentioned above.

In comparison to silicon fusion bonding (see previous section) anodic bonding benefits from considerably lower process temperatures and less strict requirements for the surface finish whilst still achieving excellent bond strengths (15 to 25 MPa). Even though anodic bonding is compatible with IC packaging (max. temperature of 450°C) a further reduction of the bonding time and/or temperature is desirable as some electronic components and prefabricated devices may not be able to withstand such temperatures at all or for such an extended period [22, 25]. Additionally, a lower bonding temperature can reduce or remove the mechanical stress and warpage after cooling due to the mismatch of CTE of the bonded materials. A simple reduction of the bonding temperature and time, however, often resulted in a diminished bond quality [25]. Therefore, research was aimed at improving these bonding processes without influencing the quality of the bond. Lee et al. [22], for example, achieved void-less bonds with high bond strength (>15 MPa) at temperatures of 300°C in considerably shorter bonding times by using a pulsed voltage technique. Instead of applying a constant, static electric field a pulsed square waveform voltage profile was used reducing the overall required bonding time by 70%. In [25] low temperature anodic bonding with high bond quality (non-bonded area <1.5% and bond strength >10 MPa) at a bonding temperature of 200°C was reported. Due to the low bonding temperature the residual stress in the sample after cooling was eliminated.

Overall anodic bonding is less harmful (considerably lower process temperatures) for devices to be packaged; however, it is restricted by some limitations. In general clean (particle-free) and smooth surfaces (surface roughness <1 µm) are required for successful bonding which can only be guaranteed in controlled atmospheres and require elaborate preparation of the bonding interfaces. In contrast to intermediate layer bonding it is restricted to bonding of materials with closely matched CTE. Even though the bonding temperature can be reduced to 200°C the heat load is applied to the entire device and thereby limiting the use of some temperature-sensitive materials (polymer and organic materials) within the package. More importantly, the strong electric fields which are applied during the bonding process prevent this technique from being applied for packaging of sensitive electronics and other prefabricated devices like RF-MEMS.

2.3 Intermediate Layer Bonding

In the previous section direct bonding, i.e. without any additional intermediate bonding layer, using silicon fusion or anodic bonding was discussed. These techniques are of great benefit if mechanically strong seals are required. However, when packaging of chemical and temperature sensitive and electronic devices is required, they are less suitable due to the high temperatures or strong electric fields necessary for successful sealing. In these cases bonding techniques using an intermediate layer are a promising alternative. Intermediate layer bonding has the advantages of less stringent requirements on the quality of the bond interfaces, a greater choice of substrate material which can be bonded, considerably lower bonding temperatures and no electric fields are required for successful bonding. Most importantly, some processes are largely insensitive to surface impurities; hence, elaborate pre-bonding wafer preparation (cleaning) and bonding in a clean room are not required. A number of intermediate layer bonding techniques, which are well established in industry already, have been developed. The three most common ones, eutectic, glass frit and adhesive layer bonding, are discussed in this chapter.

2.3.1 Eutectic Bonding

Eutectic bonding, which is also referred to as eutectic soldering, is a bonding technique using metallic intermediate layers as the sealing layer to form an eutectic alloy. The main advantage of this technique is that the melting point of the eutectic alloy, which is formed during the bonding process, is much lower than the melting temperatures of the pure materials. Typical electronic solders are a prime example of eutectic bonding materials. Eutectic bonding, which is a well-established technique in industry for single chip packaging since the early 1990's, was first applied to wafer to wafer bonding for the encapsulation of silicon microstructures by Wolffenbuttel in 1994 [28, 29]. With eutectic bonding, hermetic seals with high bond strength can be achieved at considerably lower temperatures than in direct bonding techniques. In silicon eutectic bonding, gold is the most commonly used eutectic partner as these materials are frequently utilized in MEMS fabrication already [28, 30, 31]. It forms an eutectic alloy with silicon at an eutectic composition of 19 at% (Si) and 81 at% (Au) and a temperature of 363°C, which is well below the melting point of gold (1064°C) and silicon (1414°C), as shown in the phase diagram in Figure 2.3 [29].

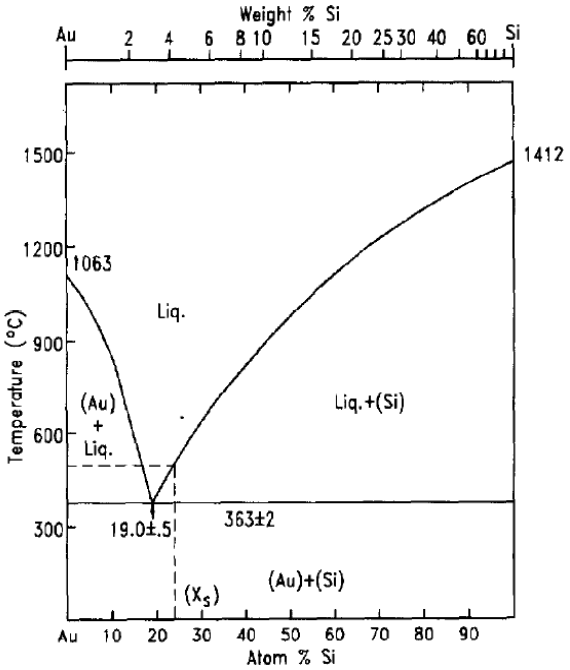

Figure 2.3: Phase diagram of silicon and gold [29]

At the eutectic concentration, a liquid phase forms directly without passing a two phase equilibrium once the mixture is heated above the eutectic temperature (363°C). The mixture will remain fluid until the temperature drops below the eutectic temperature or the concentration of the composition changes below the liquid line (see Figure 2.3). In order to bond two wafers together, gold and silicon have to be applied to the bond interfaces to form the eutectic. In most cases gold is deposited onto one of the wafers to be bonded and the silicon is provided from the bulk of the silicon wafer itself. Upon direct, atomic contact of the gold and silicon interfaces a diffusion process is started and accelerated with increasing temperatures. Above the eutectic temperature a liquid phase forms, the eutectic compound, which facilitates further mixing and diffusion, and acts as intermediate bonding layer. Normally there is an effectively unlimited supply of silicon, as it comes from the substrate directly, hence solidification starts once the silicon has reached a certain concentration in the mixture and the temperature drops below the liquid line. During cooling a strong eutectic bond is formed which consists of a gold silicon hypereutectic phase [28-30].

Eutectic bonding benefits from relatively low bonding temperatures and, therefore, lower stress in the final assembly, no out-gassing during bonding and mechanically strong bonds [28, 30, 32]. A key reason for its widespread success in industry is the fact that hermetic seals and electrical interconnects can be achieved in the same process [28, 32]. However, low reliability and uniformity (void-free bonding) of eutectic

bonding are two major concerns. If oxide layers are present on the bond interfaces successful bonding cannot be achieved [28, 30, 32]. Therefore, the surface preparation is the critical step during the procedure of eutectic bonding as the quality of the bond (strength) strongly depends upon the surface quality [30, 33, 34].

The eutectic bonding procedure is divided into three steps: substrate preparation, the actual bonding process, and the cool down. The preparation step is of utmost importance. The quality of the bond depends upon it as mentioned above. The main problem is the poor wettability and adhesion of gold on an oxide surface. Even the native oxide layer on a silicon substrate is sufficient to prevent successful bonding. There are two possibilities to overcome this problem [28, 30, 32]: the oxide layer is either removed prior to bonding or additional adhesion layers are deposited on top of the oxide. The oxide layer can be removed mechanically by rubbing the surfaces against each other during attachment and thereby breaking up the oxide or by applying ultrasound. Alternative and commonly used approaches are the use of wet chemical etching or plasma cleaning to remove an oxide layer.

Even though good adhesion of gold to silicon can be achieved once the oxide is removed, the second approach – to apply adhesive layers – is generally preferred in applications where the native oxide on the silicon substrate is required as a functional (passivation) layer for integrated circuits. A thin intermediate metal film, which must adhere well to both the oxide and the gold, is deposited on top of the oxide followed by the deposition of the gold layer. Suitable materials are titanium and chromium or a combination thereof. A typical sketch of such a substrate wafer is shown in Figure 2.4.

Figure 2.4: Schematic sketch of substrate wafer for eutectic bonding with additional adhesion layer

In case of a removal of the oxide layer, the bonding process must be conducted directly afterwards to prevent a renewal of the native oxide layer on the silicon substrate. To further ensure a high bond quality (void-free) bond, the surfaces must be kept free of contaminants (e.g. dust particles) and therefore bonding should be conducted in an inert

gas atmosphere or vacuum to avoid oxidation at high temperatures. The eutectic materials should have a thickness of several microns to cover asperities of non-planar surfaces [30]. After the wafer preparation, the wafers to be bonded are positioned on top of each other and aligned, and for the actual bonding process the wafers are heated above the eutectic temperature. To ensure intimate contact between the bond interfaces a force must be applied throughout the entire process. For eutectic bonding commercial substrate bonders are normally used as they provide these three functions: alignment, application of force and heating. The most important bonding parameters are the bonding temperature, time and force [28, 34]. Typical parameters for silicon to gold eutectic bonding are a temperature of 390°C to 400°C for up to 15 minutes and a bonding force ranging from 100 kPa to 500 kPa [28].

In eutectic bonding with silicon and gold, superior bond strengths of up to 148 MPa [35] have been reported. However, often process temperatures in the range up to 500°C are required for reliable bonding which is significantly higher than the eutectic temperature of 363°C [32, 36]. These high process temperatures can generate problems, e.g. degradation of performance, high internal stress or even complete destruction of encapsulated device, when packaging temperature sensitive materials and devices. A particular example is RF-MEMS, which typically can only withstand temperatures below 350°C without affecting the devices' performance [33, 37]. Therefore, research has focused on using different eutectic alloys to further reduce the required bonding temperature [33, 34, 36-38]. In the research laboratories of Samsung successful wafer-level packaging of RF-MEMS has been demonstrated using a gold and tin eutectic alloy [33, 34, 37]. Hermetic seals with average bond strengths of 71.5 MPa were achieved in a bonding process where the temperature was kept below 300°C. A further reduction of the bonding temperature (180°C to 210°C) has been reported in [38] by using a gold and indium eutectic system. Apart from the lower temperature budget this alloy also benefits from a high re-melting temperature of around 470°C; high re-melting temperatures are required for some applications in optoelectronic packaging (e.g. image sensor modules). For glass to glass and glass to silicon bonding, average bond strengths of 40 MPa and 20 MPa, respectively, were accomplished. Lee et al [36] also achieved hermetic seals with bond strengths ranging up to 20 MPa for silicon to silicon bonding. The bonding temperature was reduced even further below 160°C by using indium-tin alloys.

In summary, the shear force values which can be obtained for the various eutectic alloys compare well and even exceed in some cases the values of samples bonded using silicon fusion and anodic bonding (see section 2.2). Additionally, eutectic bonding benefits from considerably lower bonding temperatures and no electric fields are required for successful bonding thus making this technology more suitable for packaging of sensitive materials. The oxidation of the eutectic alloys, however, results in elaborate and costly pre-bonding wafer preparation. In some cases a stack of several metal layers (e.g. Ti-Ni-Au-Sn-Au [34]) is required for successful bonding. Furthermore, the bond interfaces must be kept free of contaminants to avoid large non-bonded areas (voids) [33, 34, 37] and thereby limiting the practicability of these processes. When joining dissimilar materials the mismatch of CTE might result in residual stress at the bond interfaces causing warpage and reliability issues [32, 34].

The temperature required during eutectic bonding still prevents the use of certain temperature sensitive materials. Lower bonding temperatures can only be achieved with adhesive layer bonding. These methods, however, suffer from low re-melting temperatures, non-hermetic seals and out-gassing during curing [38]. To overcome the issue of elevated temperatures research has been focused on combining eutectic bonding with more localised and selective heating techniques (e.g. resistive heating, laser heating). These techniques will be discussed in more detail in section 2.4. They reduce the heat input in the actual device to be packaged considerably but still some of the general limitations of eutectic bonding persist.

2.3.2 Glass Frit Bonding

Glass frit bonding is a packaging technology which uses a low temperature sealing glass as intermediate bonding layer. It is commonly used for the encapsulation of acceleration sensors, gyroscopes, micro relays, IR-bolometers, RF-MEMS and many other devices, especially sensors [39-46]. In these applications hermetic seals with long-term stability are often essential to ensure a proper functionality throughout the lifetime of the encapsulated device. Glass frit has proven to be a suitable sealant material to ensure stable conditions for several years [47-49]. Glass frit packaging further benefits from high bond strength, high process yield and good process repeatability. Due to its high wetting abilities, glass frit has non-stringent requirements for the flatness of the surfaces to be bonded. It is even possible to run signal lines through the sealing layer without affecting the hermeticity. Glass frit adheres well to

most materials commonly used in microsystems technologies which explains its widespread use in packaging technologies. For successful bonding, temperatures in the range from 300°C to 450°C are required, limiting the use of some temperature sensitive materials within the package. Furthermore, out-gassing of the glass frit during bonding and flow of the sealant material into the structures to be encapsulated are possible downsides of this technology.

Prior to bonding, glass frit is typically handled as paste and it is commercially available from companies like Schott, Corning, Diemat and Asahi Glass Company (AGC). In most cases the glass frit material is designed to enable process temperatures below 450°C, thus making this technology compatible to IC packaging and suitable for most MEMS applications [40, 41, 43-45]. Glass frit materials with a process temperature below 400°C exist and these can be used for CMOS packaging [50]. Lead or lead silicate glasses with high lead oxide content (approximately 88 at%) are often used to achieve such low bonding temperatures [43, 45, 50]. The glass is ground into small broken particles, i.e. frits. The sizes of the frits typically range from grain sizes of 1 µm to 15 µm. The glass powder is mixed with an organic binder and solvents to form a printable paste which can be dispensed onto the bond interfaces. Inorganic fillers can be added to the paste to match the coefficient of thermal expansion (CTE) to the materials to be bonded to lower the residual stress after bonding which is typically required in the case of silicon bonding [40, 41, 43-45, 50].

Glass frit bonding is divided into three process steps: (i) deposition of the paste, (ii) conditioning of the paste and (iii) the actual bonding process. The glass frit paste can be screen-printed, stencil-printed or dispensed (e.g. by syringe) onto one of the surfaces to be joined. These deposition techniques have the benefit that the bonding layer can be applied and structured in the same step. No further steps, like photolithography, are required. Furthermore, the paste can be applied selectively to the bonding area only. Deposition of the glass frit paste onto structured wafers and substrates containing high steps or holes is also possible. If using screen-printing feature sizes of around 190 µm (minimal width) with a minimum spacing of 100 µm can be achieved. A typical height of about 30 µm of the glass frit paste is recommended to ensure sufficient material during reflow [43, 44]. After deposition of the glass frit paste onto the substrate the paste must be conditioned at elevated temperatures to drive out any solvents and to burn out the organic binder prior to bonding. A typical

temperature profile of such a thermal conditioning process of the glass frit is shown in Figure 2.5.

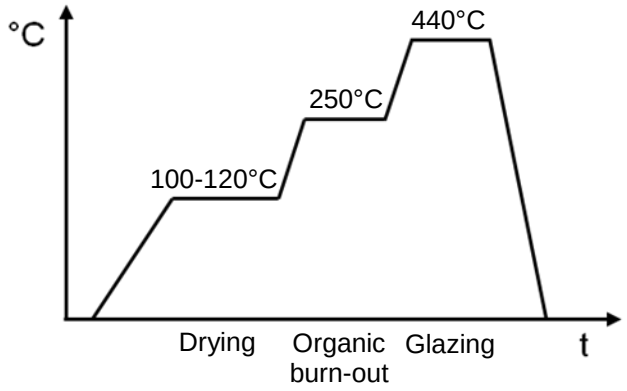

Figure 2.5: Temperature profile of thermal conditioning of glass frit material prior to bonding

The paste is first heated to a temperature of around 100°C to 120°C for typically 10 minutes to 30 minutes to dry the paste and drive out any residual solvents. The temperature is further increased to an intermediate temperature around 250°C for 30 minutes to 60 minutes to completely burn out the organic components. The exact temperature depends on the composition of the paste. In a final step, the so-called pre-melting or glazing, the paste is heated to the actual bonding temperature and fully melts. A compact glass without any voids (gas inclusions) is formed. A considerable reduction of the thickness of the glass frit layer can be observed. The inorganic fillers, used to match the CTE, melt during glazing and the final properties of the sealant layer are achieved. This thermal conditioning of the glass frit material prior to bonding is of significant importance as an insufficient burn-out will result in out-gassing and void generation during bonding; thereby lowering the bond quality (mechanical strength) and creating a potential risk of leaks [43-45, 51, 52].

Glass frit packaging is a thermo-compressive bonding process. The materials to be bonded and the glass frit are heated to the bonding temperature and a slight force, which results in reduction of the thickness of the sealing layer, is applied to facilitate the wetting of the bond interfaces. The elevated temperature reduces the viscosity of the glass frit to such a degree that even for rough and non-planar surfaces a complete wetting of the entire bonding area can be achieved. During the bonding process it is the temperature which is the critical parameter rather than the applied pressure. It must be high enough to ensure proper wetting but not too high to avoid material degradation or

flow of glass frit material into structures which should be protected. Upon cooling a strong bond is formed between the interfaces. In the case of silicon bonding additionally a very thin glass mixture is formed at the silicon to glass interface which enhances the bond strength. During cooling stress can built up due to the mismatch of CTE; however, this is only critical at temperatures above 200°C [40, 41, 43-45]. A typical cross-sectional view under a scanning electron microscope of a bonded silicon wafer pair is shown in Figure 2.6 [40]. The particles visible in the glass frit layer are not voids but the inorganic fillers used to match the CTE.

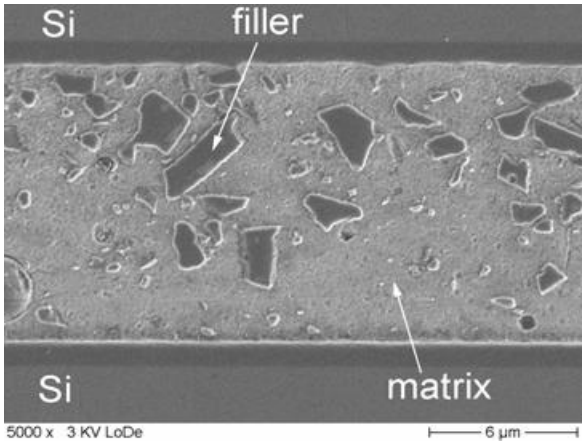

Figure 2.6: Cross sectional view of glass frit bonded wafer pair under scanning electron microscope [40]

Glass frit packaging is a simple and robust process without elaborate preparation of the bond interfaces where high yield rates above 90% can be achieved. Strong and hermetic seals with shear forces above 20 MPa have been reported [43, 44] which compares well with results achieved by anodic, fusion and eutectic bonding. In contrast to the latter, however, it is insensitive to surface steps, surface roughness, non-planar surfaces and particles due to the high viscosity of the glass frit during bonding. If signal lines are run across the seal no additional passivation is required up to temperatures of 150°C to prevent leakage currents between the signal lines as glass frit is a dielectric material [39, 43, 44]. After bonding, the glass frit sealing layer has a typical thickness of 5 µm to 10 µm which can be used as spacer between the bonded interfaces to create an internal micro-cavity for moveable structures or micro-electro mechanical components [44, 50], as shown in Figure 2.7.

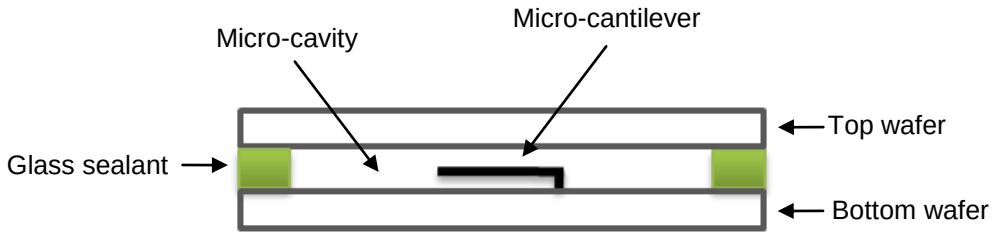

Figure 2.7: Schematic sketch of sealed micro-cantilever in cavity created by glass sealant layer between wafer pair

Successful bonding can be achieved with nearly all materials used in microsystems technologies: silicon, glass, metals (including gold), insulators and passivation layers, and polyimide [39, 43, 44, 52]. For example, in [39] strong adhesion of glass frit to silicon oxide was demonstrated which is not possible using eutectic bonding; a major drawback of the latter technology. Furthermore, no electric fields are required for bonding and bonding temperatures below 400°C make glass frit packaging compatible to IC and CMOS technology. Sparks et al [47-49, 53] have successfully applied glass frit bonding to vacuum packaging of silicon resonators. To overcome the issue of out-gassing of water and carbon from the glass frit, getters were used to achieve lower cavity pressures ($<1.13\times10^{-3}$ mbar). These getters are typically metals or alloys of Ba, Al, Ti or Fe, which are placed inside the cavity. Upon thermal activation, these getters trap various gases, which are released during the bonding process, through oxide or hydride formation, or by surface adsorption. Sparks' research underlines the superior hermeticity and long-term stability of glass frit as sealant. Over a period of 3 years no loss of vacuum inside the packages was observed even though the packages were stored at an elevated temperature of 95°C.

The major drawback of glass frit packaging are the still comparatively high bonding temperatures of 300°C to 450°C which are in general applied to the entire package. Hermetic sealing of temperature sensitive devices, e.g. functional polymers used in OLEDs (max. temperature <100°C) [54], cannot be accomplished using this technology. Otherwise, glass frit bonding would be an ideal solution for a generic packaging technique in microsystems technologies.

2.3.3 Adhesive Layer Bonding

Adhesive bonding is a technique which uses a polymer as an intermediate bonding layer; hence, it is often also referred to as polymer bonding. A wide range of polymers, including polymethylmethacrylate (PMMA), parylene, SU-8 and benzocyclobutene

(BCB), have been applied successfully to full wafer bonding, packaging of micro-fluidics devices, MEMS devices (especially RF-MEMS), and IC and CMOS packaging [3, 55-77].

Adhesive layer bonding is a low temperature process (temperatures <100°C possible) with hardly any limitation concerning the substrate materials. High bond strengths and good adhesion can be accomplished with most materials. Furthermore, no electrical fields are required during the bonding and, therefore, the process is compatible to IC packaging. Sample preparation in polymer layer bonding is compatible with standard clean room processing. The bonding procedure is a simple and robust method which is insensitive to particles, surface roughness and non-planar bond surfaces with deviations from flatness of up to a few micrometers. These reduced requirements result in considerably lower process costs. The elastic properties and often liquid-like behaviour of the intermediate layer during the bonding process results in a low stress within the materials being bonded. The thickness of the intermediate layer can be varied from tens to hundreds of microns, which means it can be used not only as the bonding layer but also as a spacer to form cavity-style packages. The limited temperature stability (glass transition temperature of most polymers t_g <400°C) and the limited long-term stability of the joints especially in harsh environments (degradation of the material properties due to moisture uptake, temperature, radiation, mechanical and chemical impacts, etc.) must be taken into account, together with the lack of full hermetic seals with such a polymer seal [3, 55, 63, 67, 70, 77].

Basically, most common adhesive bonding processes can be described as follows: (i) a polymer layer is applied to one or both surfaces to be bonded, (ii) then they are aligned on top of each other and (iii) a force is applied to ensure intimate contact of the bond interfaces. During the bonding process the polymer is transformed from a liquid or viscous form into a solid which is typically initiated by heat or exposure to ultraviolet (UV) light, or a combination thereof. The bonding mechanism in adhesive bonding is based on the fact that surfaces adhere to each other if they are placed into atomic contact. In most cases, adhesive bonding is used to join two solid interfaces together. The adhesive polymer must deform to attach to the locally rough interfaces which prevent them from bonding directly. To ensure sufficient wetting of the bond interfaces without voids the polymer must have a low viscosity, i.e. liquid-like behaviour, during some part of the bonding procedure. If the polymer is sufficiently fluid the roughness

of the surface profile can be smoothened out (see Figure 2.8) and upon hardening of the adhesive polymer, a strong bond is formed between the interfaces [3].

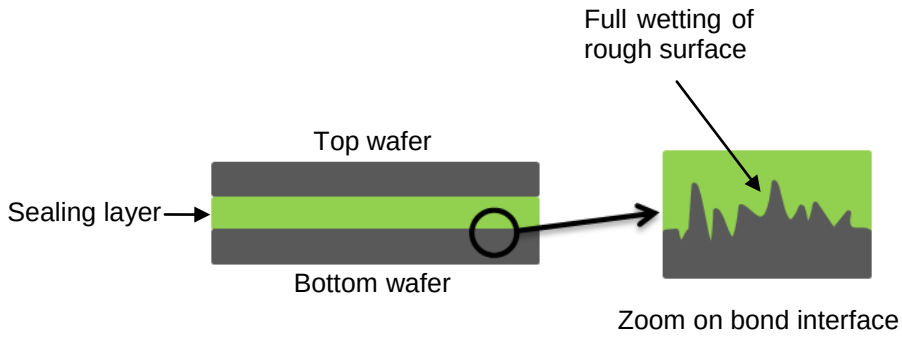

Figure 2.8: Schematic sketch of fully wetted bond interface with locally rough surface

Polymers can be grouped into four major material classes: thermoplastics, thermosetting polymers, elastomers, and hybrid polymers. Polymers of all these four classes can be used for adhesive bonding. A group, which is particular suitable for polymer bonding, are the thermosetting polymers due to their material properties. They feature a glass transition temperature of up to 300°C to 450°C, are mechanically strong and have a comparatively high chemical resistance. The bonding process is a heat-initiated polymerization process, which is also referred to as curing. During this chemical reaction the small side chains (monomers) of the polymer molecules cross-link to form a stable three-dimensional network. After cross-linking a solid polymer has formed, which cannot be re-melted or re-shaped; a full cure is pre-condition for a strong bond. As mentioned above, a liquid phase of the polymer is required at some stage of the bonding process to ensure sufficient wetting of the bond interfaces. This is achieved when the polymer is heated for the first time to initiate the cross-linking process [3, 77].

Adhesive bonding of thermosetting polymers typically comprises the following process steps: (i) cleaning of the substrates to be bonded, (ii) deposition and structuring of the intermediate layer and (iii) the actual bonding (curing) process. Prior to the deposition of the polymer the wafers are cleaned to remove any dirt particles and dried at elevated temperature to evaporate any moisture. Then an adhesion promoter (primer) – specifically composed for the adhesive polymer in use – is applied to the wafer surface to increase the adhesion between the polymer and the wafer surface. After drying of the primer, the adhesive polymer is deposited. Typically the polymer is dissolved in a solution and spin-coating is used to achieve a uniform thickness over the entire wafer

area. A pre-bake or pre-cure step must be carried out afterwards to completely evaporate any solvent out of the polymer layer. This step is of great importance as otherwise residual solvent trapped in the bonding layer will result in void formation due to out-gassing upon heating. If full wafer bonding is required the wafers can be used for bonding directly after this process step otherwise the polymer layer is patterned using lithography. After UV-exposure using a mask with the desired pattern the structures are transferred to the polymer typically using a wet develop process or deep reactive ion etching (DRIE) depending on the type of polymer. The patterning of the adhesive layer is often followed by a post-bake step to partially cross-link (solidify) the polymer already. The polymer has to be sufficiently solid so that the patterned structures can withstand the bonding process without losing their shape completely but still soft enough to conform well to the bond interface. For the actual bonding process the substrates are aligned on top of each other and a force is applied to ensure intimate contact between the bond interfaces. The polymer is heated to a typical temperature of 200°C to 300°C until it is fully cured; with the curing time dependent on the bonding temperature. Preferably bonding is accomplished in a vacuum to prevent void formation at the bond interfaces. The most important process parameters are bonding temperature, the curing time, and the force which is applied to the wafer stack. In Figure 2.9 a schematic view of the process flow is shown [3, 63, 65, 77].

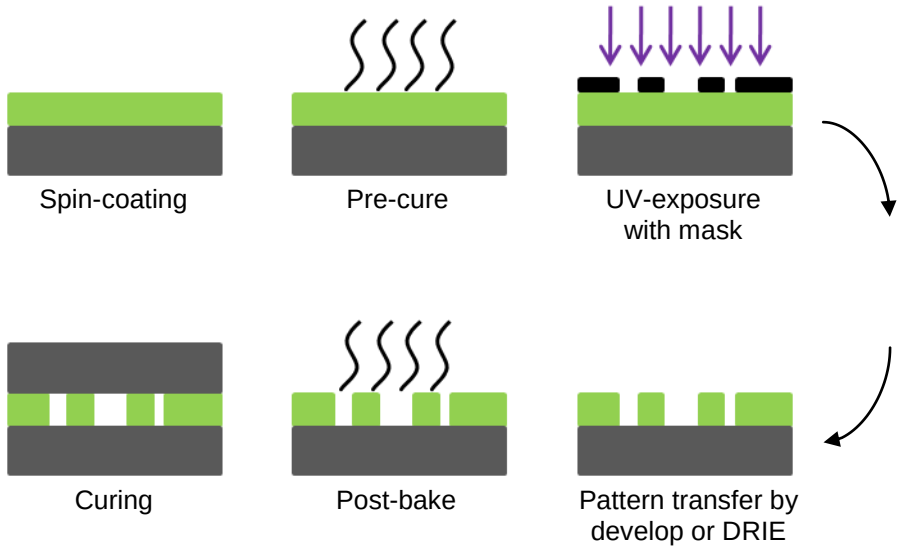

Figure 2.9: Schematic sketch of process flow for bonding using a patterned adhesive layer

Two adhesive polymers, which have seen a particular great interest by research institutes and industry for bonding applications in microsystems technologies, are SU-8 [60, 62, 68, 69, 77] and BCB [55-58, 65-67, 70-73, 76]. Both polymers have been

applied successfully for bonding in various applications and can be seen as most promising materials for adhesive bonding. SU-8 is a negative tone photoresist which benefits from particular low curing temperatures ranging from 100°C to 200°C. Due to the low bonding temperature the stress induced by the bonding process is considerably reduced resulting in high yield processes (>95%). Polymer layers of thickness from a few microns up to several hundred microns can be deposited in a single spin-coating step [60, 62, 75]. Aspect ratios as high as 17:1 can be achieved [62]; hence, the intermediate layer can also be used as spacer for cavity-style packages. Polymer bonding using SU-8 further benefits from high mechanical strength, high chemical resistivity and good adhesion to silicon. Due to its low demand on the surface quality of the bond interfaces it is suitable for low cost and high volume production [60, 62, 75].

Successful bonding of silicon to silicon with a high bond strength of 20.6 MPa at a temperature of 90°C using SU-8 as adhesive layer was demonstrated in [68, 69]. For silicon to glass bonding, typically required for MEMS applications, maximum bond strengths up to 20.9 MPa could be achieved in a process where the temperature was kept below 105°C. The main disadvantage of SU-8 is the high coefficient of thermal expansion (CTE) of SU-8 (50×10^{-6} K^{-1}) in comparison to the CTE of other materials commonly used in microsystems technologies (e.g. silicon 2.5×10^{-6} K^{-1}); posing a risk of high tensile stress and possible damage of the packaged device after bonding [75].

A further very promising polymer, which is particular suitable for adhesive bonding, is BCB [55-58, 65-67, 70-73, 76]. The heat initiated curing process of BCB (typical temperatures 200°C to 250°C) does not require any catalyst resulting in minimal out-gassing; provided the solvent has been evaporated completely during wafer preparation (see above) [67]. Furthermore, BCB benefits from low moisture uptake, high mechanical strength, high chemical resistance, bio-compatibility and low residual stress level. Its excellent electrical properties – high resistivity (10^{19} Ω cm), low permittivity (ε_r = 2.65) and low loss tangent in the range of 1 MHz to 10 GHz – make BCB a very suitable material for the encapsulation of RF-devices. The liquid-like behaviour of the polymer during curing enables bonding of non-planar surfaces and it is less sensitive to particulate contamination than direct bonding techniques. Steps created by electrical feed-through lines are sealed off during bonding. Due to the low process temperature virtually any metal can be used for electrical interconnects [56-58, 64, 65, 67, 70, 76].

Jourdain et al [56-58, 76] have intensely investigated BCB as bonding layer for silicon to glass joining for the encapsulation of RF-MEMS. After curing of the polymer at 250°C, shear strengths in excess of 37 MPa were obtained which is even higher than in anodic bonding (typically 15-25 MPa). Even after 1000 temperatures cycles (-25°C, +125°C) this high mechanical stability remained, underlining the robust properties of BCB as sealing layer. In [71-73] it was demonstrated that BCB can not only be used as intermediate layer for the encapsulation of RF-devices but also as capping material directly. A new packaging process was developed to use a thin BCB film membrane for the encapsulation process. Due to the electrical properties of BCB the performance of the packaged RF-devices was significantly improved compared to packages with a glass lid. One of the disadvantages when using BCB as bonding material, like all polymers, is the lack of full hermetic seals. Leak rates between 1.4×10^{-7} and 4.8×10^{-7} mbar l s^{-1} could be achieved, which is 3 to 10 times higher than the rejection limit of MIL-STD-883G. The hermeticity could be increased significantly by deposition of an additional diffusion barrier of silicon nitride around the polymer seal; however, despite this improvement only 'near-hermetic' packaging was achieved [65, 67]. Near-hermetic or quasi-hermetic packaging, newly introduced terms for adhesive bonding since full hermetic packaging cannot be achieved [74], often suffices for the encapsulation for applications such as MEMS mirror arrays and RF-MEMS [66]. A further drawback of BCB, which is also common for all other adhesive polymers, is the limited thermal stability. At temperatures above 300°C the mechanical stability of the seal decreases rapidly due to decomposition of the polymer [55].

Polymer bonding is a simple and robust process. It does not require extremely smooth bond interfaces. To a certain degree it is insensitive to particle contamination, and substrates can be joined in a standard laboratory without any special pre-treatment of the bond interfaces [77]. Bond strengths similar to those in eutectic and anodic bonding can be achieved without the necessity for elaborate wafer pre-treatment. However, the limited long-term stability of the seal in harsh environments and the lack of full hermetic seals are major drawbacks of this technology. Even though bonding is accomplished at considerably lower temperatures compared to other intermediate layer bonding processes, the requirement of heating the entire device to 250°C to achieve mechanically strong bonds inhibits the use of this technique with temperature sensitive devices, e.g. functional polymers used in OLEDs (max. temperature <100°C) [54].

Table 2.1: Summary of non-local heating packaging methods

Packaging Technique	Advantages:	Disadvantages:
Silicon fusion bonding	Hermetic seals High bond strength	High temp. (up to 1100°C) Surface flatness in nm-regime required Bonding in clean room (Class 10)
Anodic bonding	Hermetic seals High bond strength	Strong electric fields (400-1200 V) Relatively high temp. (400-450°C) Clean, smooth bond interfaces required (roughness <1 µm)
Eutectic bonding	Hermetic seals High bond strength Relatively low temp. (160-360°C) Less stringent surface requirements	Eutectic alloys prone to oxidation => elaborate preparation steps required Sensitive to particulate contamination
Glass frit bonding	Hermetic seals High bond strength Simple and robust process Virtually no limits for bonding materials	Relatively high temp. (300-450°C)
Adhesive layer bonding	Simple and robust process Virtually no limit for bonding materials Low temp. (<100°C possible)	Non-hermetic seals Low re-melting temperature Limited chemical and mechanical resistivity

2.4 Localised Bonding Techniques

The most common direct and intermediate layer bonding techniques for packaging in microsystems technologies have been described in section 2.2 and section 2.3. The main advantages and disadvantages of each technique have been summarised in Table 2.1. When choosing one of these technologies for a particular packaging application the choice depends on the materials to be bonded, the hermeticity requirements of the seal and the surface roughness of the bond interfaces. Often packaging of temperature sensitive materials is required. Therefore, the overall process temperature is a major selection criteria for the bonding process to avoid degradation of the performance or even complete destruction of the device to be packaged. The review of the standard bonding techniques, however, has shown that they mostly rely on global heating, typically in an oven or substrate bonder, where the entire package is heated to the bonding temperature. Often process temperatures of several hundred degrees are required for reliable and mechanical strong seal; thus limiting the use of temperature sensitive materials.

In recent years research has focused on more localised bonding techniques, namely microwave heating [64, 78, 79], induction heating [6, 80-83], resistive heating [11, 84, 85], seam sealing [86-90], and laser joining [10, 31, 54, 91-106], where the heat input is restricted to the joining area only. These techniques are used either to join two materials directly or combined with one of the previously described intermediate layer bonding methods. The main advantage of bonding using localised heating is the greatly reduced heat input into the bulk of the package which enables the use of temperature sensitive materials within the centre. Most chemical bonding reactions require a certain thermal energy to be initiated and to create a reliable bond. Generally the same bond quality can be achieved faster at a higher bonding temperature than at lower process temperatures. Localised heating, therefore, also benefits from shorter process times, a desirable process parameter in device fabrication, as high temperatures can be applied in the joining region without providing additional thermal strain on the device to be packaged [11, 84, 85]. The key features of these localised bonding techniques, including their main advantages and limitations, are discussed in the following.

2.4.1 Microwave Heating

Microwave heating [64, 78, 79] is a selective heating technique which is based on energy dissipation of dielectric materials at a high frequency. The microwave radiation is coupled to the dielectric materials through dipole orientation by the electric field thereby resulting in an increase of the temperature [64, 79]. To ensure sufficient coupling of the microwave radiation to the dielectric materials, a high imaginary dielectric constant ε'', which is often found in metals and some polymers, is required. Materials with a low ε'' are almost transparent to the radiation [78].

Parylene, an adhesive polymer, has proven to be such a suitable material. In [64, 79] successful bonding of silicon to silicon for full wafer bonding and patterned wafers with parylene as intermediate layer has been demonstrated. High bond strengths of up to 12.68 MPa could be achieved. Curing under microwave radiation is 10-20 times faster at similar process temperatures than simple heat-induced polymerisation as microwaves can accelerate chemical reactions [64]. Full hermetic packaging of silicon to silicon with gold as sealing layer was shown in [78]. The required heat energy for the bonding process was deposited into the metal layer and conducted to the bond interfaces. In both cases the substrate materials were not heated up significantly during the bonding process. Such a process is particularly useful when joining dissimilar materials with a

great mismatch in coefficient of thermal expansion (CTE) or temperature sensitive devices. A potential drawback of this technology is the limited selectivity of this heating technique. All materials with a high imaginary dielectric constant within the package will heat up to a certain degree during the bonding process.

2.4.2 Induction Heating

In recent years induction heating has generated considerable research interest [6, 80-83] as selective heating method for packaging applications in microsystems technologies. Induction heating is based on the principle of electromagnetic induction which can be used to heat electrically conductive materials. In Figure 2.10 a schematic sketch of a much simplified induction heating system is shown.

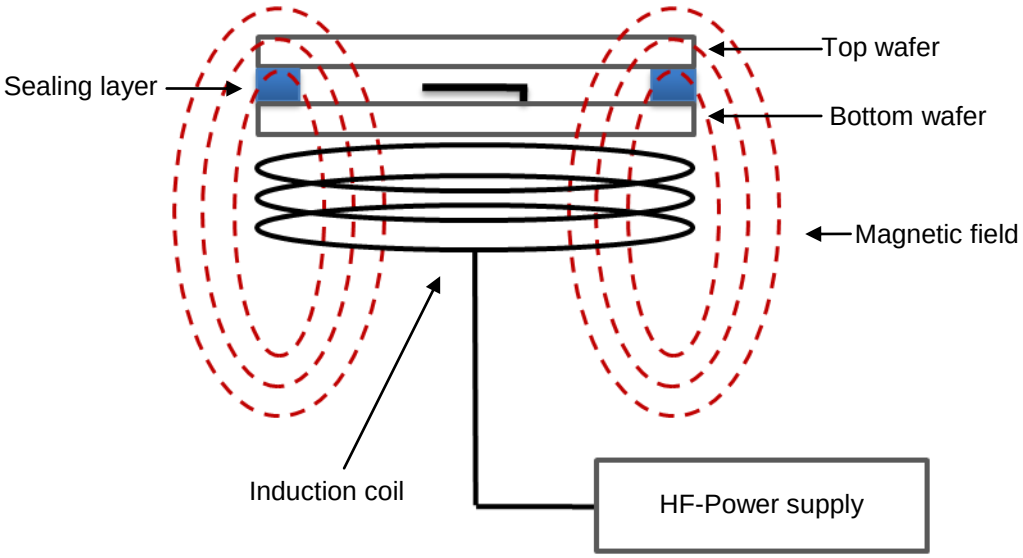

Figure 2.10: Schematic sketch of induction heating system consisting of sample which is positioned in the magnetic field generated by the coil

An induction heating system typically consists of three key elements: a high frequency power supply, an induction coil and the sample to be bonded. Using the power supply an alternating current is applied to the induction coil to generate an alternating magnetic field. The sample is positioned inside the magnetic field such that an electrical current is generated within and heat is generated due to resistive heating. The energy dissipation in induction heating is based on hysteresis loss and resistive loss. Resistive loss is the dominant heating mechanism as hysteresis loss is only present in magnetic materials. Induction heating can be used for localised, selective bonding as only electrically conductive materials get heated directly; non-conductive materials, like plastics and semiconductors, remain unaffected. If bonding of non-conductive materials

is required a thin conductive material layer can be applied in the desired joining region which acts as heater and transfers the heat energy to the bond interfaces by conduction [6, 80, 83].

Successful bonding of silicon to silicon with a lead-tin solder using induction heating was demonstrated in [82, 83]. To increase the energy absorption a thin magnetic film, a nickel-cobalt alloy, was deposited between the silicon interface and the solder layer to act as localised heating element (see Figure 2.11). Successful bonding was achieved in less than 1 minute with bond strengths in excess of 18 MPa. Thermal monitoring showed that the temperature in the device region could be kept at 110°C despite a temperature of 200°C in the joining area. Hu et al [81] applied the same principle to silicon to glass and glass to glass solder bonding. However, nickel was used for the heating element and the solder was replaced with pure tin to comply with RoHS and lead-free regulations. Due to the high mismatch of CTE of the heater and silicon, an additional buffer layer was deposited below the heater (nickel film) to reduce the stress upon cooling. For silicon to glass joining a bond strength of 3 MPa was reported.

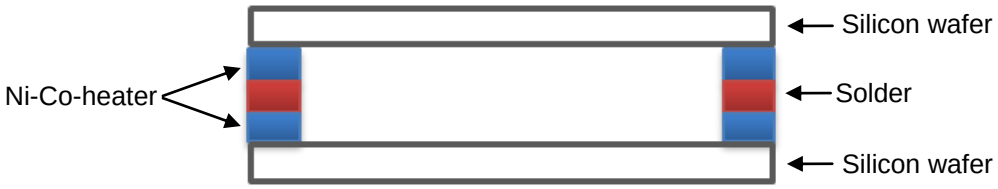

Figure 2.11: Schematic sketch of wafer stack for induction heating with solder layer and Ni-Co layer as localised heating element

Apart from silicon to silicon and silicon to glass joining induction heating can also be applied to hermetic packaging of standard ceramic packages used in the electronics industry. Typically they consist of a ceramic cavity-style substrate with metallised layers deposited at the bond interface and are solder-bonded to a Kovar^{TM} cap (compare Figure 2.13). In [80] such a package was used for hermetic encapsulation of a temperature sensitive gyroscope. Heating of the entire package to 300°C to reflow the gold-tin solder would have destroyed the device. However, by induction heating only the metal parts (the cap, solder and metallised layers on top of ceramic) are heated directly. Simulation of the bonding process suggested that lateral heat flow to the centre of the package (sensitive device area) was limited to 180°C. One of the drawbacks of induction heating is that, to ensure effective heating, the coil needs to be designed according to the layout of the bonding layer [80]. Therefore, this approach is only of

limited usability in generic packaging processes. Furthermore, induction heating is not a truly localised and selective heating technique as all electrically conductive materials within the package get heated up to a certain amount.

2.4.3 Resistive Heating

Truly localised heating for applications in MEMS packaging using thin film micro-heaters for resistive heating was studied in detail by Lin et al [11, 84, 85]. The required bonding energy is provided in a highly localised manner by micro-heaters which are deposited in the joining area only. To further confine the heat input, the micro-heaters are surrounded by insulation materials. In [11, 84, 85] successful application of this heating method to various bonding methods, including silicon-glass fusion, eutectic, solder bonding and vacuum packaging, was demonstrated. Traditionally these packaging methods rely on global heating in a furnace. The proposed bonding technique heats the joining area only. High bonding temperatures, which are generally favourable for high quality bonds and shorter process times, can be applied without the risk of excessive thermal strain on the devices to be packaged.

In [85] silicon to glass fusion bonding and silicon to gold eutectic bonding was demonstrated. In both cases silicon was used as substrate material and bonded to either glass or silicon. A silicon dioxide layer of thickness 1 µm was grown on the silicon substrate for electrical and thermal insulation. A patterned film of polysilicon (width 5 µm, thickness 1.1 µm) was deposited on the substrate which acts as the heater and also serves as bonding material for fusion bonding. A patterned film of gold (width 5 µm, thickness 0.5 µm) was used for eutectic bonding. An electrical current is applied to the micro-heaters (patterned gold or polysilicon layer) upon which the temperature increases to activate the bonding process and the surfaces are joined by applying a force. A schematic sketch of the bonding assembly is shown in Figure 2.12.

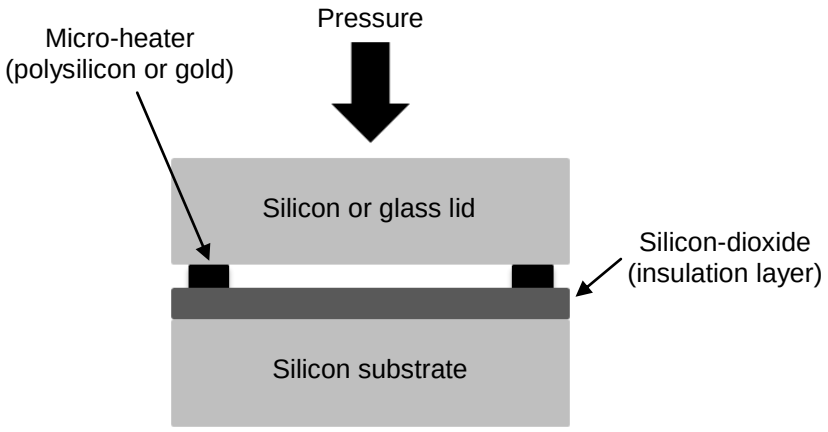

Figure 2.12: Schematic sketch of bonding principle for localised heating using micro-heaters

Successful silicon to glass fusion bonding was achieved in as little as 5 minutes with the micro-heaters being heated to a temperature of around 1300°C. In comparison, conventional fusion bonding in an oven at 1000°C typically requires a 2 hour process. At a temperature of 800°C eutectic bonding was also accomplished in a 5 minute process opposed to traditional bonding typically at 410°C for one hour (including cool down). After joining, the seals were mechanically broken apart again to investigate the quality of the bond. In both cases fracture of the silicon was observed at the bond interface suggesting bond strengths of at least 10 MPa, the fracture strength of bulk silicon. Temperature monitoring experiments with a thermocouple positioned 15 µm away from the micro-heater indicated that the temperature increased by less than 40°C at this location when the polysilicon heater was heated to its melting point (~1415°C). The high temperatures are well restricted to the area of the micro-heater; underlining the potential of truly localised heating using this approach [85].

The same research group also applied this localised heating approach successfully to solder bonding, CVD bonding and silicon to glass bonding with an aluminium sealing layer [11, 84]. In each case uniform and mechanical strong bonds were achieved. In comparison to conventional bonding methods using global heating localised micro-heaters have two main benefits: often a considerable reduction of the bonding time was observed due to locally higher temperatures and quicker temperature ramp rates, and the thermal strain on the devices to be packaged is reduced to a minimum. For bonding of single samples this method is well adapted; however, if scaled up to a wafer-level the high currents required for heating might become an issue. Heat sinking would be required to maintain low temperatures in the device area. The main drawback of this technology is the need for fabrication of the micro-heaters and their interconnections

[66]. As they are integrated in the sealing layer directly, they must be deposited on every individual wafer to be bonded; thereby adding several pre-bonding steps to the process flow and making it more complex.

2.4.4 Seam Sealing

Seam sealing [86, 88, 89] is a packaging technology typically used for hermetic sealing of chip carrier packages, commonly referred to as flat-packs, which originates from the electronic industries and still has widespread use today. A recent study [90], however, has shown that it is also of potential interest for wafer-level MEMS packaging in silicon to gold eutectic bonding. Seam sealing, like resistive heating using micro-heaters, also relies on resistive heating to generate the required bonding temperature locally in the joining area; however, the heat is applied to the outside of the package and not from within the sealing layer. Fully automated seam sealing machines for electronic packaging are commercially available [88, 89]. A schematic cross sectional view of such a typical seam sealing bonding process is shown in Figure 2.13.

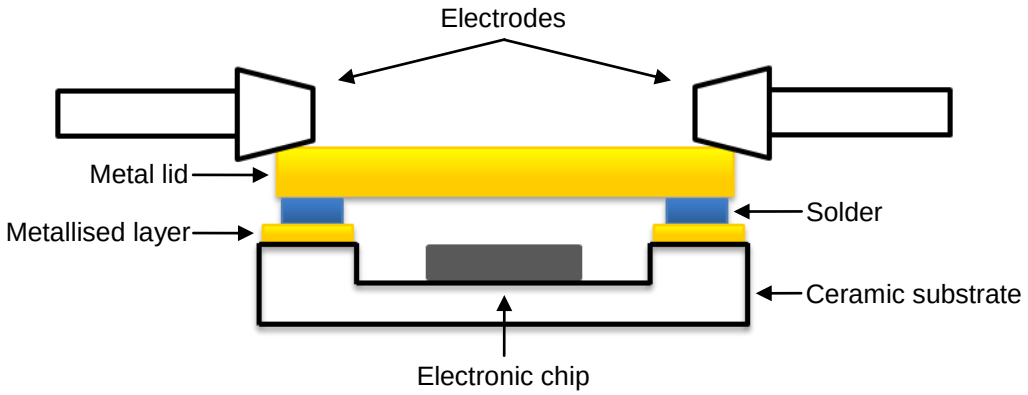

Figure 2.13: Schematic cross sectional view of seam sealing process

In most cases, chip carrier packages have a cavity-style substrate with a base which is surrounded by upstanding side walls to create a housing for the electronics to be encapsulated. Ceramic is typically used as substrate material. A thin metallised layer is deposited on top of the ceramic as a bond interface. By melting a solder ring or by welding directly, a metal lid can be hermetically sealed to the ceramic substrate. The heat required for the bonding process is applied by the electrodes which are rolled along the lid. A current, which is applied to the electrodes, results in resistive heating and a local temperature increase where the electrodes are in direct contact with the lid. Depending on the applied current temperatures in excess of 1000°C can be achieved

locally; enabling either soldering or direct welding processes. Due to the relatively low thermal conductivity of ceramic the lateral heat flow into the substrate is restricted and enables packaging of sensitive electronics [86, 88-90].

Reliable and hermetic seals, typical requirements in electronic packaging, can be achieved with seam sealing in high yield processes. Traditionally seam sealing was limited to ceramic substrates with low thermal conductivity. However, research was aimed at applying this technology to substrate materials with higher thermal conductivity, e.g. aluminium nitride [86] and silicon [90], to open up further application fields. Simulations in [90] suggest that seam sealing can be applied to silicon to gold eutectic bonding in a localised heating process where the temperature in the device centre remains at room temperature despite temperature of up to 1000°C in the joining area. The main disadvantage of seam sealing is the inflexibility of the process. Due to the electrodes only rectangular or circular packages can be joined, arbitrary shapes are not possible [87]. Precise alignment of the electrodes along the bond path is required for uniform heating which otherwise does result in non-hermetic seals and thermal damage of the package [89]. Furthermore, seam sealing will reach its limits with increasing miniaturization in packaging technologies. If the two electrodes come into close proximity, arching occurs between the electrodes and reliable bonding can no longer be achieved [87].

2.4.5 Laser Joining

Laser joining, as a localised heating technique, for packaging in microsystems technologies has generated significant research interest [10, 31, 54, 91-106] in recent years. In contrast to other techniques, laser joining benefits from several advantages [91, 95, 101, 102, 104]:

- It is a non-contact method (remote processing); hence, there is no wear and tear or contamination of the substrates to be bonded.
- Due to the quick and easy control of the laser beam processing time, temperature and the volume heated can be controlled very precisely, and even complex designs can be processed.
- Most importantly, when using a laser as the heat source, the heat input into the device can be highly localised since the laser beam can be focussed to a small spot.

In comparison to conventional, global heating techniques, the mechanical and thermal stress on the components to be packaged are considerably reduced. The wide wavelength range of available lasers from the infrared (CO_2 lasers, Nd:YAG etc) to the ultraviolet (Excimer lasers and harmonics of Nd:YAG) offers the possibility to choose the wavelength which suits the materials to be bonded best. Localised laser heating can be applied to both direct and intermediate layer bonding.

Wild et al [93-95, 105, 106] and Theppakuttai et al [104] have demonstrated silicon to glass joining using Nd:YAG lasers (1064 nm) in a direct bonding process. The process is based on the principle of laser transmission welding which requires one material to be highly transmissive but the other material must be strongly absorbing at the wavelength of the laser beam. In this case, Pyrex, a highly transparent glass (>90% at 1 mm thickness), was used. The laser at a wavelength of 1064 nm passes through the glass and is absorbed by the silicon substrate. As a result, the silicon locally heats up, melts and is bonded to the glass. A small force ensures that the materials stay in contact during the process. A schematic sketch of the direct laser joining process is shown in Figure 2.14.

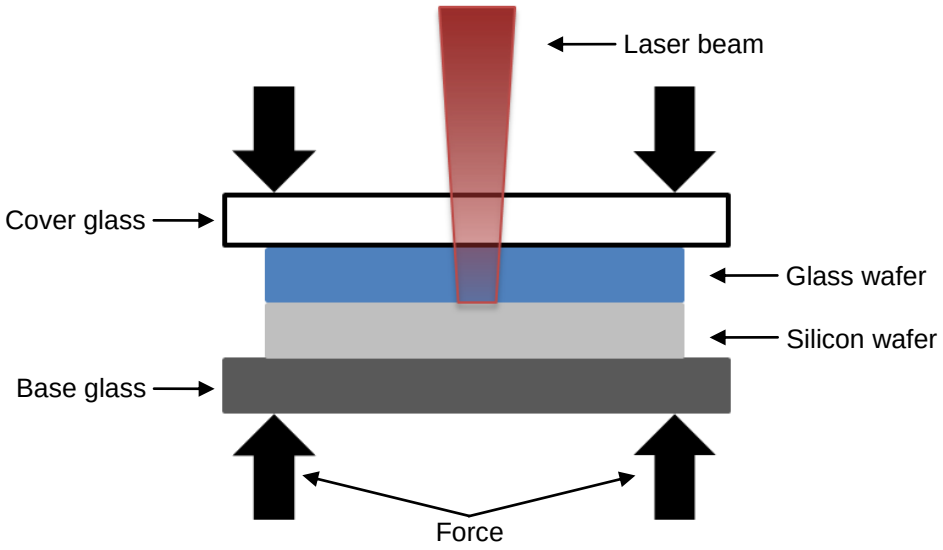

Figure 2.14: Schematic sketch of direct laser joining process for silicon to glass bonding

Using this bonding technique silicon to glass joining of single spots using single shots from a ns-pulsed laser was demonstrated in [104]. The silicon and glass were locally fused together in a process whilst the surrounding wafer material remained at room temperature. Successful bonding of consecutive lines and features was demonstrated in [93-95, 105, 106] using a continuous wave (cw) Nd:YAG laser. Hermetic seals with a

bond strength ranging from 5 MPa to 10 MPa were achieved. Typically laser powers of 12 W to 30 W and bonding speeds of 50 mm min^{-1} and 500 mm min^{-1} were used [105]. Temperature measurements with micro-thermocouples positioned 0.3 mm from the centre of the beam path showed that the temperature remained below 300°C. Closer investigation of the bonding process revealed that a precise control of the bonding parameters is required to avoid crack propagation in the glass layer due to the high thermal gradient within the material [106]. After integration of a pyrometer into the laser head for online process control of the laser power (bonding temperature) even complex micro-fluidic structures, as shown in Figure 2.15, could be joined without cracking of the glass [95].

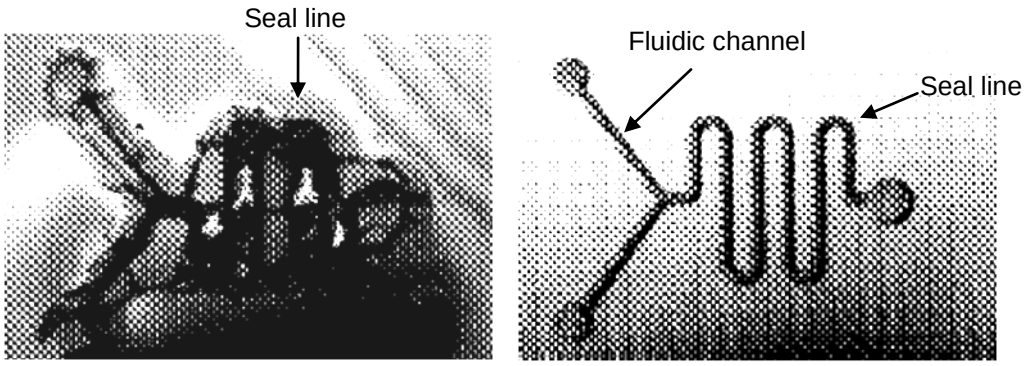

Figure 2.15: Photograph of micro-fluidic mixer with a channel width of 100 µm; structure was sealed along contour of channels. Left: constant laser power; right: pyrometric online control of laser power [95]

In [31, 97, 98, 101] laser-based eutectic bonding of silicon to glass was investigated. This process is also based on the principle of laser transmission welding as described in the previous paragraph. However, in this case the laser beam is absorbed by the eutectic solder directly instead of the silicon substrate. In [97] silicon to glass bonding with an indium intermediate layer was demonstrated using a ns-pulsed Nd:YAG laser at a wavelength of 355 nm. Thermal simulations suggest that upon laser illumination the temperature increases locally to 2500°C and rapidly decreases again to 43°C within 1 millisecond. Destructive testing was carried out to determine the bond strength which was found to be 2.6 MPa, the yield strength of indium, with the failure occurring within the indium layer. To restrict the laser irradiation zone and thereby pre-define the bonding area a mask was used as shown in Figure 2.16. Such a technique is not preferred as it limits the great flexibility which is possible in laser-based processes.

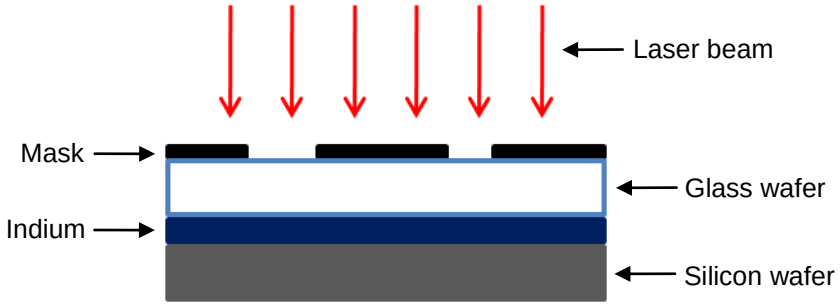

Figure 2.16: Schematic sketch of experimental setup for silicon to glass bonding with an indium intermediate layer and laser illumination through a mask

Tan et al [31, 101] also used a ns-pulsed Nd:YAG laser at a wavelength of 355 nm to achieve silicon to glass bonding with a gold-tin eutectic alloy. High quality laser bond tracks without defects and bond strengths in excess of 15 MPa were achieved, which is comparable to other localised joining techniques. In [98] superior bonding strengths above 40 MPa were reported for laser-based silicon to glass eutectic bonding with either aluminium or gold as intermediate layer. Examination of the line of breakage suggested that the bonding mechanism is a superposition of eutectic and fusion bonding. The thermal energy for the bonding process was provided by a Nd:YAG laser with a wavelength of 1064 nm which was used in pulsed and cw-mode. Bonding experiments have shown that precise control of the bonding parameters (laser power and speed) is required to avoid thermal damage of the intermediate layer. Damage occurs especially in corners of the bond track or when the laser is run in pulsed mode (see Figure 2.17).

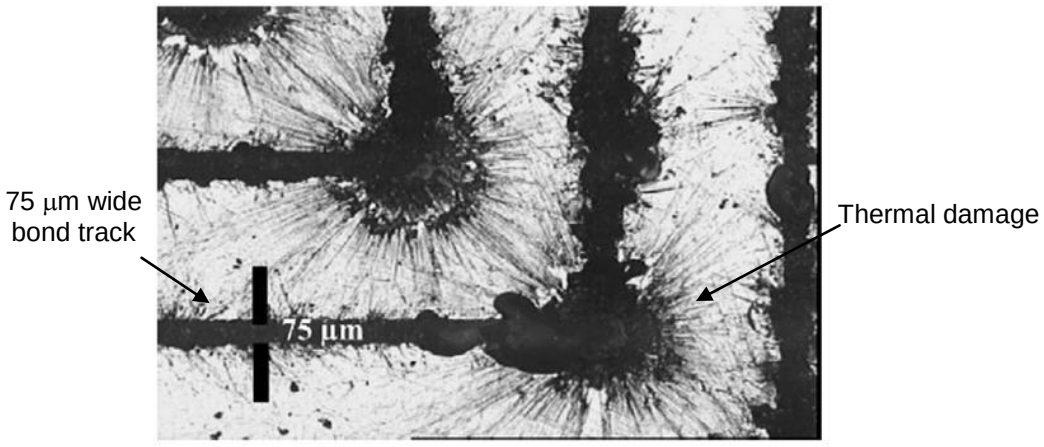

Figure 2.17: Photograph of laser track in the intermediate layer for laser-based eutectic bonding. The spots in the corner of the track indicate thermal damage due to overheating [98]

The laser-based direct and eutectic silicon to glass bonding techniques presented above show the feasibility of using laser heating in such bonding processes. However, in general they are still under development and not yet at a stage where they could be

applied to packaging in actual device manufacture. Nevertheless, current results clearly point out the benefits and potential of localised laser heating – i.e. confinement of heat to joining region. Similar to conventional direct and eutectic bonding using bulk heating, these techniques also require clean, high quality surfaces for successful bonding although the locally higher temperatures which can be achieved by localised laser heating allows for lower surface roughness requirements (1-2 µm) [101].

In [10, 99, 100, 102, 103] localised heating packaging technologies are described which can be more readily applied to actual device manufacture. In these experiments a CO_2-laser was used as heat source. Off-the-shelf ceramic quad flatpacks (CQFP) are generally used for the encapsulation of RF-MEMS where a solder preform (Au-Sn) is reflowed in an oven to join the substrate to a Kovar™ lid. The global heating process, however, results in degradation of the performance of the RF-MEMS [103]. A localised heating packaging technique was developed where a metallised silicon lid, instead of the Kovar™ lid, was bonded to the CQFP using a gold-tin solder. The package was sealed by translating a CO_2-laser beam along the edges of the lid (see Figure 2.18). Hermetic seals with bond strength in excess of 3 MPa were achieved. The pull tests resulted in failure (breakage) of the silicon lid and not the seal [103].

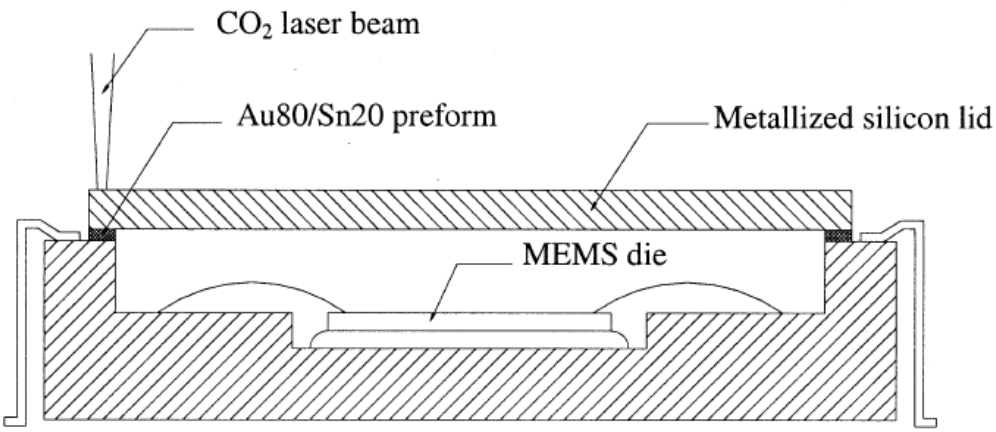

Figure 2.18: Sketch of laser-assisted silicon lid encapsulation of MEMS devices in CQFP [103]

The same research group describes in [10, 100] bonding of a ceramic lid with an epoxy seal to the same CQFP. As described above, a CO_2-laser was used to locally heat and join the package. Successful sealing of the packages with bond strengths around 2.5 MPa were achieved. Thermal modelling of the bonding process suggested that the high temperatures are confined to the joining region and only marginally affect the

centre of the package, underlining the localised heating nature of this laser-based process. In a different study [99, 102] the same research group has shown successful wafer-level packaging of silicon to silicon with a lead-tin solder in a vacuum. Again, a CO_2-laser was used to provide the bonding energy locally. Throughout the bonding process the temperature at the centre of the device remained around 100°C despite a bonding temperature above 183°C. Hermetic seals with bond strengths of up to around 8 MPa were accomplished. The yield of the process was 87.5%; of 24 packages on the same wafer 21 were successfully sealed. To ensure sufficient adhesion and to hinder oxidation several thin metal layers have to be deposited on the silicon interfaces (see Figure 2.19) requiring elaborate preparation steps of the bond interfaces.

Figure 2.19: Schematic sketch of silicon wafer with thin metal layers required for successful solder bonding using CO_2-laser heating

A promising concept for laser-based joining of glass to glass with a glass frit intermediate layer is shown in [54, 92]; however, the published material does not provide a great deal of detail about this work. In [92] a diode laser and in [54] a fibre-laser beam is scanned at high speed along the track of the bonding layer to heat it quasi-simultaneously. The laser power is absorbed by the glass frit directly and reflows evenly. Due to the low thermal conductivity of glass (typically 1 W m^{-1} K^{-1}) and the relatively short processing times (few tens of seconds) the heat is restricted mostly to the bonding area only. Despite a bonding temperature of around 450°C the temperature in the centre remains below 100°C for a package of dimension 20 mm by 20 mm. This process, however, is prone to cracking in the glass due to the high thermal gradient and therefore high stress levels within the glass.

2.4.6 Summary of Localised Bonding Techniques

A comparison of the localised heating techniques (see Table 2.2) has shown that only by resistive or laser heating, truly localised and selective heating can be achieved. Resistive heating requires deposition of the heating elements on each device to be bonded resulting in more elaborate and complex process steps. Furthermore, the high currents required for wafer-level packaging probably will tend to heat accumulation in

the substrate wafer. Seam sealing, an alternative resistive heating process, places restrictions on the package shape and dimensions. Localised direct bonding and eutectic bonding, similar to their conventional counter-parts based on global heating, require smooth, clean surfaces, elaborate pre-bonding preparation steps, and hence are less favourable. In this thesis, the combination of the advantages of intermediate layer bonding and localised laser heating is investigated in detail.

Table 2.2: Summary of localised heating techniques

Heating Technique	**Advantages:**	**Disadvantages:**
Microwave heating	Localised heating of joining area Accelerates bonding (polymerisation) process (chemical reaction 10-20× faster) Reduced heat input into bulk of package	Only partly localised/selective heating => all dielectrics within package heat up to a certain degree
Induction heating	Localised heating of the joining area Reduced heat input into bulk of package	Only partly localised/selective heating => all electrically conductive materials heat up to a certain degree Coil needs to be in shape of bonding layer => limited usability for generic process Single chip packaging
Resistive heating	Truly localised heating => only in area of micro-heater Packaging of temp. sensitive devices Reduction of time for single bonding cycle	Elaborate pre-bonding steps => fabrication of micro-heaters Single chip packaging On a wafer-level wiring and high currents for heating might pose problems
Seam sealing	Truly localised heating Reduced heat input into bulk of package	Restricted to rectangular and circular packages Comes to its limits (arching) with increasing miniaturization Single chip packaging
Laser heating	Remote and non-contact method Highly localised/selective heat input due to small focus of laser beam Easy and quick control of laser beam => precise control of processing time, temperature and heated volume Processing of complex designs Multiple device joining possible	High costs of the laser system

2.5 Previous Work at Heriot-Watt University

Prior to the start of this PhD, research into laser-based silicon to glass joining with a BCB adhesive layer and glass frit packaging was carried out within in the research group at Heriot-Watt University which I joined at the start of my PhD. These research activities were predominantly driven by the requirements and interest of several industrial collaborators. QinetiQ was interested in the silicon to glass joining process, a typical MEMS application. The research on glass frit packaging was a joint TSB project with QinetiQ and GE Aviation, which was mostly driven by GE Aviation. For both projects the key interest was to apply laser heating to packaging to confine the heat input and to enable packaging of temperature sensitive materials. The initial results of these studies are summarised below, including a brief introduction of the intermediate bonding layers under investigation in this PhD.

2.5.1 Laser Bonding of Silicon to Glass with BCB Adhesive Layer

In [107] a feasibility study on using laser-based heating for silicon to glass joining with a BCB adhesive layer is presented. BCB is a UV-sensitive negative tone photo-resist which was chosen for its high bonding strength, bio-compatibility, low out-gassing, low moisture uptake and high chemical resistivity, as mentioned in section 2.3.3. Several types of BCB resins, which differ in viscosity, are commercially available from Dow Chemical. The viscosity of the resin influences the structure height of the BCB bonding layer. In general, a thicker bonding layer allows for higher surface roughness of the bond interfaces and higher particle contamination. The BCB resin with the highest viscosity, Cyclotene 4026-46, was chosen to ensure a simple and robust process. With this type of resin final thicknesses of the BCB layer of 7 – 14 µm can be achieved which is sufficient to compensate surface inequalities and particle contamination of the bond interfaces.

BCB was chosen as bonding material not only for its excellent sealing properties but also for its fast processing (curing) times. The bonding process of BCB is a heat initiated curing process which results in cross-linking of the polymer and gives it its final properties (strength, resistivity…) once fully cured. The BCB curing process is a time and temperature dependant reaction (see Figure 2.20). The higher the temperature the shorter the curing time, provided that the maximum temperature is kept below 350°C where the polymer starts to degrade. A full cure of BCB can be achieved in as short as 1 second if bonded at a temperature of 350°C. In [108] it was demonstrated

that rapid thermal curing (RTC) of BCB in an IR belt furnace with a cycle time of 5 minutes (ambient to ambient) and a peak temperature of 315°C is possible. The high ramp rates for the temperature did not show any negative influence on the quality of the seal. In laser heating even higher temperature ramp rates are feasible and very fast process cycle times in the order of a few seconds are expected.

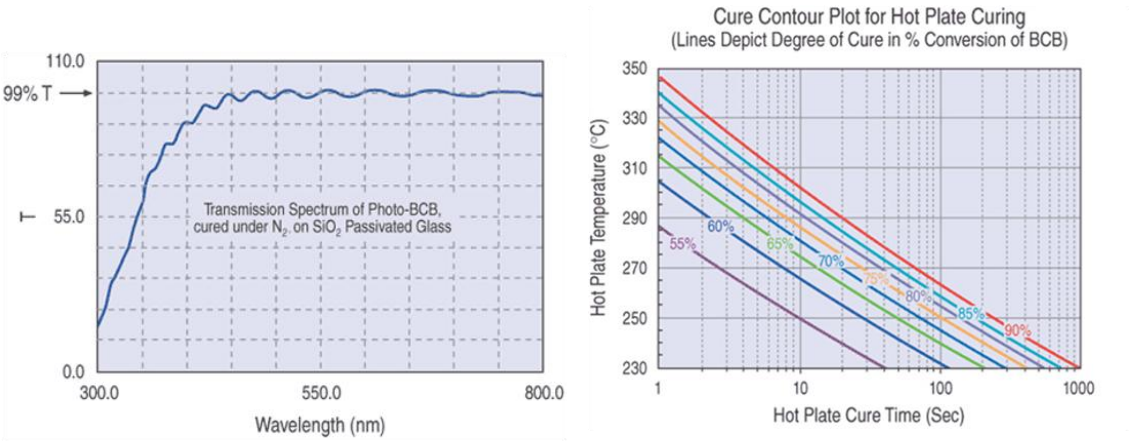

Figure 2.20: Transmission spectrum of BCB (left) [109] and cure contour plot for hot plate curing of BCB (right) [110]

The laser bonding process of silicon to glass with a BCB adhesive layer is based on the principle of laser transmission welding. For the experiments a continuous wave direct diode laser at a wavelength of 810 nm was used. The BCB polymer transmits 99% of the light in the visible and near-infrared (see Figure 2.20), it therefore cannot absorb the energy of the laser directly and the bonding process relies on absorption of the laser energy in one of the bond interfaces and subsequent thermal conduction of the heat energy into the bonding layer. Since the glass is highly transparent (>90%) at the wavelength of the laser, the laser energy is absorbed by the silicon substrate. A schematic sketch of the bonding setup is shown in Figure 2.21.

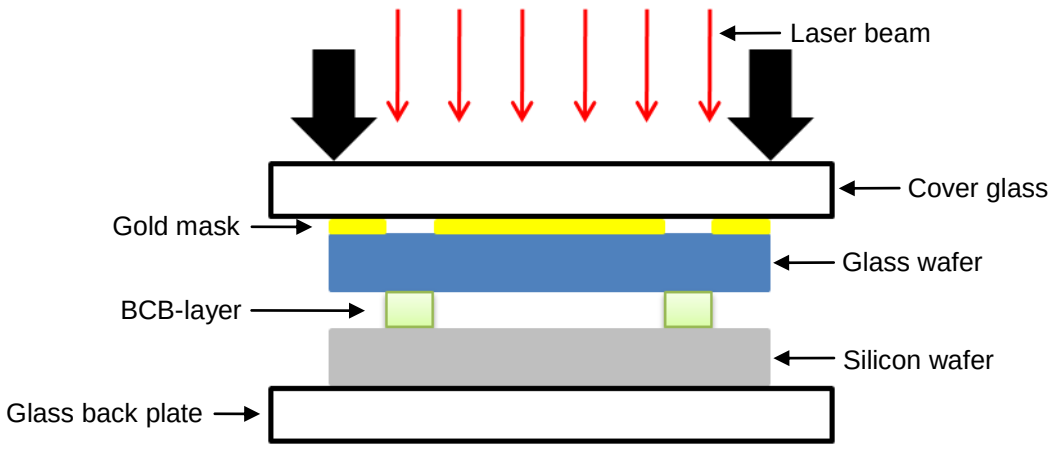

Figure 2.21: Schematic sketch of the laser joining setup for silicon to glass joining with BCB adhesive layer using a mirror mask

To protect the centre of substrate from direct exposure to the laser radiation a mirror mask was used so only the bonding area was illuminated directly and the location of a thermally sensitive device is shielded from the incident laser radiation. During bonding a slight pressure was applied to the sample to ensure intimate contact of the bond interfaces. Experiments showed that successful bonding in as little as 2 seconds could be achieved although the best results were obtained for exposure times of 15 s. Shear force testing of these samples showed that bond strengths up to 270 N were achieved which compares well to shear forces of around 200 N reported in [56] for samples bonded using conventional flip-chip bonding. These samples were of similar sealing area; however, a minimum bonding time of 10 minutes at 250°C was required. This study clearly showed the feasibility of laser-based silicon to glass bonding with a BCB intermediate layer and demonstrated the possibility of considerably reducing the process time without affecting the quality of the bond.

Even though only the bonding area was heated selectively with the centre of the device protected from direct irradiation by the mask, the potential benefits of truly localised heating were not fully achieved. The entire device still heated up due to lateral heat flow caused by the high thermal conductivity of silicon (150 $W\,m^{-1}\,K^{-1}$) as the bonding experiments were accomplished on a glass back plate. This aspect demonstrated that this technique is not perfectly suitable in order to avoid or minimise heating of a temperature sensitive MEMS device located in the centre of a package. Furthermore, it was a highly energy inefficient process as more than 80% of the laser power was reflected by the mask which was used to protect the centre of the package from direct exposure. The mask also limited the flexibility of this process as a new mask would have to be produced for every different shape of bonding layer. Based on these initial results the further development to a truly localised heating bonding process and wafer-level packaging were investigated in the work of this PhD.

In parallel to the work of this PhD, a second research group at Heriot-Watt University has also been investigating an alternative technique, to improve on the findings of the feasibility study. Their work is reported in [111-113]. Instead of using a mask to protect the centre of the package from direct exposure to the laser beam custom designed beam forming optical elements were used. The laser beam was shaped to

match the outline of the bonding layer. Only the joining area was illuminated selectively. Lateral heat flow still caused the entire device to heat up as bonding was achieved on a thermal barrier. This technique suffers from the same drawback as the mask technique described at the beginning of this section (2.5.1) in that it is a rather inflexible technique as the beam shaping optics must be optimised for every different shape of bonding layer.

2.5.2 Laser-based Glass Frit Packaging of Miniature Devices

The work presented in [114] is a feasibility study on using laser heating in glass frit packaging. GE Aviation and QinetiQ had a joint interest in laser-based hermetic packaging of a range of miniature packages and materials. They are hoping to exploit this technology for packaging of temperature sensitive devices. The research at the initial phase of this study was solely carried out by Qiang Wu, a research associate who worked in the group at the time, but the results presented in [114] were obtained in collaboration between Wu and the author, during the first year of this PhD. The main aim of the study was to show the ability of the laser to provide the required localised heating. A range of packages was sealed successfully as shown in Figure 2.22.

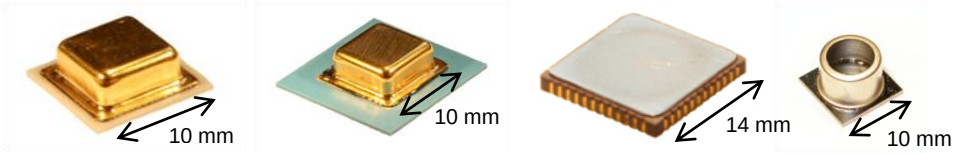

Figure 2.22: Photographs of laser-bonded samples. Left to right: aluminium-nitrate and LTCC substrate to top-hat cap, LCC package, and silicon to TO5-cap

To provide the required thermal energy for the bonding process a laser beam (940 nm) was scanned quasi-simultaneously at high speed along the track of the glass frit layer. The bonding process used in this work is very similar to the approach explained in detail in chapter 3 and differs only in minor aspects. The main difference is that for simplicity the samples to be joined were placed on top of a thermal barrier (glass slide) for these early investigations. As no measures were taken to prevent heating inside the devices due to lateral conduction, the whole sample was raised to a high temperature despite the localised heat input into the sample. Full hermetic sealing of all the samples, shown in Figure 2.22, was achieved in high yield processes using this laser-based heating technique; highlighting the benefits of glass frit as a sealant. Even laser-machining of micro-channels of depths up to 100 µm into the bond interfaces did not

affect the hermeticity of the seals. Glass frit has the ability to conform well to naturally rough surfaces and can also reflow entire micro-channels, as shown in Figure 2.23.

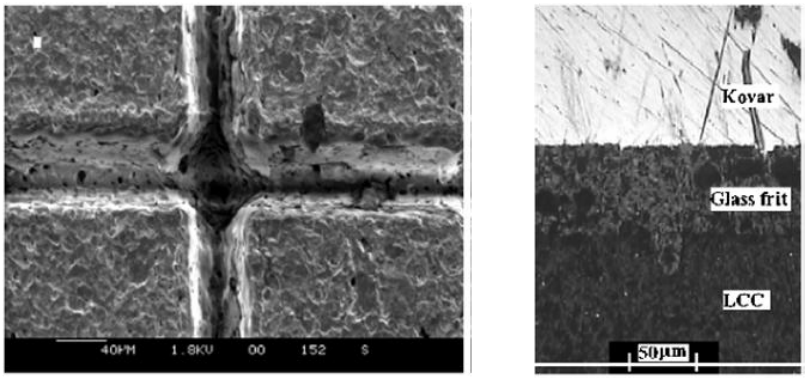

Figure 2.23: SEM image of LCC substrate with laser-machined channels (left) and micrographs of cross-section of bonded sample

A further development of this laser-based technique to a truly localised heating packaging process where active cooling is applied to restrict the lateral heat flow and vacuum packaging are described in this PhD thesis.

Diemat Glass Frit

The glass frit material, which was used for the feasibility study and will be continued to be used for bonding experiments in air described in this PhD thesis, is the glass frit paste DM2700P/H484 manufactured by DIEMAT [52]. It is designed to hermetically seal low thermal expansion materials such as silicon, alumina, Kovar^{TM}, and borosilicate glasses. According to the manufacturer strong adhesion can be achieved to most surfaces, including gold. It is particularly suitable for laser-based packaging processes for two main reasons: in comparison to other glass frit materials it has a particularly short bonding time and it can tolerate the high temperature ramp rates possible in laser processes. Reliable, hermetic seals are achieved in as little as 1 minute when the bond interfaces are sealed under slight pressure at a peak temperature of 375°C. The only drawback of this material is that it is not suitable for vacuum packaging. As previously mentioned in chapter 2.3.2, a thermal conditioning process must be carried out before glass frit can be used for bonding to ensure void free bonds. The recommendations for the firing profile are summarised in Table 2.3.

Table 2.3: Firing profile for Diemat glass frit material

Process step:	Temperature (°C):	Duration (min):
Drying	100	10 – 15
Organic burn-out	250	30
Glazing	350	1

AGC Glass Frit

For bonding in vacuum the glass frit paste 51115HT1 from Asahi Glass Company (AGC), a lead-free paste specially developed for vacuum packaging, will be used. Not much information is available on this material. Only some guidelines and recommendations for the firing profile were provided by the manufacturer [51]. Prior to bonding the paste must undergo a thermal conditioning process. The recommendations for the firing profile are summarised in Table 2.4.

Table 2.4: Firing profile for AGC glass frit material

Process step:	Temperature (°C):	Duration (min):
Drying	120	30
Organic burn-out	270	30
Glazing	440	10

According to the manufacturer a hermetic seal can be achieved if the glazed surface is mated for 10 minutes under slight pressure to the substrate at a firing temperature of 440°C followed by a controlled cool down of maximum 10°C min^{-1}. These figures are based on furnace heating where only low temperature ramp rates and slow cool down rates are possible. Following these guidelines would result in a rather long process time of 50 minutes for a single bonding cycle, which would make the laser process very costly since only a single sample can be bonded at a time. Furthermore, the company did not have any experience in applying this material for actual vacuum packaging. Their recommendation of this material for vacuum packaging was solely based on the composition of the paste. Therefore, a great deal of interest was put into investigating the actual suitability of the material for vacuum packaging and optimising the bonding parameters towards a much improved process time.

2.6 Quality Assessment / Military Standard Testing

In this section the test methods which are used to assess the quality of the seal of the packaged devices will be described. These test method are standardised to ensure

comparable results. Most of the test results described in this thesis were obtained according to the test methods described in MIL-STD-883G [115]. In the following a brief summary and explanation of the methods used throughout this thesis will be given.

2.6.1 Definition of Hermeticity and Leak Testing

One of the most common methods to assess the quality of a seal is to determine its hermeticity. The term *'hermetic'* describes a seal that is completely gas tight or impermeable to gas flow. In conjunction with microsystems technologies it stands for an air tight seal which will keep gases and moisture out of the sealed package, thereby eliminating failure of the device due to condensing water vapour inside the package. A full hermetic seal can ensure that a package remains dry and at a high vacuum for years. As no seal is perfect, standards had to be defined up to which leak rates seals are still considered as hermetic. For cavity style packages (all packages described in this thesis are of this particular type) these standards are defined in test method 1014.12 of MIL-STD-883G. Depending on the size of the cavity a maximum leak rate is defined at which the package is still regarded as fully hermetic.

In the following fine and gross leak testing according to MIL-STD-883G Method 1014.12 will be described. Packages are said to have a gross leak when their leak rate exceeds 10^{-4} mbar l s^{-1}. Leaks with a rate $<10^{-4}$ mbar l s^{-1} are termed fine leaks. Devices with a leak rate below 10^{-8} mbar l s^{-1} have passed the leak test and are regarded as hermetic.

The test method 1014 is divided into five test conditions:

- Test Condition A: Fine Leak using Helium tracer gas
- Test Condition B: Fine Leak using Radioactive tracer gas
- Test Condition C: Gross and Fine Leak Test Techniques
- Test Condition D: Gross Leak using a Dye Penetrate (Destructive)
- Test Condition E: Gross Leak by Weight Gain Measurement

Only Test Condition A and C are described as only these two techniques were applicable for the actual leak testing used in the work presented in this PhD.

Test Condition A: Fine Leak Using Helium Tracer Gas

For helium leak testing according to '*Test Condition A',* a helium "bomb" chamber and a helium leak detector are required. First the packaged device is pressurised in a 100% helium atmosphere (typ. 3-5 bar for 2-10 h depending on the cavity size) in the helium "bomb" chamber. This process is also referred to as "bombing" and if the package has a leak some helium gas will enter the cavity. The amount of gas entering the device depends on the size of the leak, the bomb pressure and the bomb time. After "bombing" the device is transferred into the chamber of a helium leak detector. The chamber is pumped down and the absolute amount of helium escaping from the package is measured. The measured leak rate depends on the amount of helium inside the package, the size of the leak and the volume of the cavity.

Table 2.5: Rejection limits for fine leaks using Test Condition A

Volume of package (cm^3):	Reject limit (mbar l s^{-1}):
< 0.01	5×10^{-8}
0.01 – 0.4	1×10^{-7}
> 0.4	1×10^{-6}

The rejection limit/failure criterion for a device depends on its internal cavity volume (see Table 2.5). If the measured leak rate is lower than the rejection limit the device has passed the leak test and the seal is considered as hermetic.

Test Condition C1: Gross Leak "Bubble" Test

The bubble test only indicates gross leaks. Therefore, it is always applied in conjunction with fine leak testing. The fine leak test has to be done before the bubble test (gross leak test) because the detector fluid used within the process might cover fine leaks. In a first step, the packages to be tested are placed into a bath of lower boiling fluid (type I detector fluid, boiling point <100°C) and pressurized for a given time. Afterwards the packages are transferred to a higher boiling fluid (type II detector fluid, boiling point >125°C) and the temperature is elevated above the boiling point of the type I detector fluid. If any liquid entered the package while immersed in the type I fluid, it would boil off and produce a stream of bubbles indicating a leak. A part has passed the gross leak test if no definite stream of bubbles or less than two large bubbles originating from the same point are emerging from the package.

Through-hole Leak Testing

These above mentioned methods for determining the hermeticity were specially developed for electronic devices (microcircuit packages). As there are no particular standards present for MEMS devices themselves, therefore, the same standards and test methods as for electronic devices are applied. Jourdain et al showed that these methods are not fully applicable for all MEMS due to their small volume [56-58]. MEMS typically have internal cavity volumes as small as 0.001 nl to 1000 nl. That is at least 1000 times smaller than described in MIL-STD-883G. The non-detection of helium does not necessarily mean that the package is hermetically sealed as the leak rate also depends on the cavity volume. Therefore, Jourdain et al [56-58] developed a new test method which is independent of the internal cavity volume and can detect both gross and fine leaks (leak-rate 5×10^{-12} – 10^{-3} mbar l s^{-1}). It is called through-hole testing method as the samples are fitted with a hole in the bottom chip. A schematic sketch of the test setup is shown in Figure 2.24.

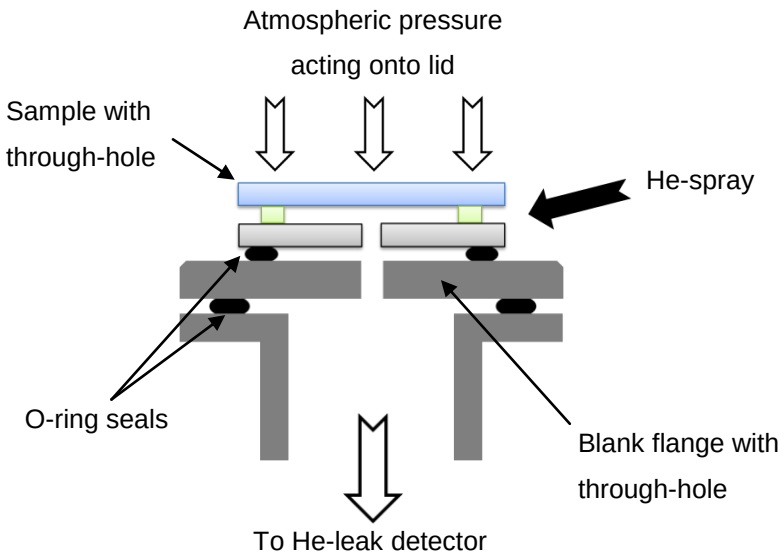

Figure 2.24: Sketch of through-hole helium leak testing setup

For this technique a helium leak detector with the same specifications as for the fine leak test according to MIL-STD-883G is required. Before testing, no pressurising of the samples with helium is required but the samples can be placed directly onto the helium leak detector. An O-ring with vacuum grease is used to seal the sample and the detector hermetically. In order to detect leaks in the packaged device helium is sprayed around the seal and the rest of the device. Leaks will be indicated by helium rates above the background level. Two drawbacks remain with this test method: no information about

the long-term stability of the seal is provided; and not the actual device but a modified version is tested – all the devices have to be fitted with a hole in order to be tested.

2.6.2 Residual Gas Analysis

Residual gas analysis (RGA), which is described in test method 1018.5 of MIL-STD-883G, can be used to obtain the actual level of vacuum inside the cavity of a package which has been sealed in a vacuum environment. In RGA, the package is transferred into a vacuum chamber which is connected to a mass spectrometer. The lid is pierced under vacuum, inside the vacuum chamber, and the escaping gas is analysed by a mass spectrometer. The spectrum of the residual gas inside the package is compared to the spectrum of a normal air atmosphere and from that the residual pressure (level of vacuum) inside the package can be calculated. Furthermore, this technique can also be used to detect if any out-gassing of the sealing layer occurred during the bonding process. These would be visible as peaks in the spectrum which are not present in a standard air atmosphere.

2.6.3 Shear Force Testing

Shear force testing, which is described in test method 2019.7 of MIL-STD-883G, is used to test the mechanical stability of the seal of a packaged device. The substrate of the bonded sample to be tested is clamped securely to prevent movement during testing. A shear tool is aligned to one side of the lid of the device. The side (edge) of the lid and the substrate should form an angle of approximately 90°. An increasing force is applied in perpendicular direction to the seal until mechanical failure of the seal occurs. A sketch of the shear force test procedure is shown in Figure 2.25.

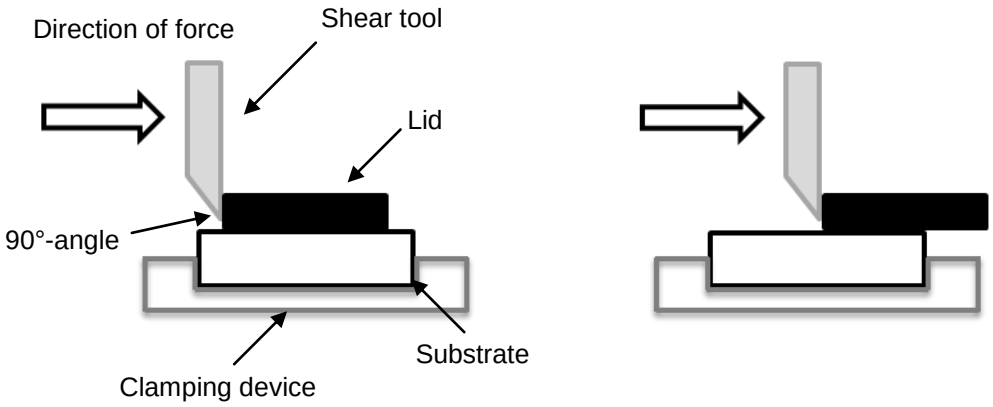

Figure 2.25: Schematic sketch of shear force test procedure

Inspection of the line of breakage after shear force testing allows conclusions to be drawn about the failure mechanism of the seal. If the fracture occurred within the sealing layer the bond strength clearly exceeded the mechanical stability (fracture strength) of the bonding material itself. If parts of the lid or substrate material remain stuck to the line of breakage the seal exceeded the mechanical strength of one of the bond partners. If, however, the intermediate bonding layer remains completely attached to either bond partners insufficient wetting of the particular interface was the reason for the failure of the bond.

3 Development of Laser Bonding Setup

In this chapter the development of a laser bonding setup is described. This setup is used for all the bonding experiments described in the following chapters.

Two of the main objectives of this PhD are the development of:

(i) a wafer-level bonding process and

(ii) hermetic packaging of components under vacuum.

These two objectives are based on initial feasibility studies on laser-based silicon to glass joining with a Benzocyclobutene (BCB) intermediate layer and glass frit bonding of Leadless Chip Carrier (LCC) packages at Heriot-Watt University, as described in section 2.5. In order to allow for these advanced packaging processes the originally used setup for the feasibility study had to be completely redesigned and a main aim of the redevelopment was that it should be possible to use one setup for all these bonding processes without major changes to the components or setup when switching between the processes. A description of the former bonding setup, the requirements and the development of the new setup, including a thorough discussion of its features, will be given.

3.1 Requirements on Setup

To give an overview of the status quo at the start of this PhD, the former bonding setup is described briefly. Its features are discussed and compared to the requirements on the novel bonding setup. The required changes and upgrades to fulfil these specifications are identified.

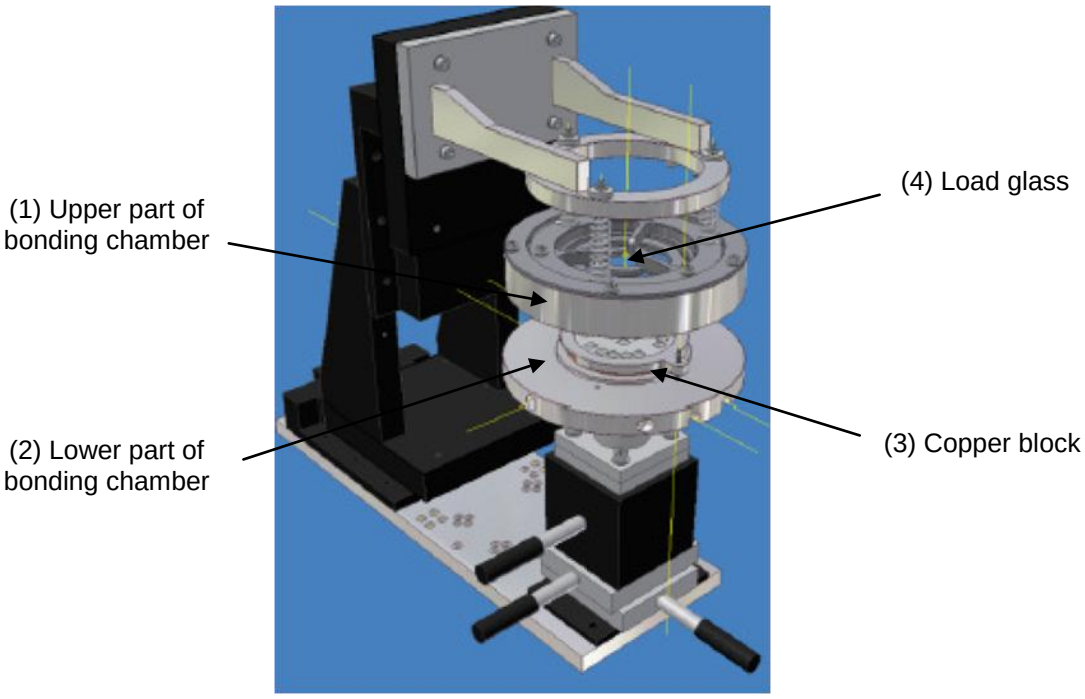

Figure 3.1: Sketch of former bonding setup [116]

The former setup mainly consists of two parts – the upper (1) and lower (2) part of the bonding chamber (see Figure 3.1). A water-cooled copper block (3), which is designed to hold 3" wafers, for cooling of the substrate during the bonding process is incorporated into the lower part of the bonding chamber. A window (4) is integrated into the upper part which applies the required pressure via a linear stage during the bonding process; hence, this window is referred to as the load glass. The setup is placed below the scan head of a laser system which provides the focused thermal energy for the actual joining process. The focused laser spot is scanned across the specimen through the load glass in order to bond the samples. The setup has been designed for vacuum packaging or bonding in an inert gas atmosphere. When the chamber is evacuated, however, atmospheric pressure acting on the load glass creates an additional force which is directly transferred to the samples below (see Figure 3.2).

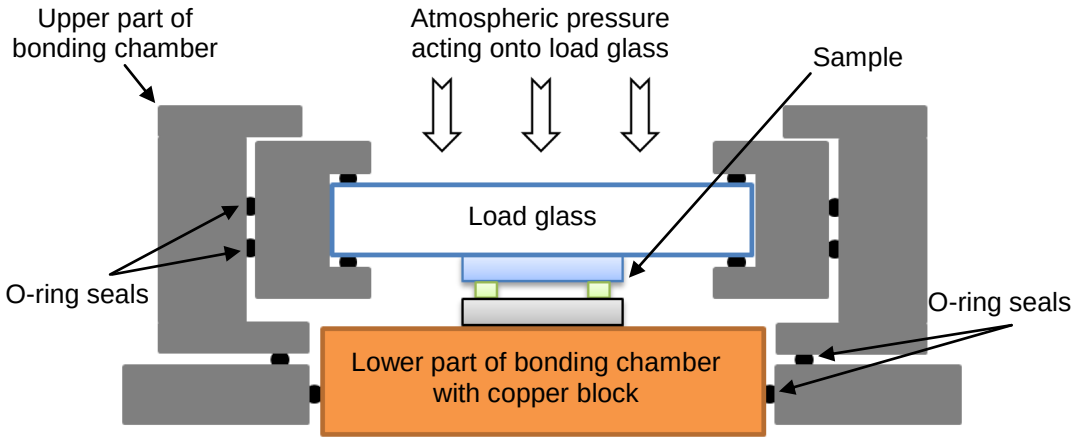

Figure 3.2: Schematic sketch of cross sectional view of upper and lower bonding chamber

This prevents the use of the system with low vacuum pressures, since otherwise the force acting onto the samples becomes too high. If the chamber is evacuated to <1 mbar a force of about 1.3 kN is acting onto the devices. Although bonding experiments thus far have shown that a force must be applied, this only needs to be about 5 N for single samples. If the existing setup was to be used for vacuum packaging more than 200 samples would always need to be bonded in parallel (placed on a single 3" wafer) which is not really feasible. Therefore, even though the setup is vacuum-tight, it is not suitable for vacuum packaging. Furthermore, it is not possible to run electrical connections for sensors like thermocouples into the bonding chamber, as required for temperature monitoring during the bonding process.

The main objective of the new bonding setup is that it should to be universal (flexible). It must fulfil all the requirements for chip and wafer-level packaging, including vacuum packaging. To apply the force required for bonding independently of the level of vacuum, i.e. the atmospheric pressure acting onto the load glass, the mechanism to generate this force must be moved inside the bonding chamber. A water-cooled copper block for cooling the substrate, and a load cell for measurement of the bonding force, which were already integrated in the previous setup, are required again. A backfill of the bonding chamber with inert gas after initial evacuation to prevent oxidation of the bonding layer is a desirable option for applications where a vacuum is not required. Therefore, several feed lines for the electrical connections, vacuum port, gas backfill and water-cooling need to be run from the outside to the inside of the bonding chamber without significant influence on the vacuum capability of the setup (i.e. the level of vacuum inside the setup). Additionally, a method for temperature monitoring during the bonding cycle is required to gain a better understanding of the entire process and

allow process optimisation. A detailed discussion of the different options available is given in section 3.3. The bonding setup should be reasonably compact so that it can be easily fitted under the galvo-scanhead of the laser system in use, and it should be designed in such a way that it can be easily adapted (upgraded) to the various requirements of different bonding processes.

3.2 Development and Description of Setup

3.2.1 Bonding Setup

To enable vacuum packaging, one of the key objectives of the new bonding setup is to move the mechanism to apply the force inside the evacuated volume which requires a considerably larger bonding chamber than previously available. The upper part of the former setup could be integrated into the new setup without any major changes as it was intended to be vacuum-tight in its original design phase already. All interfaces are fitted with O-ring seals (see Figure 3.2). The original load glass of thickness 4 mm and diameter 100 mm was replaced with one of thickness 13 mm so it can withstand the atmospheric pressure without bending or the risk of breaking once the setup is evacuated. Borofloat glass is used for the load glass because it has very good transmission at the laser wavelength of 940 nm (see Figure 3.18).

The lower part of the bonding setup was completely redesigned to accommodate a pneumatic cylinder to apply the required force for bonding. One important design rule when constructing a vacuum apparatus is to keep its dimensions as small as possible to facilitate the evacuation of the chamber and to minimise the surface area where water molecules can adhere to. A review of the options available to apply this force has shown that pneumatic cylinders are the ideal solution. They are the most compact devices which can still exert forces in the order of a few hundred Newton and they are inexpensive. Other alternatives like vertical lift stages or piezo actuators are expensive and either rather large or can only apply forces of a few Newton which would not suffice for wafer-level bonding. The only risk of using pneumatic cylinders, a device which is operated with compressed air, inside a vacuum is a potential for slight air leaks. A compact double action pneumatic cylinder from SMC (CDQMB25-30) with a stroke of 30 mm and a maximum force of 500 N was chosen, which should be sufficient for bonding up to 100 samples at a time. In case higher forces should be required the cylinder can always be exchanged for a more powerful one of similar outer dimensions

which would still fit into the chamber. A sketch of the bonding setup is shown in Figure 3.3.

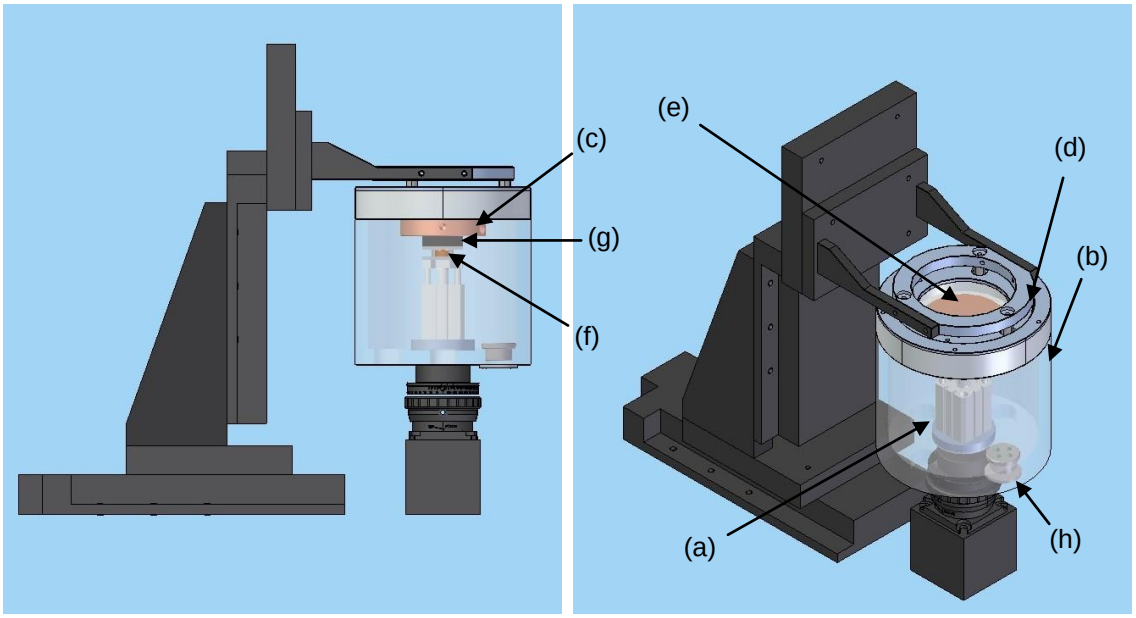

Figure 3.3: Sketches of new bonding setup with enlarged bonding chamber and integrated pneumatic cylinder

The pneumatic cylinder (a) is centred in the lower part of the bonding chamber (b), which is basically a hollow aluminium cylinder with a solid base. To further enhance the benefit of localised laser heating the samples are placed onto a copper block (c) for bonding to restrict the lateral heat flow and to keep the temperature in the sensitive device area in the centre of the package as low as possible. Active water-cooling is integrated into the copper block to keep it at a constant temperature even during the extended time period of several tens of minutes of some bonding processes. In the previous setup the upper part of the bonding setup (d) was used to exert the bonding force and the copper block as part of the lower one was locked into position. With the new setup, the copper block, which is mounted on top of the pneumatic cylinder, is used to press the samples against the load glass (e) inside the upper part of the setup (lid). The lid is sealed (pressed) flush against the bonding chamber and is held in a fixed position by a linear stage, and in case of bonding in vacuum additionally by the atmospheric pressure acting on top of the lid. Hence, the bonding force is independent of the level of vacuum inside the chamber as only the force acting onto the lid is increased once the chamber is pumped down; the force acting onto the samples remains unchanged.

To measure the applied force, a miniature compression load cell (CDF-0.5kN) supplied by Omni Instruments with a range of 0-0.5 kN (f) is placed between the copper block and the pneumatic cylinder. The load cell is connected to a load cell indicator (Tracker 243 by Data track) which displays the load with an accuracy of ±0.01 kg. The load cell is sandwiched between two aluminium plates; one containing a recess to centre it and the other one is to provide a flat, hard surface to press against to minimise measuring errors. Prior experiments have shown that for high quality bonds with full contact of the interfaces along the bond line it is essential that the load glass and the copper block are absolutely parallel. Since several components (pneumatic cylinder, load cell with aluminium plates and copper block) are stacked on top of each other there is a risk of a slight tilt between the load glass and the copper heat sink if the connection between all components is rigid. Hence, the components are not bolted together tightly, but held in place and guided by rods to permit a slight play (see Figure 3.4). In addition, a pliable cushion material (g) is placed between the copper block and the aluminium plate above the load cell which compensates for any tilt in the assembly ensuring that the two are aligned in parallel.

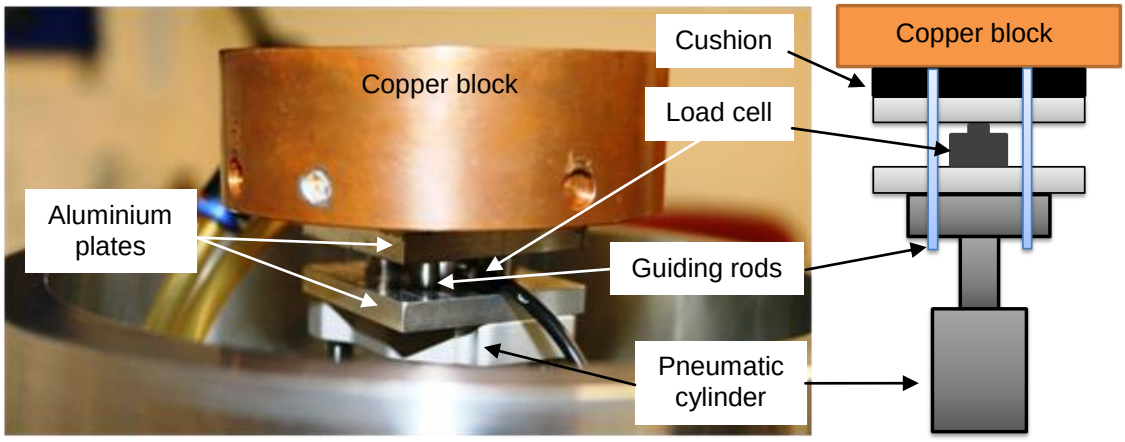

Figure 3.4: Photograph and schematic sketch of copper block and load cell on pneumatic cylinder

All the feed lines for cooling water, compressed air, etc. are put through feedthroughs (h) in the bottom of the bonding chamber. Instead of sealing those in directly vacuum-tight coupling interfaces were designed which allow easy replacement of the feed lines in case they break without the need for elaborate repairs. For that reason four holes of diameter 25 mm are drilled into the base of the bonding chamber; one of them is fitted with a DN-ISO FN16 flange to which the vacuum pump is connected and the remaining ones are sealed with customised plugs machined out of brass. For the feed lines for the cooling water and compressed air one of these plugs is equipped with four through-

holes fitted with push-in fittings (SMC) on either side (Figure 3.5). The connection pipes on the in- and outside of the bonding chamber can easily be connected and replaced if needed. According to the supplier (SMC) the fittings seal well down to pressures of at least 10 mbar which should suffice for this purpose.

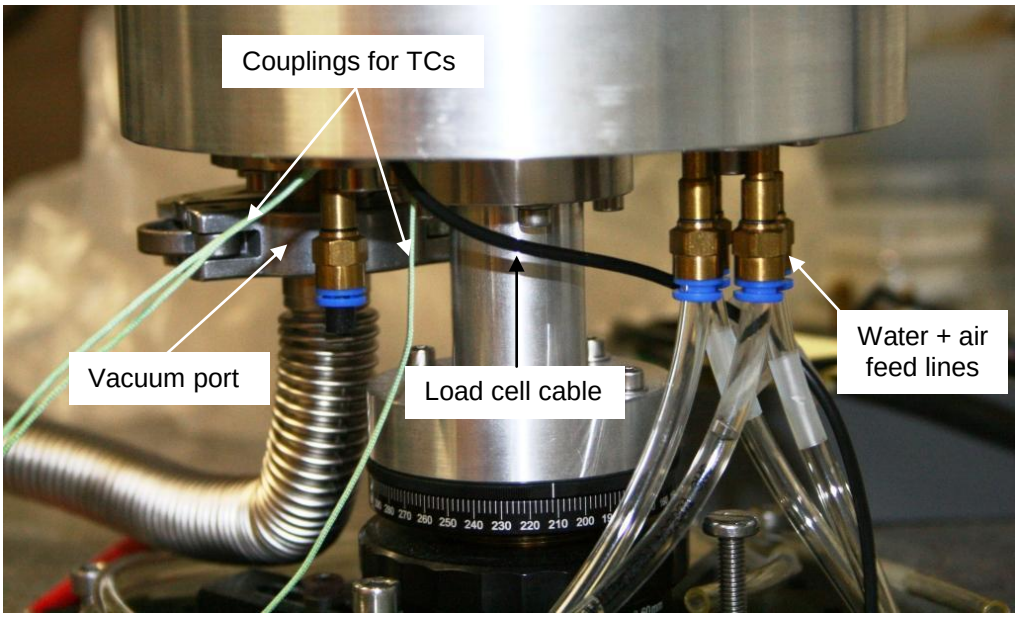

Figure 3.5: Photograph of bonding setup with vacuum-sealed feed lines

A second plug is used for the electrical connections to the load cell and the wires are sealed using a vacuum compatible epoxy (Torr Seal, Varian). The remaining three holes are used for the electrical connections of thermocouples. Instead of sealing the thermocouples in directly interchangeable couplings with connectors on either side were made (Figure 3.6). The wires for the electrical connection of the thermocouple were fed through the centre hole of such a threaded push-in fitting, as already used for the pipe connections, and sealed in using the vacuum epoxy. These couplings have two major advantages rather than sealing in the thermocouples directly: if a cable break occurs within the coupling it can simply be unscrewed and replaced by a new one, and also in case a thermocouple breaks it can be exchanged by simply unplugging it. The fourth plug is a blank which is left in case any further feedthroughs, for example nitrogen for back-filling the bonding chamber, are needed in future.

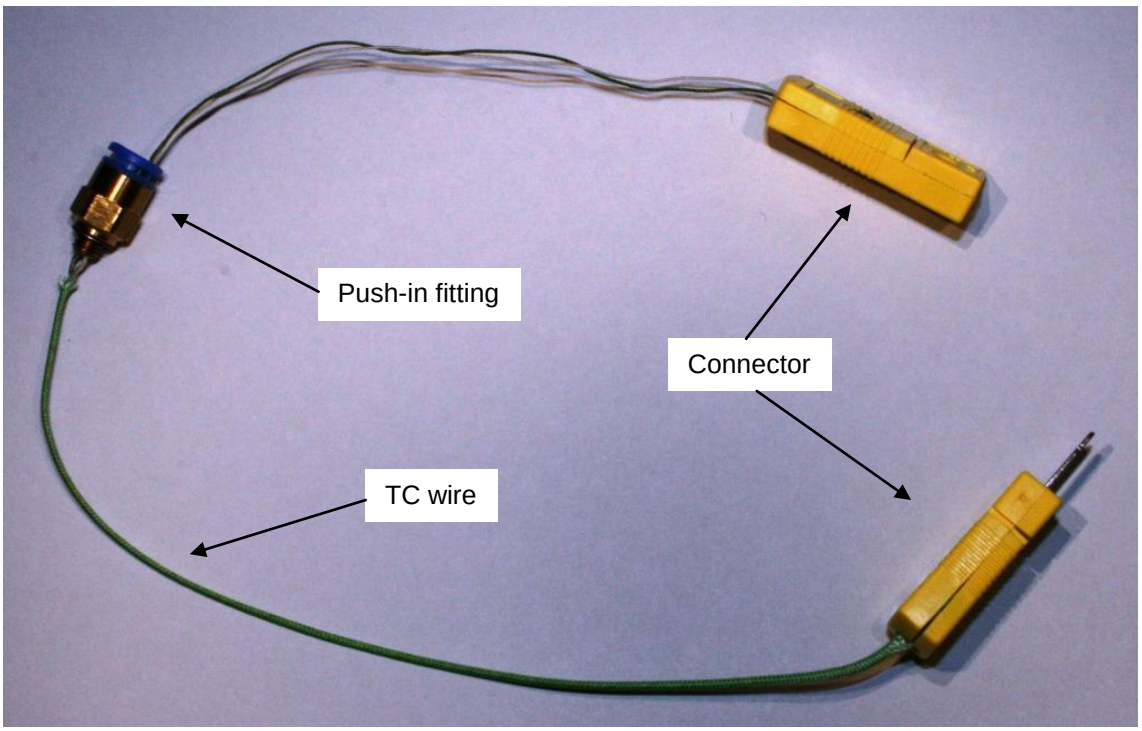

Figure 3.6: Photograph of vacuum-tight, interchangeable coupling for thermocouple

A rotary vacuum pump (DUO 5M) and a Pirani gauge (PT441 930-T) by Pfeiffer Vacuum Ltd. are used to evacuate the chamber and to monitor the level of vacuum in the system. A bleed valve is fitted to break the vacuum prior to re-opening the chamber after bonding. Initial vacuum tests of the setup have shown that a final pressure of around $3x10^{-2}$ mbar was achieved with the pneumatic cylinder moving up and down inside and the water-cooling switched on. Despite all the feedthroughs and potential, slight air and water leaks – fittings only specified for vacuum down to ~10 mbar – a final pressure inside the bonding chamber close to the limit of rotary pumps (typically around $<5x10^{-3}$ mbar) was achieved. Thus a very flexible and modular bonding setup has been developed where various, interchangeable connections are fed into a vacuum chamber without breaking the vacuum. The entire bonding chamber is placed onto a compact lab jack (LJ750/M, Thorlabs) so its height can be adjusted into the focal position below the scan head of the laser system.

3.2.2 Laser System

At the initial phase of this project (before the start of this PhD), when the laser system was specified, only the silicon to glass joining process was under investigation. Therefore, laser sources with a wavelength well matched to the maximum absorption of silicon were of particular interest. As can be seen in Figure 3.7 the absorption is particularly high in the wavelength range between 800 nm and 950 nm, where it peaks

at around 68% before the absorption sharply decreases again. In this wavelength range diode lasers are available with typical output wavelengths at 808 nm, 910 nm and 940 nm.

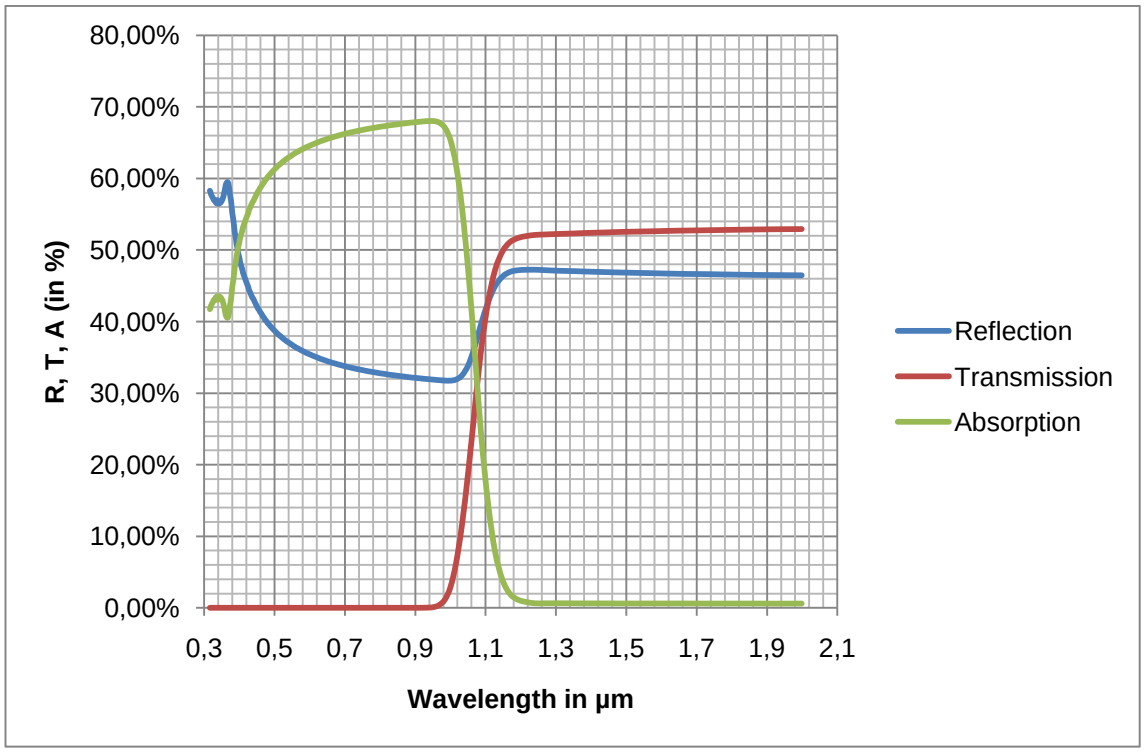

Figure 3.7: Absorption, transmission and reflection spectra of double-sided polished 600µm thick single crystalline silicon at room temperature [117]

In laser material processing applications, like cutting and drilling, short pulsed laser systems are often desirable to maximise the peak power. Due to the high beam quality of these systems, i.e. high focusability, very high laser intensities can be achieved on the workpiece. These enable vaporisation (removal) of the material without the extended heat affected zones often observed in cw-laser processes due to the continuous heat input into the material. The bonding procedures under investigation are purely heat initiated processes with bonding times ranging from seconds to several minutes. Therefore, cw-lasers (rather than pulsed lasers) are the ideal solution. As the bonding processes are aimed at industrial application, efficiency and cost of the laser source are important factors for the choice of the system, hence a diode laser was chosen.

This diode laser has an output wavelength of 940 nm (Laserline, optical output power 200 W) because the wavelength is well matched to the absorption of silicon, it is efficient (diode lasers can have high wall plug efficiencies of up to 50%) and it is a relatively cheap source of photons. Further requirements on the laser system are that

the heat input into the sample must be localised, i.e. a focal spot size of less than a few hundred microns is required, and the beam must be easy to control. For the beam delivery system a fibre delivered system in combination with a galvanometer scan head was chosen. The fibre core diameter is 200 µm. The scan head has a working area of approximately 45 mm by 45 mm and a focused spot size of around 250 µm at a working distance of 84.5 mm using a telecentric f-theta lens of focal length f = 80 mm. At the end of the fibre the beam is collimated to a diameter of 30 mm to match the aperture of the scan head and is coupled into the scan head through a 90° deflector (see Figure 3.8). The deflector is placed into the beam path as coupling unit for auxiliary components. It has a port at the backside of the 45° mirror for optional integration of a pyrometer or a camera into the setup for advanced process control.

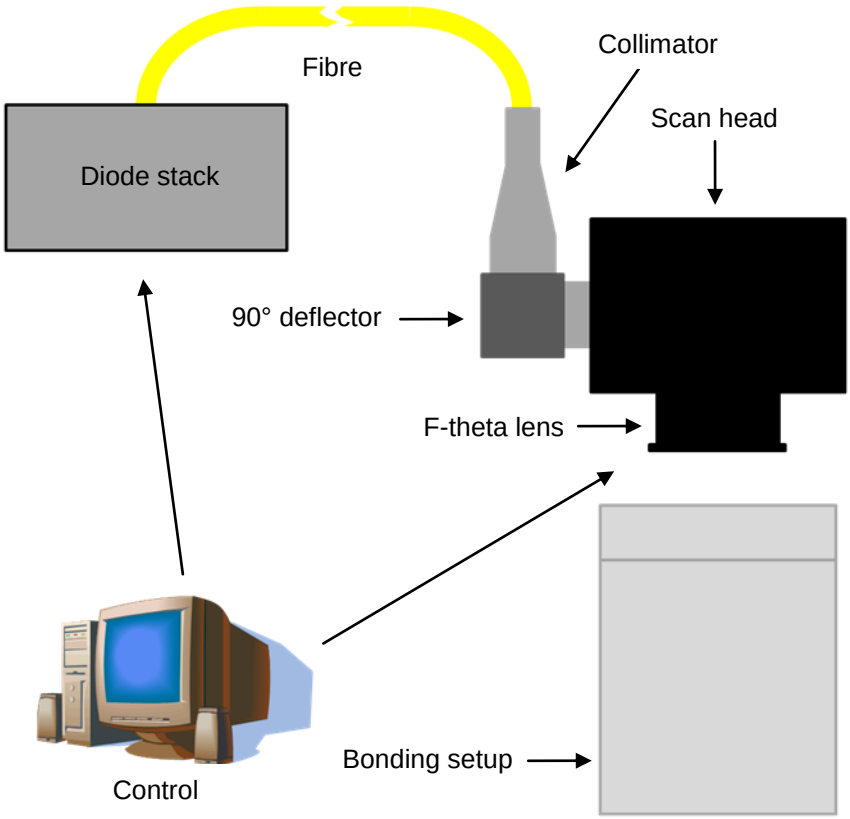

Figure 3.8: Schematic sketch of computer-controlled laser system with scan head and bonding setup

A sketch of the laser system is shown in Figure 3.8. Both the laser and the scanner are controlled via computer with the Scanner Application Software (SCAPS) SAMlight. The user interface is a simple 2D CAD software to draw the scanning (beam) path of the laser on the sample, and to assign the laser power and scanning speed. The beam path can be adjusted very easily for various samples of arbitrary shape without the need for

any mechanical changes to the bonding arrangement. Only the beam path needs to be changed in the software according to the shape of the sample to be bonded.

3.2.3 Laser Bonding Process

In the following the two joining processes – silicon to glass bonding with a BCB intermediate layer and glass frit packaging of LCC packages – demonstrated in this thesis are described briefly. Both processes, which can be done in the same setup without the need for any changes, are based on the same principal with only slight differences to the heat transfer within the sample. A photograph of the bonding setup and a schematic presentation of the bonding process are shown in Figure 3.9. Due to the long time-constants of the processes (up to several minutes) appropriate heat sinking is essential to prevent lateral heat flow into the centre of the device. The sample to be bonded is placed onto the water-cooled copper block to remove the excess heat during the bonding process and to protect the centre of the device from high temperatures. The bonding chamber is closed with the upper part of the bonding setup which is moved by computer-controlled linear stages. Then the sample is pushed with a light pressure against the load glass using the pneumatic cylinder to apply the required bonding force. The bonding setup is positioned at such a height below the scan head that the laser is slightly defocused (1.4 mm) to a beam diameter of around 400 µm (to match the width of the sealing layer). The beam waist is below the bond line. The laser beam is scanned at high speed (1000 mm s^{-1}) along the bonding track of the sample to heat the entire sealing layer quasi-simultaneously. At the same time as the sample is heated from the top the excess heat is drawn away through the bottom of the substrate.

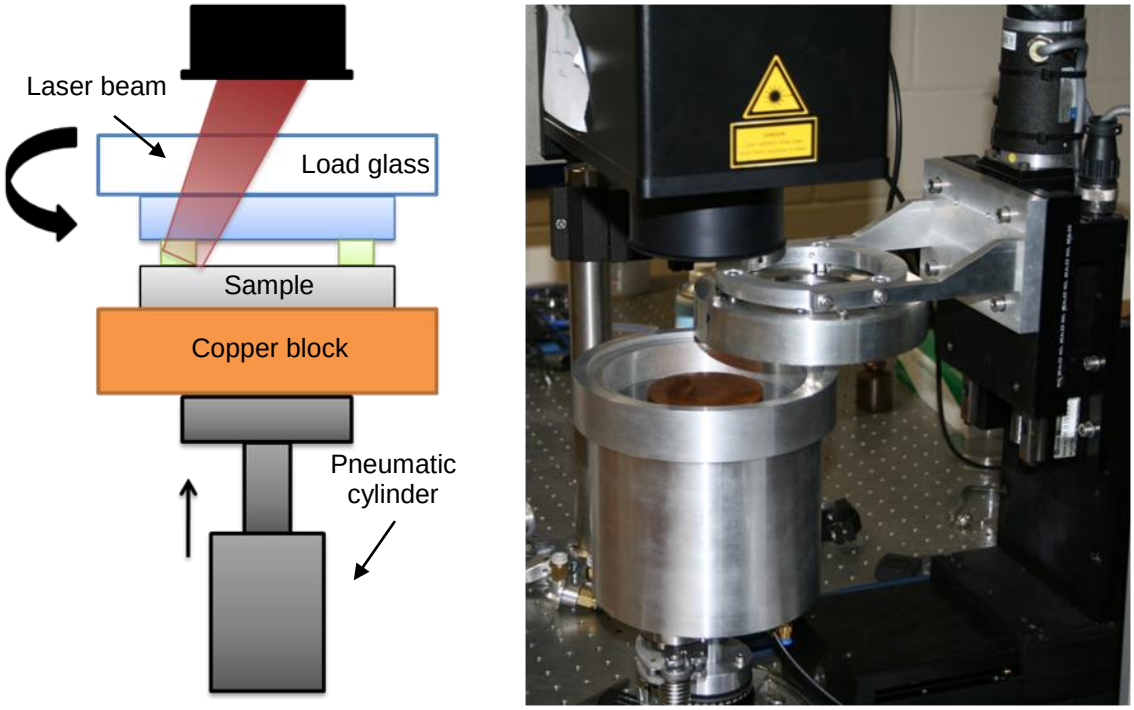

Figure 3.9: Sketch and photograph of laser bonding setup

3.2.3.1 Silicon to Glass Joining Process with BCB Adhesive Layer

The silicon to glass bonding process with the BCB intermediate layer is a transmission bonding process. Both the Borofloat glass and the BCB are highly transmissive at the laser wavelength of 940 nm but the light is strongly absorbed by the silicon substrate. At room temperature the absorption of silicon accounts for around 68% with the remaining 32% lost due to the surface reflectivity, as shown in Figure 3.7. The optical absorption of silicon is temperature dependant; increasing temperatures result in higher absorption. Furthermore, the optical properties in Figure 3.7 are valid for a silicon to air interface. In a silicon to polymer interface the reflection losses are reduced. These effects, however, are not investigated further in this work as they act in favour by increasing the overall optical absorption. A qualitative representation of the heat flow during the laser bonding process is shown in Figure 3.10.

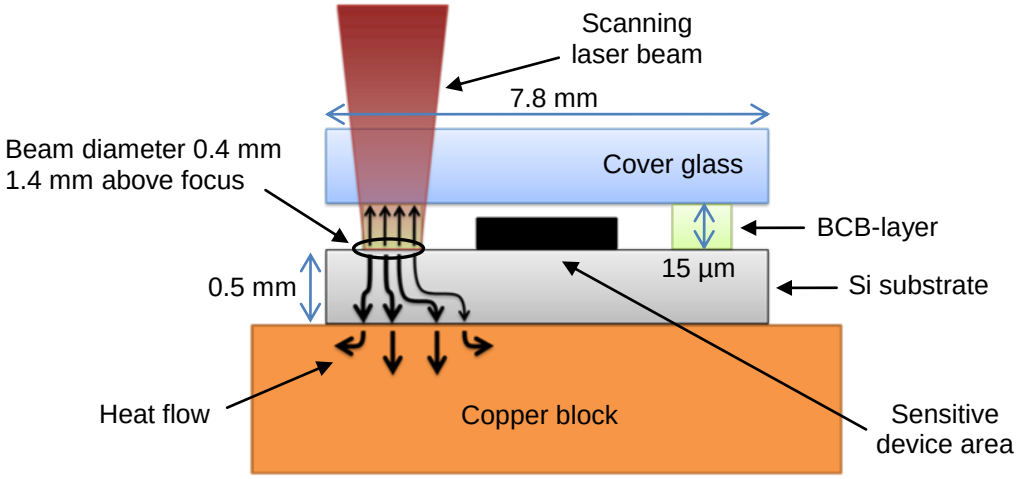

Figure 3.10: Sketch of qualitative representation of heat flow during laser-based BCB joining process (cross sectional view)

The curing process of the BCB sealing layer relies on the upwards heat conduction from the silicon through the BCB to the glass interface; i.e. the bonding layer is heated from bottom to top. Systems and structures located at the centre of the silicon substrate require protection from excess heat. A water-cooled copper block placed below the silicon wafer provides a heat sink to minimise the lateral heat flow within the silicon substrate. The high thermal conductivities of the silicon (149 W m^{-1} K^{-1}) and the copper block (401 W m^{-1} K^{-1}) ensure that the excess heat is removed instantly from the joining area, thereby protecting the sensitive device area in the centre of the package from elevated temperatures. The comparatively low thermal conductivity of the BCB (0.3 W m^{-1} K^{-1}) initially results in a very steep thermal gradient within the joining layer of thickness 15 µm. A sufficient long heating (bonding) time must be guaranteed to ensure the temperature within the BCB reaches a steady-state and the entire volume is heated (cured).

As a first estimate and for a more quantitative description the heat flow was calculated assuming steady-state conditions and a one-dimensional flow. Even though such a much simplified approach does not reflect the complex interactions of the real bonding process it helps to understand the main directions of heat flow within the sample. In steady-state conditions, the one-dimensional heat flow per area by conduction through a layer can be calculated as follows:

$$Q/A = \frac{k(T_1 - T_2)}{x} \text{ for } T_2 < T_1 \qquad (3.1)$$

Where k is the thermal conductivity of the material, T_1 and T_2 are the face temperatures and x is the thickness of the layer.

In Table 3.1 the results for the main directions of heat flow within the silicon and the BCB are summarised.

Table 3.1: Results of one-dimensional heat flow per area by conduction for the silicon to glass joining process

Layer:	Direction of Flow:	Q/A in MW m-^{2}:
BCB	vertical	6
Silicon	vertical	89.4
Silicon	horizontal	13.15

For T_1 a typical bonding temperature of 320°C and for T_2 room temperature (20°C) was assumed. To calculate the heat flow within the silicon substrate in horizontal direction the radius of the BCB ring (r = 3.4 mm) was taken for the thickness of the layer as the sample is radially symmetric. As can be seen from the results in table X, upon laser irradiation the main direction of the heat flow (89.4 MW m^{-2}) within the silicon substrate is in vertical direction towards the heat sink. The heat flow towards the centre of the substrate (13.5 MW m^{-2}) is considerably lower and therefore it should be possible to protect temperature sensitive devices located at this position from excess temperatures. As mentioned above, the lowest heat flow (6 MW m^{-2}) is through the BCB sealing layer and the bonding time must be adjusted to ensure uniform heating of the entire volume. The temperature of the copper heat sink was assumed to remain constant due to the constant heat removal by active cooling and its much larger mass (~1.5 kg) in comparison to the sample (few grams). For future investigations Finite Element Analysis should be taken into to consideration to model the heat flow for a more detailed analysis.

3.2.3.2 Glass Frit Packaging Process of LCC Devices

The joining process of the LCC packages also relies on heat conduction but the gold-plated lid used with this substrate is highly reflective (>90%) at the laser wavelength of 940 nm. To overcome the very limited absorption at this wavelength and to be able to couple sufficient energy for bonding into the sealing layer a square piece of silicon of thickness 500 µm is placed in good thermal contact on top of the lid, thereby increasing the effective absorption to around 68% (see Figure 3.7). The remainder of the power is lost mostly due to reflection. As explained in the previous section, these values are valid at room temperature only and the absorption increases with the temperature of the

silicon substrate. A qualitative representation of the heat flow during the LCC bonding process is shown in Figure 3.11.

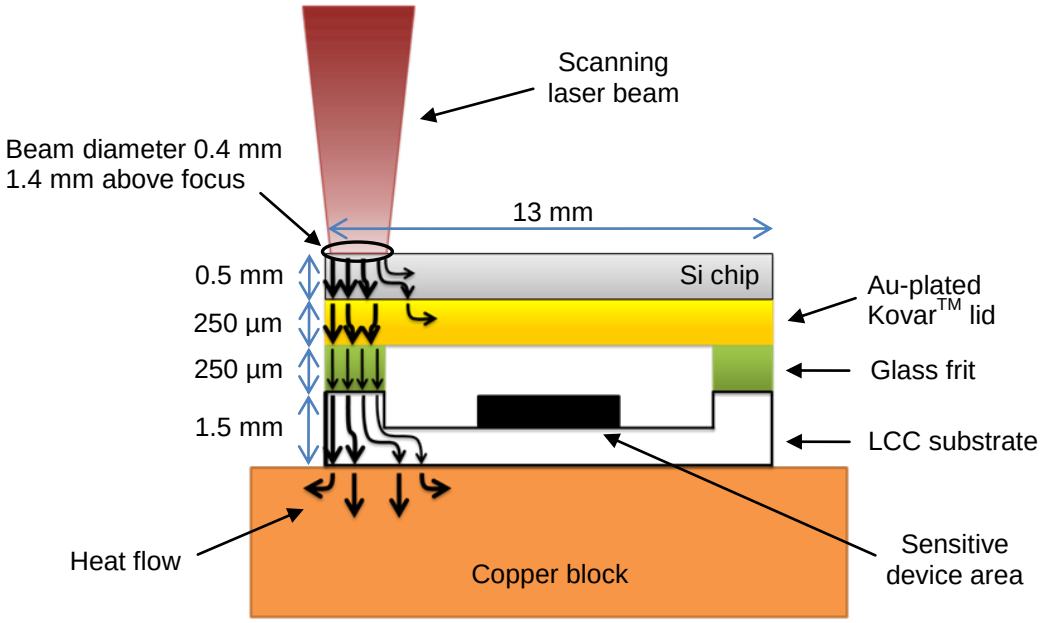

Figure 3.11: Sketch of qualitative representation of heat flow during laser-based glass frit packaging process (cross sectional view)

The laser light (energy) is absorbed by the silicon chip and the heat is conducted from top to bottom through the lid and glass frit to the substrate. This process relies mostly on heat conduction. Due to the high thermal conductivity of silicon (149 W m^{-1} K^{-1}) the entire lid heats up. Nevertheless, the heat input into the LCC substrate is still localised as the only conduction route to the substrate is via the glass frit layer. The part of the heat flow path within the sample with the highest thermal resistance is the glass frit layer. In comparison to the Kovar™ lid (17 W m^{-1} K^{-1}) and the substrate, which is mostly made of alumina (18 W m^{-1} K^{-1}), the glass frit has a low thermal conductivity of 0.9 W m^{-1} K^{-1}. The lateral heat flow in the LCC substrate is restricted by the copper heat sink (401 W m^{-1} K^{-1}) below. The excess heat is drawn away through the bottom of the substrate protecting the sensitive device area in the centre of the package from elevated temperatures. Even though the centre of the device should be protected from high temperatures the heat transfer between the substrate and the heat sink must be carefully balanced. If too much heat is drawn away, e.g. by improving the thermal transfer rate through the use of heat conductive materials, a steep thermal gradient occurs within the glass frit layer of thickness 250 µm and the entire volume of glass frit cannot be reflowed.

For a basic, more quantitative discussion the main directions of the heat flow during the glass frit bonding process were calculated using equation (3.1) as described in the previous section. The results for the heat flow per area by conduction of the individual layers are summarised in Table 3.2.

Table 3.2: Results of one-dimensional heat flow per area by conduction for the glass frit packaging process

Layer:	Direction of Flow:	Q/A in MW m^{-2}:
Silicon	vertical	105.79
Silicon	horizontal	8.14
Kovar^{TM}	vertical	24.14
Kovar^{TM}	horizontal	0.93
Glass frit	vertical	1.28
Alumina	vertical	4.26
Alumina	horizontal	0.98

For T_1 a temperature of 375°C – the bonding temperature of the glass frit packaging process in air – and for T_2 room temperature (20°C) was assumed. To calculate the heat flow in horizontal direction half of the side length of the LCC substrate (x = 6.5 mm) was taken for the thickness of the layer as the sample is mirror symmetric. Due to the high scanning speed of the laser beam the sample is heated quasi-simultaneously from both sides of the substrate during the joining process.

Upon laser irradiation the silicon chip heats up and conducts the thermal energy to the Kovar^{TM} lid which is in direct contact. Due to lateral heat flow the entire silicon chip (8.14 MW m^{-2}) and Kovar^{TM} lid (0.93 MW m^{-2}) heat up, however, the main direction of the heat flow (Si: 105.79 MW m^{-2}, Kovar^{TM}: 24.14 MW m^{-2}) is in vertical direction. The heat flow through the glass frit layer (1.28 MW m^{-2}) is comparatively low because of the small thermal conductivity of the glass frit material. A comparison of the heat flows in the substrate (alumina) shows that the direction of the main heat flow is towards the heat sink (4.26 MW m^{-2}) and not the centre (0.98 MW m^{-2}), i.e. a temperature sensitive device located at the centre of the substrate would be protected from high temperatures. These initial calculations are sufficient for a basic description of the heat flow. Future work, however, should be focused on modelling of the bonding process using Finite Element Analysis to get a better understanding of the entire process and to take the effect of active cooling into account.

3.2.4 Development of Method for Application of Bonding Force

Preliminary bonding experiments have shown that it is hard to obtain reliable seals with full contact of the interfaces along the entire bond line with high repeatability if the sample is pressed flush against the flat load glass. This is a particular problem when bonding multiple samples on the same wafer but can also be the case for single chip packaging. To achieve full contact the force must be applied absolutely uniform over the entire sealing area. Despite the efforts to align the copper cooling platform in parallel to the load glass by compensating for any tilt with the pressure pad it is difficult to ensure an even distribution of the bonding force. This issue was resolved by applying the force only in a discrete spot (single contact point) rather than pressing against a flat surface. In a first instance a small cut-out round piece of a silicon wafer of diameter 1 mm and height 0.5 mm (a small cylinder) was placed on top of the lid in the centre of the sample to be bonded. High quality seals with full contact of the interfaces along the bond line were achieved with high repeatability resolving the issue of applying the force evenly. The only drawback of this method is that the small piece of silicon always needs to be centred carefully on top of the sample prior to bonding. Great care has to be taken that the lid and substrate do not get misaligned during the progress. This effort might be feasible for bonding of single samples (on a chip level) but is not practical anymore if a larger number of samples should be bonded at the same time.

Apart from that the key problem when packaging at a wafer-level using localised laser heating is how to apply the force required during bonding individually for every single sample on the wafer, since a scanning beam is used to sequentially illuminate the samples in contrast to bonding in commercial substrate bonders where all samples are heated in parallel. On heating with the scanning laser beam the polymer layer locally softens or starts to melt and is compressed. The cover wafer might flex slightly resulting in a change of pressure applied to the remainder of the samples on the wafer, perhaps even leading to void generation in the bonding layer. Additionally, it results in stress accumulation in the cover wafer which might cause devices bonded in an earlier step to split apart (see Figure 3.12). Therefore, the main concern in scaling this process up to a wafer-level is to apply the force homogeneously and individually for every single sample.

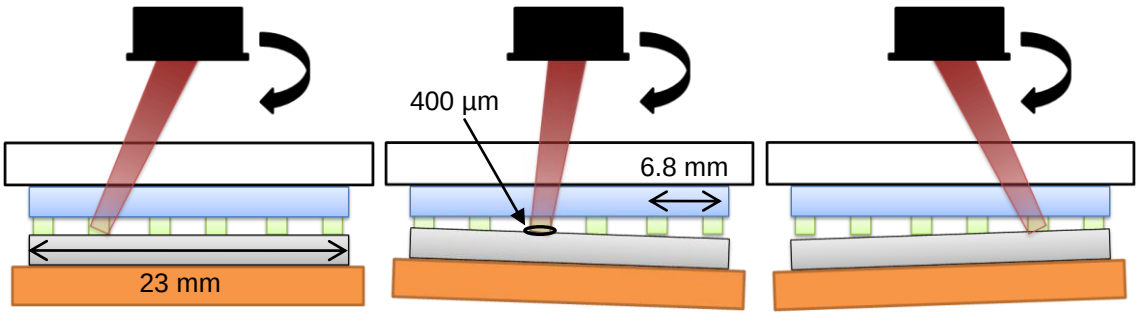

Figure 3.12: Sketches illustrating the issue of applying bonding force in sequential laser heating; as the laser moves along samples joined earlier split apart again.

A possible solution to this problem would be to place small devices with a high spring constant and slightly smaller dimensions as the devices to be packaged between the load glass and the cover wafer. Those "springs" would apply the pressure locally for each single device and could adapt to any flexing of the cover wafer. An almost equal pressure on the entire surface of the wafer throughout the bonding process could be guaranteed. Great care, however, has to be taken when choosing such a device especially regarding its spring constant and dimensions as the spring must be stiff enough to compensate for any flexing of the cover wafer but still compact enough not to obstruct the beam path of the laser (beam clipping). This becomes a particular issue when bonding at the perimeter of the scan field (working area) of the scan head where the laser beam hits the sample to be bonded at a flat angle.

As an alternative, glass spheres of diameter around 2 mm were chosen to apply the pressure. This approach relies only on flexing of the cover glass and not of the device which is used to apply the localised force itself. Glass spheres have two main advantages: they are compact and solid, and they only apply the force at a single point (minimum contact area possible). Above the centre of each device to be bonded a glass sphere is positioned to apply the pressure in discrete spots (rather than pressing the entire surface area against the flat surface of the load glass). On applying the pressure the cover glass flexes slightly where it is in contact with the spheres (Figure 3.13). Although the glass partly relaxes again once the polymer layer softens during the laser bonding process, the pressure on the remaining non-bonded devices on the same chip should not be altered significantly. The pressure should be distributed equally over the entire bonding area, provided the glass sphere is centred precisely in the middle of the ring structure. Reliable seals with full contact of the bond interfaces should be achievable in processes with high repeatability using this method.

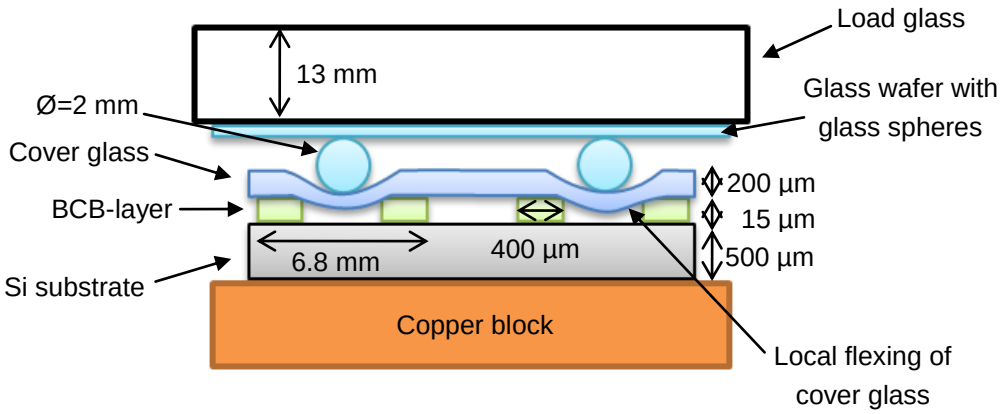

Figure 3.13: Sketch illustrating force application in distinct spots (flexing of cover glass) using glass spheres

The risk of using such an approach for applying the bonding force locally is that by flexing of the cover glass additional stress is generated which might cause already bonded samples to split apart again or might result in fracture of the glass. To estimate the impact of the localised force application on the cover glass the maximum deflection and the maximum bending stress were calculated. As simplifications an evenly distributed load was assumed and the BCB layer was regarded as solid columns; at room temperature BCB is fairly stiff and only melts and compresses upon heating. In the calculations only the curvature of glass and not the compression of the BCB was taken into account. The maximum deflection of a circular glass plate which is supported along its perimeter can be calculated as follows:

$$\delta = 0.764 \, \frac{w \, a^4}{E \, t^3} \tag{3.2}$$

Where a is the radius of the plate, t the thickness, E the Young's modulus of glass (Borofloat: 64 kN mm^{-2}) and w the evenly distributed load. The maximum bending stress is described as:

$$\sigma = 1.208 \, \frac{w \, a^2}{t^2} \tag{3.3}$$

As radius a length of a = 3 mm was used which is equal to the length non-supported glass within the BCB ring. For the bonding force and the thickness of the glass typical values were chosen which were used in the actual bonding experiments (see chapter 4). All the calculated results are summarised in Table 3.3.

Table 3.3: Calculated results for the maximum deflection on bending stress in the cover glass upon force application

Glass Thickness:	Bonding Force:	Max. Deflection:	Max. Bending Stress:
200 µm	2.7 N	11.46 µm	25.82 MPa
500 µm	6.0 N	1.66 µm	9.22 MPa

For the cover glass of thickness 500 µm only a slight deflection of 1.66 µm upon force application of 6 N was calculated and the maximum bending stress of 9.22 MPa remains well below the maximum bending strength of Borofloat glass (25 MPa). For the glass of thickness 200 µm even the reduced force of maximum 2.7 N is sufficient to result in a deflection of 11.46 µm in the centre and a maximum stress of 25.82 MPa, which is in the order of the maximum bending strength. As confirmed by bonding experiments (see chapter 4) the bonding force should not exceed 2.7 N which otherwise results in fracture of the glass.

For ease of handling and to ensure they remain in fixed position throughout the entire bonding process, the glass spheres were attached to a glass wafer. As described in chapter 4, chip-level and wafer-level packaging using simplified patterns of five and nine samples on the same chip are investigated in this thesis. For packaging of single devices, a single glass sphere was simply glued to the centre of a glass wafer using the vacuum epoxy Torr Seal which has proven to be a good choice for this purpose due to its high temperature resistance and strong adhesion to glass. To fully explore the options of this laser-based wafer-level packaging approach different spacings between the neighbouring devices of the pattern of five and nine samples on the same chip were investigated. For each one of them a glass wafer with glass spheres attached to the particular positions of the pattern was produced. To ensure a high positioning accuracy of the glass spheres small recesses in the form of half spheres were machined into the glass wafers using a CO_2 laser marker (Epilog). The recesses accommodate the glass spheres in their particular positions and avoid shifting while they are glued in. A photograph of such a glass wafer with nine glass spheres attached to it is shown in Figure 3.14.

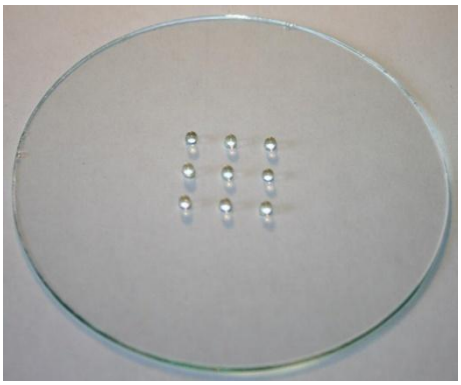

Figure 3.14: Photograph of glass wafer with glass spheres attached to it acting as single point loads

Depending on the pattern of devices to be bonded, the glass wafer was attached to the load glass in the upper part of the setup using small pieces of double-sided tape. The wafers could be easily removed and exchanged by carefully levering along the edge of the wafer and the load glass using a scalpel. This method for applying the necessary bonding force was used for the polymer bonding process and also for the glass frit packaging process. Initial bonding experiments with the LCC packages have shown that the overall bonding force is not critical but an even force distribution across the lid is required for sufficient wetting of the bond interfaces and hermetic seals in a high yield process.

3.2.5 Development of Method for Localised Cooling

Earlier investigations in collaboration with Qiang Wu, using the former bonding setup (see Figure 3.1), have shown that successful bonding cannot be achieved if the entire substrate area is in direct contact with the copper block in the silicon to glass joining process [118]. This failure is due to the high thermal conductivity of silicon (149 $W\,m^{-1}\,K^{-1}$) which leads to too much heat being drawn away to achieve high enough temperatures in the bonding area required for the curing process of the BCB sealing layer. Even when running the laser at the maximum output power of 200 W, the temperature does not reach the minimum curing temperature of 230°C. Hence, the area which is in direct contact with the heat sink has been reduced in size to protect only the sensitive device area in the centre from elevated temperatures rather than the entire area. This adaptation has led to a more energy efficient process since a considerably lower laser power (energy) is required to achieve the desired curing temperature. This is an important factor for industrial applications. Specially designed cooling platforms with either five or nine raised copper bosses of diameter 4.5 mm with appropriate spacings corresponding to those of the patterns to be bonded were manufactured to facilitate this efficiency improvement. A recess in the bottom ensures accurate centring and sliding onto the existing water-cooled copper block inside the bonding chamber. Special attention was paid to the flatness and roughness during machining of this face to ensure a good thermal contact between these components (copper block and cooling platform).

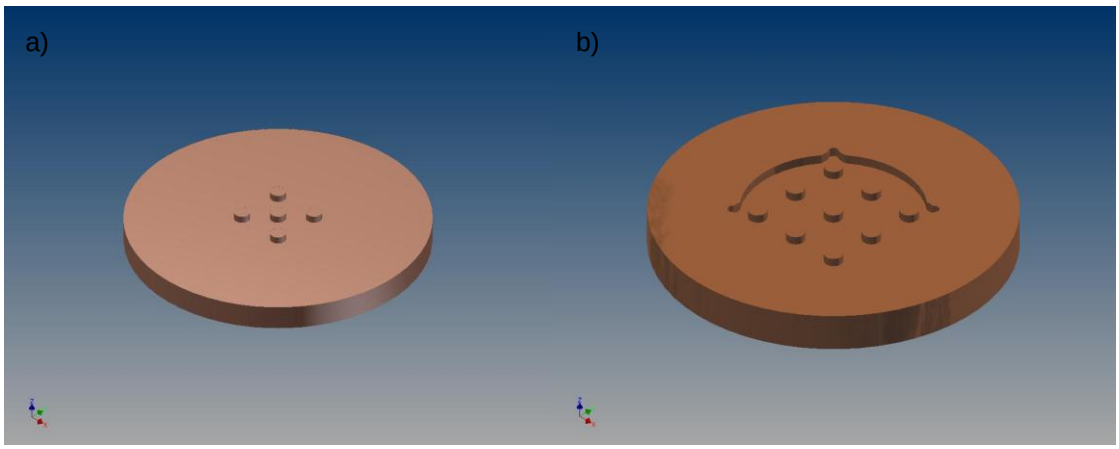

Figure 3.15: Sketches of copper adaptors with copper bosses; a) pattern of 5, and b) pattern of 9.

The first experiments with the pattern of five samples on the same wafer showed that it was difficult to align the silicon substrate and the cover glass with the patterned BCB-layer to the exact positions of the copper bosses underneath as they only consisted of the raised bosses without any reference for alignment (see Figure 3.15a). Also there was the risk that the non-bonded sample could shift slightly while raising the entire assembly using the pneumatic cylinder to apply the required bonding force. For the pattern of nine, therefore, a different design for the cooling platform was used. The array of copper bosses is surrounded by a raised layer with cut-outs in the corners to hold the square silicon substrates into position (Figure 3.15b). Only the corners and not the entire length of the silicon substrate are supported (in direct contact with the copper platform) as this would act as additional heat sinking resulting in higher laser powers required for curing or possibly preventing successful bonding at all.

Before joining of a specific pattern, the particular glass wafer with glass spheres and the cooling platform with the corresponding spacing need to be integrated into the bonding setup. To ensure the copper bosses, and hence the ring structures to be bonded, and the glass spheres on the glass wafer are precisely aligned, the glass wafer is placed onto the cooling platform and the spheres are carefully centred on the copper bosses. Then the bonding chamber is closed. The pneumatic cylinder is used to raise and press the glass wafer against the load glass and it is attached with double-sided tape, as described above. For the glass frit joining process with the LCC packages the entire substrate can be placed in direct contact with the copper block. Due to its considerably lower thermal conductivity ($12\ W\ m^{-1}\ K^{-1}$) the 200 W laser is sufficiently powerful to achieve the required bonding temperature in the joining region.

3.2.6 Integration of Camera for Alignment into Bonding Setup

For precise alignment of the laser beam to the bonding track, i.e. the perimeter of the silicon chip in case of the LCC packaging process or the BCB ring in case of the silicon to glass joining process, a camera was integrated into the beam path of the laser system. A sketch of the optical setup is shown in Figure 3.16. A black and white CCD camera (Baxall camera CDSP 9752) was chosen for this application as it is also sensitive in the near infrared spectrum and can display the laser beam of wavelength 940 nm. The reflection of the laser beam from the sample is viewed from the rear of the 45° mirror. The collimated beam is magnified and focused onto the chip of the CCD camera using a zoom lens (Computar No. 250006). Absorptive ND-filters are placed into the beam path for attenuation of the light to avoid saturation of the camera. With this optical arrangement the sample can be viewed through the galvo-mirrors of the scan head in the same position as the laser spot. The camera is connected via a Hauppage USB Live video digitizer to a computer and in combination with Win TV the video is displayed on the monitor.

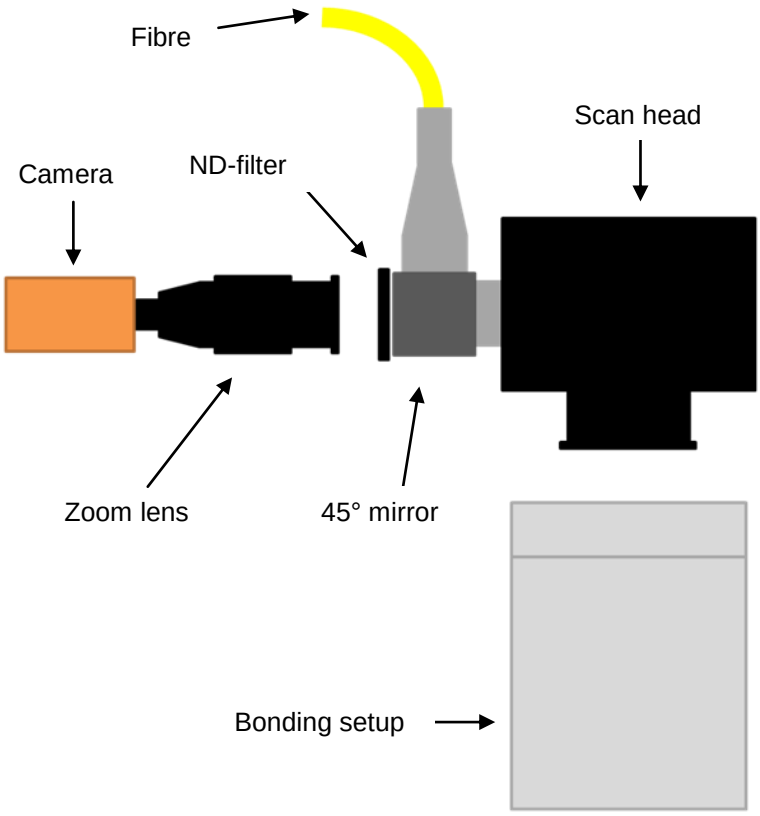

Figure 3.16: Schematic sketch of bonding setup with camera integrated into beam path of the laser

The laser offers the possibility to be run at threshold only. This is sufficient to illuminate an area around three times as large as the beam diameter, which can be seen

on the camera, but still has no significant thermal effect on the sample. If the scanning speed is reduced to 1 mm s^{-1} the beam path of the laser on the sample can be followed easily on the screen. By adapting the sketched beam path in the scan head control software (SamLight), the beam path can be aligned exactly to trace the bonding track of the sample to be bonded with an accuracy of ±10 µm.

3.3 Temperature Monitoring

Both joining methods are heat initiated processes and therefore temperature control is one of the most important process parameters to achieve successful bonding with high process yield.

3.3.1 Temperature Monitoring of Silicon to Glass Joining Process

As shown in Figure 3.17, the BCB curing process is a time and temperature dependent reaction; the higher the bonding temperature the shorter the curing time. In order to avoid degradation of the BCB polymer, however, the maximum temperature has to be kept below the glass transition temperature t_g = 350°C. In case of BCB, the bonding (curing) time can be reduced from tens of minutes to seconds simply by increasing the bonding temperature. Therefore, accurate monitoring of the temperature profile during the bonding process would be beneficial for process control and optimisation.

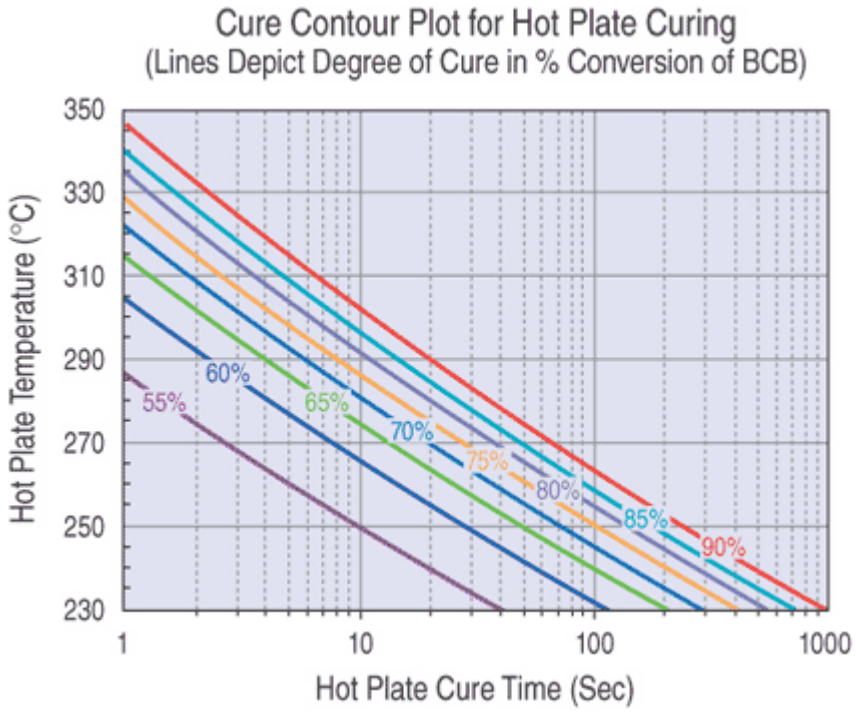

Figure 3.17: Cure contour plot for hot plate curing of BCB [110]

To give a true representation of the temperature profile during the bonding process a non-destructive and non-invasive real time temperature monitoring method without any changes to the bonding setup would be the ideal solution. Care has to be taken to prevent the temperature monitoring from influencing the "natural" heat flow within the sample. A common method for non-contact, remote temperature monitoring is the use of bolometer-based IR-cameras which typically operate at a wavelength range from 8 µm to 14 µm. Borofloat glass, however, like most types of glass is highly absorbent for infrared radiation (Figure 3.18) and therefore solely the temperature on top of the load glass as part of the upper bonding chamber rather than of the sample itself would be measured.

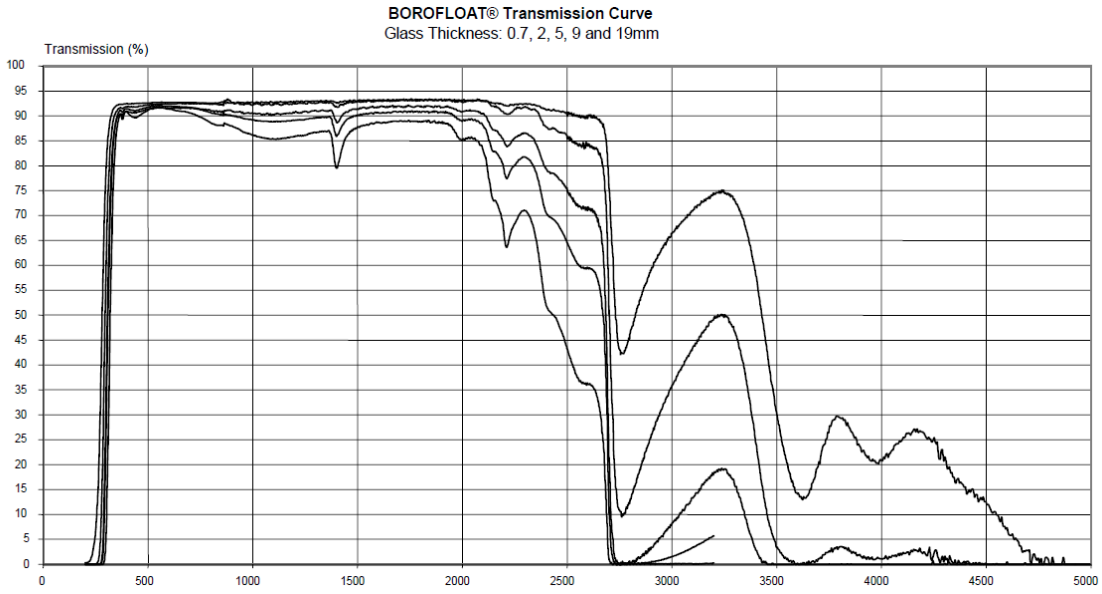

Figure 3.18: Plot of transmission curve for Borofloat glass of thickness 0.7, 2, 5, 9 and 19 mm [119].

An alternative non-contact and remote temperature measurement method is the use of pyrometers. Pyrometers have a built in detector which measures the thermal radiation emitted by the target object. The thermal radiation of this object is related to its temperature through the Stefan-Boltzmann law and the emissivity of the object. Pyrometers typically use IR-photodiode detectors; e.g. Ge-photodiodes with a lower cut-off wavelength of around 2 µm where glass is still fairly transparent (see Figure 3.18). Commercial laser systems with an integrated pyrometer in the laser processing head/scan head are available which ensures that the pyrometer measures the temperature in almost the same position as the laser spot. The main advantage of these systems is that the laser power is controlled online via a feedback loop even during the process. The desired process temperature is fed into the system and the laser power is regulated

accordingly achieving an even temperature distribution throughout the entire process. In [95] selective laser radiation bonding with integrated thermal process control in the laser processing head is demonstrated, where a Nd:YAG laser system is used for direct bonding of glass to silicon. The bonding experiments with thermal process control showed continuous bonds with improved quality in comparison to bonds at a constant laser power.

Upgrading the existing laser system and galvanometer scan head with such a pyrometer and control unit for advanced process control was considered. The infrared pyrometer EP60 (Dr. Mergenthaler GmbH & Co. KG) with a temperature range from 140°C to 650°C at a wavelength range from 1.6 µm to 2.0 µm [120] is such an example. At these wavelengths Borofloat glass is highly transmissive (>85%) even for a thickness of up to 19 mm as can be seen in Figure 3.18. Temperature measurements directly on the sample through the load glass should be possible. Dr. Mergenthaler GmbH & Co. KG, a supplier specialising in engineering such systems with turnkey solutions, was consulted about integrating temperature control into the laser system in use. Major changes to the existing laser system would have been required; these steps include: integration of the pyrometer into the system, adaptation of the galvo-mirrors to the pyrometer signal – application of a second coating at the backside of the mirrors with high reflectivity at the wavelength of the pyrometer, integration of the control unit with the controller of the laser system and the overall calibration of the entire setup. All these modifications would have been quite costly and would have resulted in longer downtimes of the system. For the silicon to glass joining process, nevertheless, this would be the ideal solution especially in industrial applications as the temperature could be measured and controlled in the joining region at the silicon interface – both the cover glass and the BCB intermediate layer are transparent at the wavelength of the pyrometer.

An alternative solution is the use of micro-thermocouples which are integrated into the bonding layer directly. Initial temperature monitoring experiments showed, however, that this technique cannot be used for silicon to glass joining process with a BCB intermediate layer. Both the cover glass and the BCB-layer are transparent to the laser beam but it is strongly absorbed by the wires of the thermocouple thereby heating the thermocouple junction. Instead of measuring the temperature of the joining layer the temperature of the laser beam was recorded. As no feasible approach for temperature

monitoring could be identified without longer downtimes of the laser system and considerable cost, the optimum bonding parameters were determined by trial and error. If the research on the silicon to glass joining process is to be pursued further beyond the scope of this PhD thesis the integration of pyrometer control into the laser system as described above should be reconsidered to facilitate and improve the process control considerably.

3.3.2 Temperature Monitoring of Glass Frit Packaging Process

Knechtel et al. [43, 44] have shown that temperature control is the most important factor in glass frit packaging, hence precise temperature control is essential during the bonding process. For the LCC packaging process with the glass frit intermediate layer a pyrometer cannot be used to measure the temperature in the sealing layer directly. The gold-plated Kovar™ lid is highly reflective at the wavelength of the pyrometer and the signal is not able to penetrate through this layer. A piece of silicon is placed on top of the Kovar™ lid to overcome the limited absorption of gold at the laser wavelength as described in subsection 3.2.3.2. In this case, the pyrometer would measure the temperature on top of the lid (in the silicon chip) rather than the one in the sealing layer below. In the case of the LCC package, however, thermocouples can be used to monitor the temperature directly in the sealing layer as they are protected from direct exposure to the laser beam by the lid. Three thermocouples were integrated into the LCC package to monitor the temperature both inside the sealing layer and in the centre of the device during the bonding process. The three positions of the thermocouples are shown in Figure 3.19. Two of these thermocouples are placed along the bonding track – in the middle of one side and in one corner – to investigate the heat distribution and to measure the temperature inside the sealing layer. A third thermocouple is placed in the centre of the device to demonstrate the localised heating nature of this laser bonding process and to what extent the lateral heat flow to the centre is restricted.

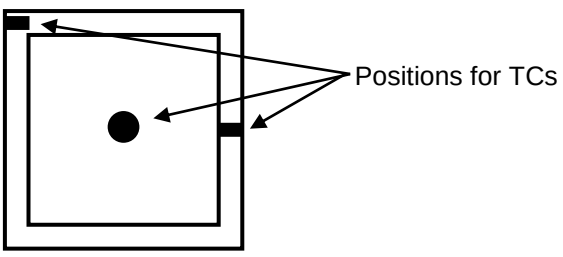

Figure 3.19: Sketch of LCC substrate for temperature monitoring with positions for thermocouples (TCs); two in joining area and one in the centre of the device.

Thus, a temperature monitoring method was developed which minimises changes to the geometry and "natural" heat flow within the package as much as possible. Miniature K-type thermocouples of wire diameter 0.25 mm (5SRTX-GG-KI-30-1M, Omega Engineering) are used to keep the thermal mass of the thermocouples as low as possible. They are the smallest commercially available thermocouples which still withstand temperatures above 440°C (bonding temperature of AGC glass frit material). They have a glass braid insulation (maximum temperature 480°C) and comply with EN 60584-2 Tolerance Class 1, i.e. an accuracy of ±1.5°C. To monitor the temperature directly at the interface between the glass frit layer and the substrate, small grooves were laser-machined with a nanosecond pulsed Nd:YVO_4 laser into the substrate to accommodate the thermocouples. The grooves are of dimensions 1.2×0.9 mm by 0.35 mm deep so the thermocouples are flush with the substrate surface once placed into the cut-outs and sealed in. The thermocouples were sealed in using glass frit as other adhesives would not withstand such high temperatures and their different thermal conductivities would falsify the result of the temperature monitoring results. A photograph of such a LCC substrate with the two thermocouples sealed in along the bonding track is shown in Figure 3.20.

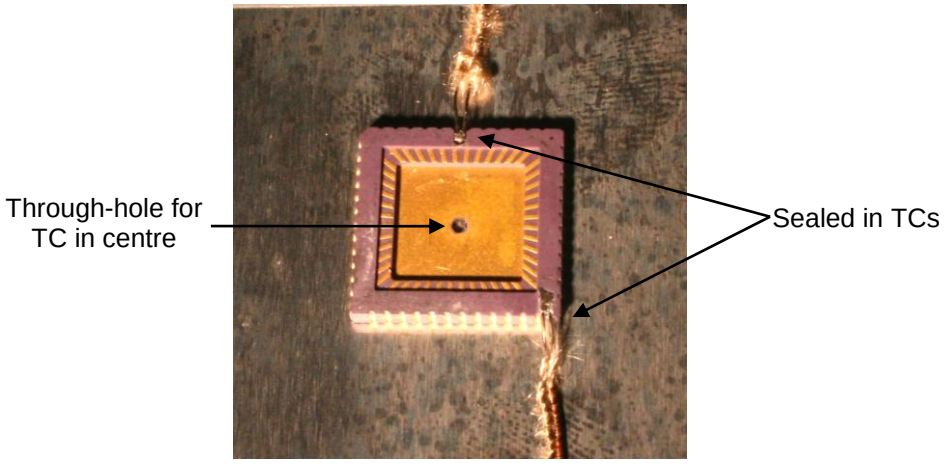

Figure 3.20: Photograph of substrate with sealed in thermocouples and through-hole in centre

For the third thermocouple a through-hole of diameter 0.4 mm was laser-drilled in the centre of the substrate. The third thermocouple required a special cooling platform to be made, with a through-hole and a slot at the rear of the platform. This enables the LCC package to be cooled in the same way as in the normal bonding experiments (Figure 3.21). The special cooling platform simply slides on and centres onto the existing cooling copper block inside the bonding chamber (just as the platforms for wafer-level bonding). Unlike the other thermocouples, this one was sealed in place with

the vacuum adhesive Torr Seal since it is not directly in the path of the laser and it can withstand relatively high temperatures. The temperatures required to seal in the thermocouple with glass frit would have caused the other two thermocouples to disassemble again.

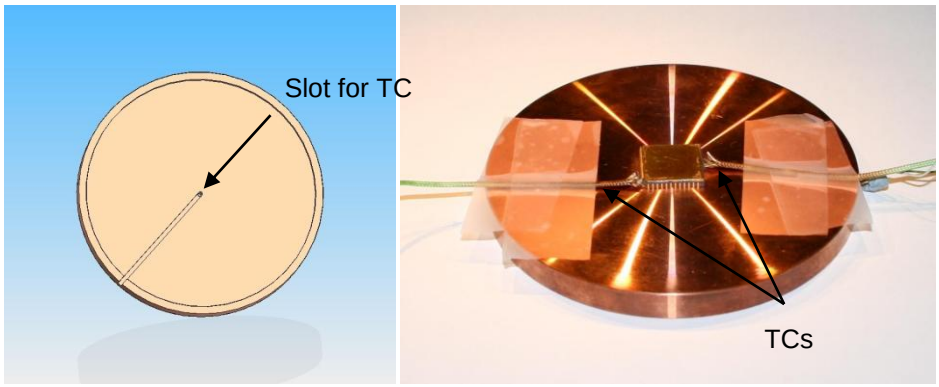

Figure 3.21: Left: Sketch of adaptor with slot for thermocouple; right: photograph of cooling platform with integrated thermocouples

The thermocouples are read out with high accuracy thermocouple thermometers (HH802U, Omega Engineering) which have a sampling rate of 1 Hz and a reading accuracy of 0.05% of full scale. The thermocouples are connected to the read-out unit using the couplings described in section 3.2.1. The signal can be fed from inside the bonding chamber to the outside without breaking the vacuum. While assembling the coupling great care was taken that all the connectors and wires are of type K materials, the same as the thermocouples. Otherwise, additional junctions would be created which would result in measuring errors. The thermometers were connected to a computer via USB and the temperature monitoring data could be saved directly onto the hard drive for precise analysis later on.

A further method, which was also used to determine the temperature in the centre of the device in the glass frit packaging process of LCC devices, was the use of a thermo-chromatic paint (Tempilaq, Tempil). These paints change their appearance once heated past a certain trigger temperature from a previously matt and porous surface to a shiny and glossy surface after a phase change at a specific temperature. The paint is easily applied, does not influence the "natural" heat flow within the package and does not require elaborate sample preparation as with the thermocouples but the results are rather limited. The paint does not give an explicit temperature, but only shows whether or not it was heated beyond its particular trigger temperature. Due to the high viscosity of the

paint it is hard to apply it in a discrete spot. As a result, the spatial resolution of this approach is rather limited. The major drawback of this method is that the temperature (phase change of the paint) can only be obtained after the bonding process once the package has been split open again, i.e. destroyed. Therefore, this method was only used initially to get a rough idea of the temperature range in the centre of package. For more accurate results thermocouples were used as described above.

3.4 Conclusions to Chapter 3

In microsystems technologies packaging is often application specific and hence accounts for a major part of the overall production costs of such a device. A generic packaging process would result in a considerable reduction of the packaging costs. In this chapter, the development of a multi-purpose bonding setup has been described. The bonding setup meets numerous requirements for different intermediate layer bonding processes. Only minor modifications to the bonding arrangement are required when switching between processes and these can be achieved within a few minutes.

Typical requirements of these bonding processes and the setup are:

- packaging in a vacuum or inert gas atmosphere,
- application of a bonding force,
- temperature control of the bonding process, and
- suitability for wafer-level packaging.

One of the key objectives of this PhD is to develop bonding processes where the thermal load on the bulk of the package is as low as possible. Therefore, an additional requirement has been to enable active cooling of the device substrate during the bonding process. The design of this setup was particularly aimed at providing for all the requirements of two novel laser-based bonding processes: glass frit packaging of LCC packages in air and vacuum, and silicon to glass joining with a BCB intermediate layer on a wafer-level.

For the bonding setup a design was chosen where all components are placed inside a bonding chamber. A controlled atmosphere is provided for the bonding process since often packaging in an inert gas atmosphere or in vacuum is required. Optical access for the laser beam, which supplies the energy for the bonding process, is provided by a

window integrated into the lid of the bonding chamber. A pneumatic cylinder is used to apply the bonding force which is monitored by a load cell. A water-cooled copper block is used as heat sink. As all these components operate inside the bonding chamber great care was taken for the design of the feed lines to avoid leakage. A camera was integrated into the beam path of the laser system to facilitate the alignment of the beam path to the bonding track on the sample.

For the silicon to glass joining process on a wafer-level two major challenges were to develop a method to apply the bonding force and to introduce localised cooling. The bonding force must be applied individually for every device on the wafer since they are bonded in sequence rather than in parallel. A glass sphere is centred over every device to be bonded. This approach relies on local flexure of the cover glass to provide the bonding force. If the entire substrate is in contact with the heat sink the laser is not powerful enough to ensure sufficient high process temperatures in the bonding area. Specialised cooling platforms, which are mounted on top of the copper block, were designed to provide localised cooling of the centre of the devices only.

The main challenges for the glass frit packaging process of LCC devices were the development of an accurate temperature monitoring method for process control and to ensure that the bonding force is distributed evenly across the entire sample. Temperature is the key process parameter for glass frit bonding. A temperature monitoring method was developed where miniature thermocouples were integrated into the joining area of the substrate to calibrate the laser power to the process temperature. Additionally, a technique was developed to integrate a thermocouple into the centre of the substrate to monitor whether localised heating can be achieved, i.e. the high temperatures are restricted to the bonding area. A specialised cooling platform was designed to integrate this thermocouple without significant influence on the natural heat flow within the sample. In glass frit packaging, the overall bonding force is not critical, however, it must be applied evenly to ensure sufficient wetting of the bond interfaces. The same approach as for the silicon to glass joining process was chosen. A glass sphere was used to apply the force in a single contact point to the centre of the package rather than pressing against a flat surface.

Online process control of the laser power, i.e. bonding temperature, using a pyrometer integrated into the beam path of the laser would be highly desirable. The current setup

does not allow for process temperature monitoring of the silicon to glass joining process with a BCB adhesive layer. This shortcoming could be overcome if pyrometric control were to be integrated into the existing laser system but has been deemed too expensive and time consuming to be implemented during this PhD project. Nevertheless, it would facilitate and improve the process control considerably.

4 Silicon to Glass Joining with Benzocyclobutene Adhesive Layer

Adhesive wafer-level bonding is an excellent solution to meet the stringent requirements in micro-electro-mechanical systems (MEMS) packaging. Packaging is one of the major challenges in MEMS manufacturing and as discussed in section 2.1, accounts in some cases for more than 90% of the total device costs. A range of bonding processes have become established in industry, however, in many or even most cases heating of the entire package to the bonding temperature is required to effect efficient and reliable bonding.

In this chapter, the experimental results of a laser-based adhesive layer bonding process are presented which addresses and eliminates the need to heat the entire package to the required bonding temperature. The process minimises the total heat input into the sample to be joined by selectively heating only a small cross-section of the device where the bond line is to be formed. The development of this process from chip-level to wafer-level packaging and quality testing of the packaged devices are also described in this chapter.

As described in chapter 2, adhesive layer bonding is a universal, low temperature bonding process which, in many applications, has several advantages over traditional direct bonding techniques. One of the main advantages of polymer bonding is that high bond strengths and good adhesion are achieved with most surfaces to be bonded. Hardly any limitations exist concerning the choice of the materials commonly used in MEMS manufacture. The elastic properties, and often liquid-like behaviour, of the intermediate layer during the bonding process result in low stresses within the materials being bonded and high process yields can be accomplished.

BCB is a particular promising intermediate layer and is investigated in this work. As discussed in section 2.3.3, this thermosetting polymer benefits from low moisture uptake, high chemical resistance and relatively low bonding temperatures. It is also bio-compatible which is essential in bio-medical applications. A number of BCB bonding processes have been developed using commercially available substrate bonding machines and are used widely in industry. In these systems the entire packages are heated to the required bonding temperature. Even though the temperatures involved in adhesive layer bonding (typically 200-300°C) are considerably lower than those used in

direct bonding techniques (up to 1100°C) the use of highly temperature sensitive materials within the package is still restricted.

A high power laser is an ideal heat source since it allows the generation of a highly localised heat input by focussing the beam to a small diameter and very flexible, remote positioning of the focal spot by beam steering in a 2D (X/Y) scan head. In this chapter, the development of a highly versatile bonding process which combines the advantages of localised laser heating and adhesive layer bonding is demonstrated. An example application, the packaging of silicon to glass with a BCB intermediate layer, materials commonly used in MEMS manufacture, is investigated. Due to the high thermal conductivity of the substrate material (silicon) and the long time constant (tens of seconds) of the bonding process appropriate heat sinking was applied to further restrict the lateral heat flow to the sensitive device area. All the bonding experiments are carried out in the newly developed bonding setup described in chapter 3, underlining the versatility of this novel piece of equipment.

4.1 Sample Preparation

There are several types of BCB resins available from Dow Chemicals. A. Jourdain et al at IMEC in Belgium – a former collaborator specialised in micro- and nanosystems– achieved good results with the Cyclotene 4026-46 advanced electronic resin. According to the supplier [121], a BCB layer thickness of 7 – 14 µm can be obtained with this type of resin, which is sufficient to compensate for surface roughness of the bond interfaces and to allow for compression during the bonding process. It was decided to use this particular resin and the associated chemicals, which are required for patterning process (Adhesion Promoter AP3000, Developer DS2100).

The deposition and structuring of the resin were carried out according to the prescribed processing procedures [121] with the BCB layer being deposited onto the glass substrate and patterned via UV-lithography using standard clean room processes. The entire process consists of three steps: Deposition, Patterning and Developing. Although most process parameters are given in [121], they can only be used as a rough guide with the exact parameters, especially the developing time, obtained by experiment.

Initial bonding experiments have shown that a final thickness of the BCB intermediate layer of 15 µm before joining is ideal for the purpose of this silicon to glass bonding process. Even though this is slightly outside the specifications (final thickness 7-14 µm) experiments have shown that structures with an even thickness of 15 µm across the entire wafer can be achieved with this type of resin. Several test wafers with a final structure height aiming at around 15 µm were fabricated in order to determine the exact parameters. During initial experiments in collaboration with Q. Wu two alternative illumination techniques – axicon and scanning laser beam – were investigated. An axicon lens generates an annular laser beam which can be focused to match the dimensions of the BCB bonding layer. Since the axicon illumination is limited to the generation of ring-shaped beam profiles, such a bond line was used in both experiments to allow comparison of the two techniques. The rings have an outer diameter of 6.8 mm and a width of 400 µm.

All the work was carried out in the class 1000 clean room of the MIcroSystems Engineering Centre (MISEC) group within Heriot-Watt University. The use of a clean room is required for two reasons:

1) the polymer should not be contaminated with particles (e.g. dust);
2) BCB is a photosensitive resin and therefore should not be exposed to UV radiation before developing apart from the exposure itself.

Once the polymer has been exposed and developed it can be taken out of the clean room.

The BCB polymer is applied to the sample by spin coating. In order to achieve good stiction (adhesion) of the BCB layer to the substrate an adhesion promoter (AP3000) is applied to the substrate. The adhesion promoter is dispensed statically, i.e. the wafer is at rest, then spread and finally spun dry, leaving a very thin film of <1 µm thickness. Directly afterwards the liquid-like BCB is dispensed statically, spread and finally accelerated to a high speed to ensure an evenly thick layer throughout the wafer. About 2 ml of resin are sufficient to cover a complete 3" wafer. The pre-exposure thickness of the BCB layer depends on the final speed of the centrifuge. The exact parameters for the coating procedure are summarised in Table 4.1.

Table 4.1: Parameters for photolithographic patterning of BCB

Parameters for spin coater (Speed, Acceleration, Time)	500 rpm / 100 m s^{-2} / 20 s 2000 rpm / 200 m s^{-2} / 20 s
Softbake	90°C for 6 min
Exposure	1050 mJ cm^{-2}
Pre-develop bake	85°C for 60-90 s
Developing time	4-6 min
Post bake	90°C for 1 min

After spin coating the wafers are soft baked on a hot plate (90°C for 6 min) to drive out any residual solvent. The temperature and duration depend on the thickness of the BCB-layer and the composition of the substrate. Before photolithography the wafer has to cool down to room temperature. BCB is a negative tone photo-resin, meaning that exposed areas remain after the development and non-exposed areas are washed away. The exposure should be carried out within 24 hours after drying. The required exposure dose depends on the thickness of the polymer layer and the reflectivity of the substrate wafer. For Cyclotene 4026-46 resin on silicon wafers the specified exposure is 60 mJ cm^{-2} μm^{-1}, thus for 15 µm about 900 mJ cm^{-2}. Experiments showed that a slightly higher dose (1050 mJ cm^{-2}) is required for the system configuration in use. This is probably due to fact that glass wafers were used as substrate instead of silicon wafers which have a higher reflectivity. Too little exposure can be recognized easily with the film wrinkling during the developing step or the fact that it is simply washed away completely. The exposure is followed by the pre-development bake (85°C for 60-90 s). Instead of developing the wafers according to the so-called "Puddle Develop Process" on the spin coater as described in [121] they are developed in a Petri dish; thereby the developer can be recycled and reused for more than one developing process. As mentioned above, the developing time which depends on the thickness of the BCB layer was obtained by trial and error. Under- or overdeveloping the exposed structures results in imperfect edges which are easily visible under a microscope. The appropriate developing time results in distinct, square edges otherwise slightly rounded features are observed as shown in Figure 4.1.

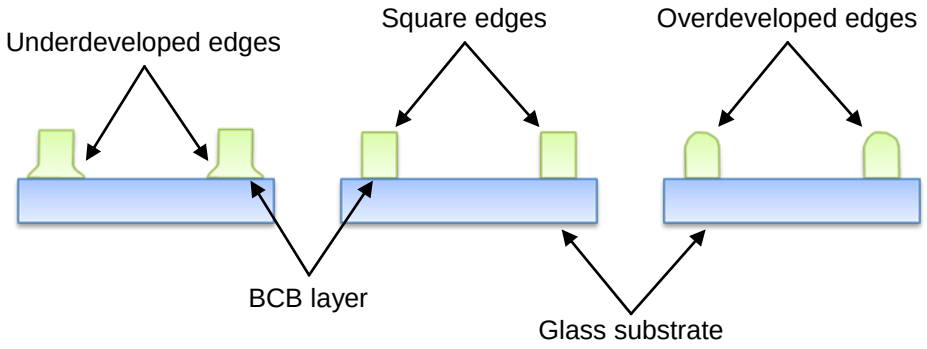

Figure 4.1: Sketch showing underdeveloped, square and overdeveloped edges of BCB layer on glass substrate (from left to right)

A developing time of around 5 minutes has proven to deliver the best results. Immediately after developing the wafers are baked again on a hot plate (post-development bake at 90°C for 1 min) otherwise inconsistencies in the shape of the structures may be observed. The parameters for each individual step listed in Table 4.1 result in the best shape for ring samples with a final height of around 15 µm. After the photolithographic processing the samples are ready for curing/bonding. A time delay between developing and cure does not affect the film thickness or the adhesion.

Using the method described above samples for both chip-level (see section 4.2) and wafer-level (see section 4.3) packaging were produced. Borofloat glass is used as substrate material since its coefficient of thermal expansion is closely matched to that of silicon resulting in considerably less stress during the bonding process. For chip-level packaging the entire 3"-glass wafer of thickness 700 µm is covered with ring structures. Around 60 individual rings fit onto a single wafer given an outer diameter of 6.8 mm of the ring structure. A photograph of such a wafer with BCB rings is shown in Figure 4.2. Prior to bonding the wafer is diced into square, single chips of dimensions 7.8 mm×7.8 mm. Double-sided polished square silicon pieces (thickness 500 µm) of slightly larger dimensions (10 mm×10 mm) are used as substrates.

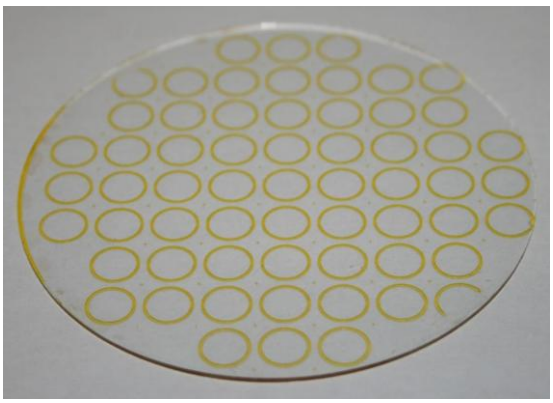

Figure 4.2: Photograph of 3" Borofloat glass wafer covered with BCB rings

The term wafer-level packaging describes bonding processes where the entire wafer is covered with structures to be bonded (see Figure 4.2). To prove the feasibility of applying a laser-based approach to wafer-level packaging, however, more simplified patterns with fewer samples were chosen, as shown in Figure 4.3. A very basic pattern of 5 samples (Figure 4.3a) was chosen for initial wafer-level bonding trials. For better comparison with wafer-level bonding a more complex pattern of 9 samples (compare Figure 4.3b) was designed where the gaps in the previous pattern have been filled in and the device in the centre is surrounded by the maximum number of neighbours. This is the most densely packed pattern possible, given the requirement that the patterns can be diced after bonding by making linear cuts with a mechanical dicing saw. Once these basic processes have been demonstrated they can be readily extended to a larger number of samples on a single wafer.

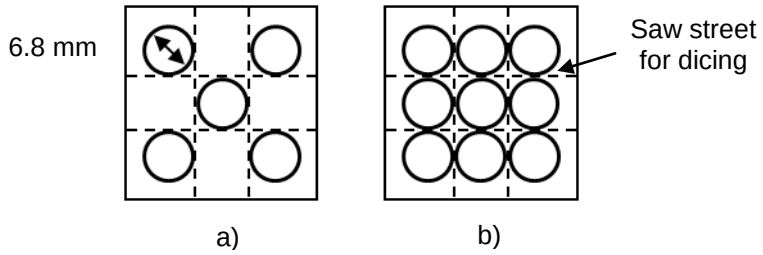

Figure 4.3: Sketches of BCB patterns used to join silicon to glass, where each ring of BCB will provide the seal for an individual device

To verify the influence of the distance between the neighbouring samples on the quality of the bond two different designs of the patterns of 5 and 9 were investigated:

(i) a centre-to-centre spacing of 7 mm (the smallest possible given the ring outer diameter of 6.8 mm and the dicing saw blade width of 0.2 mm), and

(ii) a 12.2 mm spacing.

Two different thicknesses of Borofloat glass substrates are used; 500 µm thick for the pattern of 5 and 200 µm thick for the pattern of 9. The individual application of the bonding force for every single sample of the pattern relies on local flexure of the cover glass, as explained in section 3.2.4. The thinner glass provides for the greater flexibility requirements for the more densely packaged pattern in this case.

The silicon wafers used are 500 µm thick and polished on both sides. Prior to bonding, as indicated in Figure 4.3, the glass and the silicon wafers are diced into square pieces of slightly larger dimensions than the particular pattern to be bonded.

4.2 Chip-Level Packaging

As mentioned in chapter 2, the entire project on laser-based packaging of micro-devices for this PhD thesis evolved from a feasibility study on laser bonding of glass to silicon with a BCB intermediate layer. The results of this study are reported in [107] and briefly summarised in section 2.5.1. The study showed that it is feasible to use a laser as a remote heat source to cure a BCB bonding layer between glass and silicon surfaces and thereby joining them together. Excellent bonding was achieved with a uniform illumination from the laser across the whole device. A diode laser with a collimated beam was used to provide the required thermal energy for the bonding process. To protect the inside of the MEMS device from direct exposure a mask was used resulting in a highly energy inefficient process as more than 80% of the laser power was reflected by the mask. In this technique, the devices were placed on a thermal barrier to ensure an even heat spread, however, this leads to the entire device being heated up due to lateral heat flow.

Such a technique is clearly not suitable when heating of a temperature sensitive device located in the centre of the package should be avoided. Furthermore, the mask also limited the flexibility of this process as for every different shape of bonding layer a new mask had to be produced.

In collaboration with Q. Wu a further development of this bonding process to localised heating techniques using selective laser heating in combination with active cooling to restrict the lateral heat flow was demonstrated in reference [118]. Two alternative techniques, axicon and scanning laser illumination, were investigated to achieve

selective heating of the bonding area only. The investigations of Q. Wu were mainly on the illumination technique using the axicon. The work of this thesis, meanwhile, focuses on the technique of using a scanning laser beam to provide the thermal energy required for bonding (see chapter 3.2) as virtually no limitations as regards the shape of the bonding layer exist.

4.2.1 Bonding Experiments

The bonding experiments were carried out according to the laser-based localised heating joining process described in section 3.2.3.1. As mentioned in [118] and in section 3.2.5, initial experiments have shown that successful bonding – a full cure of the BCB layer – cannot be achieved if the entire area of the substrate is in direct contact with the copper block. Therefore, heat sinking is only applied to the centre of device via a copper boss as otherwise too much heat is drawn away and the laser is not sufficiently powerful enough to achieve the required bonding temperature. A schematic of the bonding procedure and the localised heat sinking using the copper boss are shown in Figure 4.4.

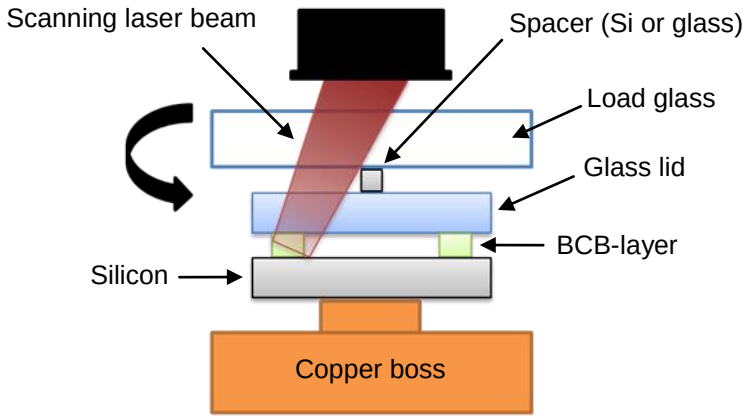

Figure 4.4: Sketch of laser bonding procedure for silicon to glass joining process with copper boss heat sink and spacer as point load

For bonding the sample was placed onto the water-cooled copper boss to protect the centre of the device from elevated temperatures during the bonding procedure. For the substrate silicon chips of dimensions 10 mm×10 mm by 0.5 mm thick were used. Borofloat glass chips (7.8 mm×7.8 mm) with the adhesive layer attached to it were used as lids. The BCB rings were deposited according to the photolithographic procedure described in section 4.1. The laser beam was scanned continuously at high speed (1000 mm s^{-1}) along the bonding track for the required bonding time. The beam was slightly defocused (~1.4 mm above focus) to match the spot size to the width of the

BCB ring. During the bonding process a slight pressure was applied to ensure good contact of the bond interfaces.

The BCB bonding mechanism is a heat-initiated curing process and a full cure is a precondition for strong and reliable seals. A full cure is achieved when >90% of the polymer is cross-linked. The curing time depends on the curing temperature (see section 3.3.1). It can vary from several tens of minutes (~230°C) to as short as only a few seconds (~350°C). For the reasons described in section 3.3.1 no adequate temperature monitoring method during the bonding process could be integrated into the setup. Therefore, the bonding parameters had to be obtained by trial and error. The degree of cure (quality of the bond) of the BCB intermediate layer after bonding was assessed visually under a microscope. The uncured BCB film exhibits a yellow-green colour which vanishes when it becomes cured. Overheating results in void (bubble) formation which is followed by charring of the film if the heat input is continued.

Two sets of experiments were accomplished to investigate the potential of this laser-based joining process. The feasibility study in [107] has shown that the BCB polymer can be cured within a few seconds using a laser-based process without degrading the properties of the BCB. For these initial experiments no measures were undertaken to restrict the lateral heat flow within the substrate and the entire device still heated up as in conventional techniques. The first set of experiments, therefore, aimed at optimising the bonding parameters, i.e. the shortest possible bonding time, when the substrate (Si-chip) is in contact with a heat sink. These experiments were carried out using the former bonding setup as the newly developed setup was still under construction. A small, round cut-out of silicon wafer (diameter 1 mm) was placed between the load glass and the lid of the sample to apply the bonding force in a discrete spot rather than pressing against the flat surface of the load glass (see Figure 4.4). A range of parameters (laser powers and bonding times) were established where successful joining could be achieved. The shortest bonding time achieved was 1 s. During these experiments a bonding force of around 4 N was applied. Taking the bonding area (~4.15 mm^2) into account this translates to a bonding pressure of around 0.96 MPa. Some typical bonding parameters are summarised in Table 4.2.

Table 4.2: Laser bonding parameters for chip-level silicon to glass joining with BCB adhesive layer using former setup (scan speed: 1000 mm s^{-1}, force: ~4 N) including leak test results

Laser Power (W):	Bonding Time (s):	Leak Rate (mbar l s^{-1})
50	15	2.9×10^{-10}
60	10	2.9×10^{-10}
70	5	6.9×10^{-10}
90	2	3.8×10^{-10}
140	1	3.9×10^{-10}

The heat sink is removing energy from the system, and to get an estimation of the temperature in the centre of device and to establish the level of heat flow, some initial temperature monitoring experiments using the thermo-chromatic paint (Tempilaq) were carried out. A small amount of the paint was applied to the centre of some silicon substrates and the samples were bonded at a laser power of 140 W for 1 s. A full cure of the BCB layer was achieved which indicates that the local temperature in the joining area was in the order of 350°C. The estimation of the temperature in the bonding region is based on the cure contour plot for hot plate curing of BCB shown in Figure 3.17. In order to achieve a full cure in as little as 1 s a temperature of 350°C is required. The paint demonstrated that the temperature in the centre of the substrate was always higher than 204°C but less than 232°C despite an assumed temperature of around 350°C in the joining area.

In summary, a laser-based silicon to glass joining process with a BCB intermediate layer was demonstrated where the temperature in the centre of the device can be kept below 232°C by heat sinking despite a temperature of around 350°C in the joining area. Although this experiment demonstrated the significant temperature gradient between the bonding area and the centre of the device which could be achieved using selective heating and heatsinking, the bonding was insufficient and weak for any processing times shorter than 5 seconds. Devices with a short bonding time ranging from 1 s to 5 s had only a limited mechanical stability of the seal since they split open when dropped from a height of 10-15 cm. The failure of the joint occurred at the BCB to silicon interface. Even though these samples appeared to have been fully cured and visual inspection under the microscope indicated a fully cured BCB, the bonding layer did not attach properly to the surface of the silicon substrate.

A second set of experiments was carried out which aimed to improve the mechanical stability of the seals, investigating whether the short bonding time has an influence on the bond strength. These bonding experiments were carried out using the novel bonding setup which had been finished in the meantime. Instead of the small silicon piece a glass sphere was attached to the load glass to apply the bonding force in a discrete spot as described in section 3.2.4 (see Figure 4.4). Again, a range of bonding parameters with different power levels and bonding times were investigated. The best results were achieved with parameters listed in Table 4.3. As it is very difficult to achieve constant forces lower than 5 N using the pneumatic cylinder, which is used to apply the bonding force in the new setup, a slightly higher bonding force of around 8 N (bonding pressure ~1.93 MPa) was chosen.

Table 4.3: Laser bonding parameters for chip-level silicon to glass joining with BCB adhesive layer using the new and improved setup (scan speed: 1000 mm s^{-1}, force: ~8 N)

Laser Power (W):	Bonding Time (s):
30	90
35	40
40	8

For closer investigation of the mechanical stability of the seals four samples were bonded for each set of parameters and subjected to shear force testing. Further bonding experiments showed that a further reduction of the bonding time below 8 s along with an increased laser power again resulted in a limited mechanical stability of the samples. If dropped from a height of 10-15 cm onto a hard surface the packages split open at the BCB to silicon interface.

4.2.2 Shear Force Testing

The 12 samples bonded at the three different exposure times (90 s, 40 s and 8 s) were shear force tested according to TM2019.7 described in MIL-STD-883G. Shear force testing determines the mechanical stability of the bonded samples, i.e. the force required to break the package open along the bond line. As suitable equipment was not available at Heriot-Watt, this testing was carried out by Optocap Ltd., a service provider specialising in packaging and assembly in microelectronics and optoelectronics. One of the samples, which was bonded at a laser power of 40 W for 8 s, broke during transport; hence, no result was obtained for this sample. A graphical presentation of all the shear force test results is shown in Figure 4.5.

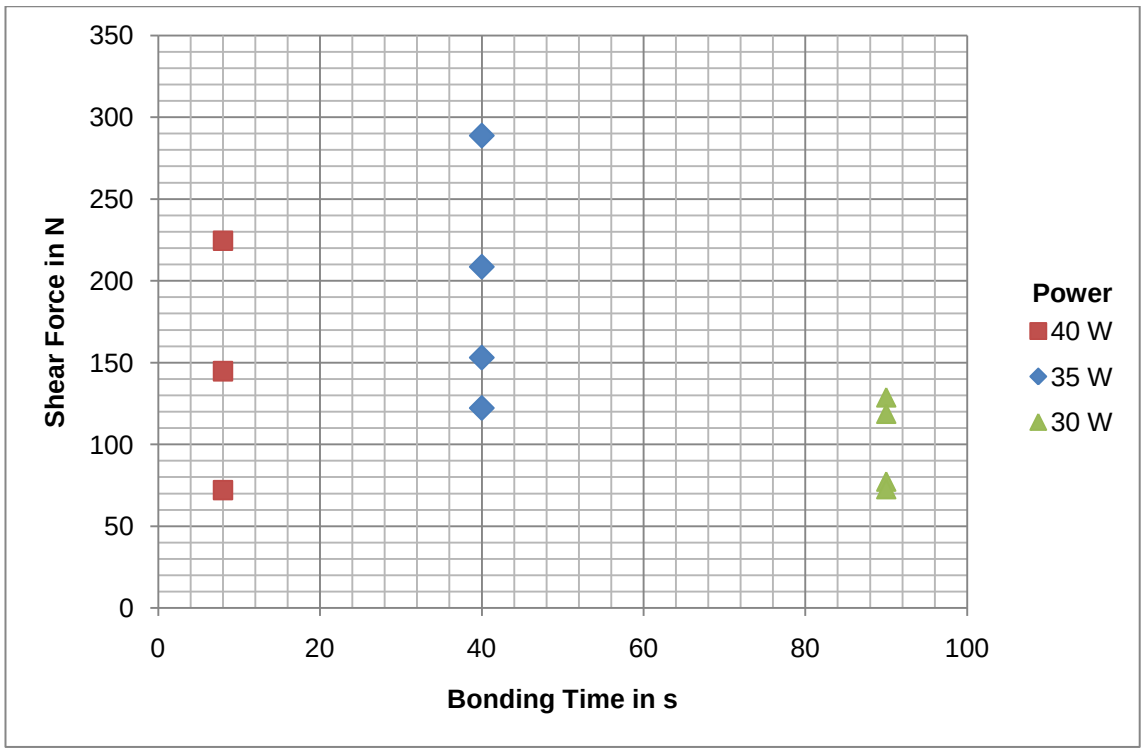

Figure 4.5: Plot of shear force test results for chip-level packaged silicon to glass packages with BCB adhesive layer

The breakage line, i.e. where the join failed, of the samples bonded for 8 s and 40 s occurred exclusively at the interface between the glass lid and the BCB joining layer, i.e. hardly any of the BCB remained attached to the glass onto which it was originally deposited. In contrast to the samples bonded for 5 s and less – where the failure occurred at the BCB to silicon interface – good adhesion between the bonding layer and the silicon substrate was achieved. Shear forces averaged around 150 N with a maximum of 290 N. These results are comparable to the shear force results for samples with a similar sealing area which were bonded using conventional flip-chip bonding (typically ~200 N) [56] and the results (typically ~170 N) presented in the feasibility study [107]. The selective laser heating and the heat sinking therefore have little or no effect on the mechanical stability of the seal.

Against expectations, the lowest bonding strengths were obtained with the samples bonded at a laser power of 30 W for 90 s – the longest bonding time. As the bond failure occurred at the BCB layer to glass interface, the adhesion of the BCB to the glass is the limiting factor rather than the "laser-generated" seal at the BCB to silicon interface. One possible explanation for these results is that the reasons for the limited adhesion of the BCB to the glass are connected to the sample preparation – the photolithographic patterning of the BCB rings. It is possible that the adhesion promoter

was spread unevenly on the wafer which would also explain the wide spread of shear force test results for the same bonding parameters (see Figure 4.5). A further refinement of the photolithographic procedure and in particular the application of the adhesion promoter should overcome these issues and should give more repeatable results. An alternative explanation could be that the BCB layer was insufficiently cured, i.e. not the entire volume of the joining layer was heated through. Hence, the join failed at the BCB layer to glass interface – the position furthest away from the heat input – where the BCB had its least mechanical stability due to a lower degree of cross-linking of the polymer. Ultimately the wide spread of the shear force values might simply depend on the overall low number of tested samples which does not allow for a significant statistical analysis.

4.2.3 Through-hole Leak Testing

One of the major requirements in many packaging applications is the need to hermetically seal or encapsulate the device to prevent dust and moisture ingress, to evacuate or to fill the device with a protective atmosphere to ensure a proper functionality for an extended life-time. The standard hermeticity test used in microsystems production is helium leak testing according to TM1014 described in MIL-STD-883G. As discussed in chapter 2, however, this test method cannot be applied for this particular sample (cavity volume ~0.5 mm^3) as it is not designed for such small cavity volumes (<1 mm^3). Therefore the samples were tested according to the so-called through-hole testing method developed by Jourdain et al [56-58] which is independent of the internal cavity volume (see section 2.6.1). As this test method requires a through-hole in the substrate additional samples with a hole of diameter 1 mm in the centre of the substrate were packaged using the bonding parameters shown in Table 4.2. A schematic of the testing arrangement is shown in Figure 2.24.

The leak testing was accomplished following the test procedure described in section 2.6.1. The background signal was measured at $<1.0\times10^{-11}$ mbar l s^{-1}, the detection limit of the helium leak tester. For the samples with the through-hole slightly higher leak rates ranging from 2.9×10^{-10} to 6.9×10^{-10} mbar l s^{-1} were obtained (see Table 4.2); no influence of the bonding parameters on the leak rate was observed.

While the leak test was carried out several limitations of this test method were noted. The leak rates listed in Table 4.2 suggest that full hermetic seals can be achieved using

BCB as sealing layer. However, if the helium was sprayed continuously around the BCB seal for a few seconds a gradual increase of the measured helium leak rate was observed due to diffusion of the helium through the adhesive layer and the O-ring seals. Therefore, the measured leak rate is rather the leak rate of air than the helium leak rate; hence, the unexpectedly low leak rates as air is a much larger molecule. Unlike in He-leak testing according to MIL-STD-883G the measured leak rate in trough-hole testing does not correspond to the actual helium leak rate of the seal. This test method does not offer any information on the long-term stability of the seal. Further investigations showed that this test procedure is merely a qualitative test method. In case of a leak – physical gap in the seal – the leak testing unit will show a direct, sharp increase in the level of detected helium. If no leak is present a slow, gradual increase will be observed till the detector is saturated due to diffusion of the helium through the sealing layer. Therefore, this test method only reveals if there are any voids or gaps present in the sealing layer but it offers no information on the actual helium leak rate of the seal. Based on this assumption qualitative testing of the samples was carried out and all samples passed the leak test.

A further limitation of this test method is that some smaller leaks or voids in the seal might be shielded by the test procedure itself. During the test the helium leak detector and the cavity of the sample are evacuated. The atmospheric pressure acts as additional force onto the lid and presses it down (see Figure 2.24). Due to the elastic properties of the BCB the sealing layer squeezes slightly and smaller voids might be temporarily closed. Further testing showed that if leaks were detected using this through-hole method they were also visible under an optical microscope. The leak test, therefore, was substituted by non-destructive, visual inspection using a microscope as the samples can be tested directly and do not need to be fitted with a through-hole.

In summary, chip-level packaging of silicon to glass with a BCB adhesive layer was demonstrated in a laser-based process. By selective laser heating and heat sinking the lateral heat flow to the centre of the silicon substrate was reduced considerably. Initial experiments indicated that the temperature in the centre of the device was kept below 232°C despite a temperature of around 350°C in the joining area. The localised heating technique has no adverse effect on the quality of the seal. Shear forces averaged around 150 N, although with some samples achieving up to 290 N, which is comparable to previous results within the same group [107] and work of other researchers [56].

Optimisation of the bonding parameters has shown that there is a trade-off between the bonding speed and the mechanical stability of the seal; bonding times shorter than 8 s should be avoided if rugged packaging is required.

4.3 Wafer-Level Packaging

The development of the wafer-level packaging process is presented in this section, together with details of the bonding experiments and quality testing of the seal. Comparisons were made with samples bonded on a chip-level.

In the previous section chip level packaging was presented, yet as mentioned earlier, state of the art MEMS packaging technologies often rely on wafer-level packaging. The main advantages of wafer-level packaging over chip-level packaging are (i) parallel processing, thereby reducing production time and costs, and (ii) protection of the device to be encapsulated from dust and water ingress prior to the dicing process [3]. In order to compete with these bonding techniques whilst still benefiting from the localised laser heating approach the development of such a wafer-level packaging method is investigated; a feasible solution to the challenges involved is presented. The key problem when packaging on a wafer-level using localised laser heating is how to apply the force required during bonding individually for every single sample on the wafer as discussed in section 3.2.4. The approach presented in this work is to apply the pressure only at a single point in the centre of each sample using glass spheres. This concept is demonstrated using simple patterns of samples with different spacings, firstly a pattern of 5, and secondly a pattern of 9. To investigate the influence of this bonding method on the bond quality the wafer-level packaged devices are shear force tested after dicing and a comparison of the results with packages bonded on a chip-level is accomplished. The basic process techniques used are described in section 3.2.3.1.

4.3.1 Feasibility Study on Basic Pattern

In this section the feasibility of multiple device joining on the same wafer in a laser-based process is investigated. A simplified pattern of 5 samples (see Figure 4.3 a) is used in order to verify whether it is possible to resolve the issue of applying the force individually for every single structure and to achieve successful bonding, i.e. sufficient contact of the bond interfaces of a non-bonded structure which is surrounded by already bonded ones. To examine the influence of the distance between neighbouring samples on the bond quality, bonding experiments of the pattern of 5 with both spacings are

presented. For simplicity the pattern with a spacing of 7 mm will be referred to as "small spacing" and the one with 12.2 mm as "large spacing".

4.3.1.1 Bonding Experiments

The patterns of both spacings were produced using the photolithographic procedure as previously described in chapter 4.1. The samples were bonded using the laser-based localised heating joining process described in section 3.2.3.1. Before the joining process, the particular glass wafer with the five glass spheres attached to it and the cooling platform with the corresponding spacing were integrated into the bonding setup. To ensure effective cooling and more importantly even force distribution during the bonding process, the spheres, the cover glass with the BCB rings and the copper bosses must be centred precisely on top of each other (see Figure 4.6). Misalignment of the spheres with respect to the centre of the BCB rings results in insufficient contact of the bond interfaces, and so only parts of the sealing layer are successfully joined as shown in Figure 4.7a).

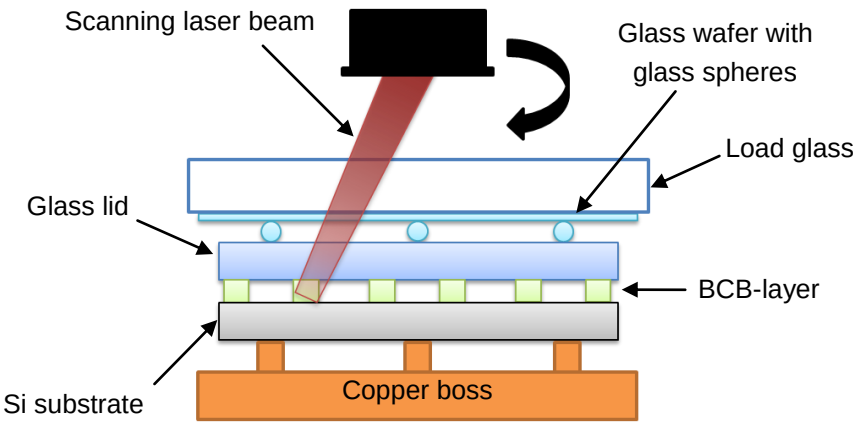

Figure 4.6: Sketch of laser bonding procedure for silicon to glass joining process on a wafer-level

For initial bonding experiments the BCB adhesive layer was deposited on Borofloat glass substrates of thickness 700 µm. Successful bonding for all five individual ring structures with both the small and large spacing could be achieved showing the feasibility of laser joining in multiple device (wafer-level) packaging. A full cure of the BCB and a good contact along the bond line could be realized as shown in Figure 4.7b). For the small spacing, however, after relieving the pressure (applied to the samples during the bonding process) at the end of the process two of the five bonds split apart again (Figure 4.7c)). The flexibility of the cover glass does not compensate sufficiently

for the flexure in the joining area when the single devices are so close together and due to the high stress in the cover glass the bond breaks apart.

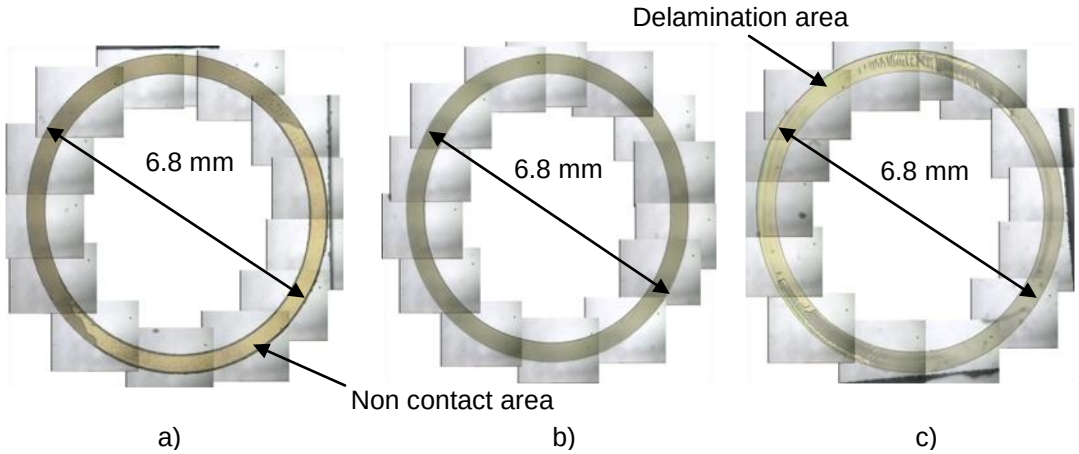

Figure 4.7: Microscope picture of BCB ring after laser joining process: a) incomplete contact of bond interfaces; b) full contact; c) partial delamination of seal. These images are composed by stitching together individual images.

Further bonding trials were carried out with Borofloat glass substrates of reduced thickness (500 µm), and hence greater flexibility, in order to reduce the stress inside the cover glass. A number of samples were bonded successfully with high repeatability. Once the pressure applied to the samples was relieved after the bonding process all five individual rings remained bonded for the large spacings. In some of the 'small spacing' samples, slight cracking and delaminating of the BCB film in parts of the bonding area were observed but not over the entire width of the seal. A photograph of such a typical bonded pattern is shown in Figure 4.8. The numbers indicate the sequence in which the individual BCB rings have been bonded; however, it does not have any influence on the results.

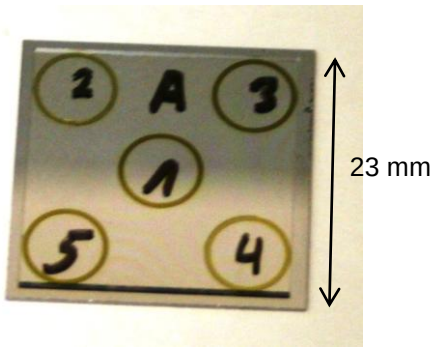

Figure 4.8: Photograph of bonded sample; small spacing pattern of 5. Numbers indicate sequence in which rings have been bonded

For the following parameters the best bonding results were achieved. A total bonding force of around 30 N was applied to the pattern of 5 during bonding, resulting in a force of 6 N for each individual device. Taking the bonding area into account this translates to a bonding pressure of around 1.45 MPa. For the small pattern a laser power of 30 W was applied for 50-70 s to each individual ring and for the large pattern 33 W for 57-77 s. During the bonding experiments it was noted that the BCB ring in the centre, in particular for the small spacing, required a slightly longer bonding time for a full cure as the surrounding copper bosses act as additional heat sinks and draw away some of the heat energy. With the small pattern, Borofloat glass of thickness 500 µm was used, whilst a thickness of 700 µm was used with the large pattern.

4.3.1.2 Shear Force Testing

In order to test the mechanical stability and therefore the quality of the seal the samples with the five bonded structures on the same wafer were sectioned into individual samples using a dicing saw. The stress and forces acting during the mechanical dicing process sometimes caused samples to split apart or resulted in partial delamination of the BCB film along the bond line, hence weakening the seal. Shear force testing according to TM2019.7 described in MIL-STD-883G showed that at least similar shear forces are obtained with these samples, packaged using this simplified wafer-level laser joining process, as with samples which have been packaged on a chip-level, provided that the BCB intermediate layer is fully cured. For the small spacing shear forces of around 95 N on average and for the large spacing of around 165 N could be achieved. For comparison, devices packaged on a chip-level withstood forces of typically 150 N (see section 4.2.2) before the seal failed. A graphical presentation of the shear force test results is shown in Figure 4.9; the testing was carried out by Optocap Ltd.

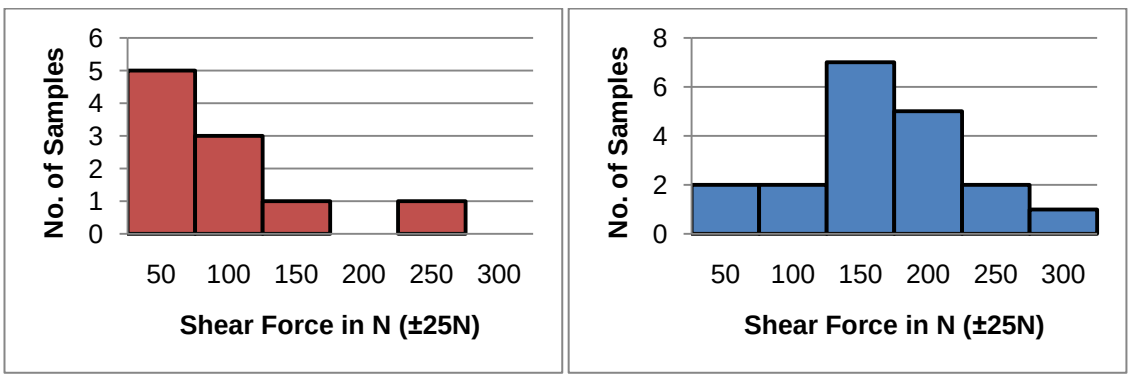

Figure 4.9: Plot of shear force test results for laser-bonded silicon to glass packages using pattern of 5. Left: small spacing; right: large spacing

In some cases, especially when the cover glass of thickness 500 µm was used, splintering and cracking of the glass was observed indicating that the strength of the seal exceeded the mechanical strength of the glass. This 5 sample pattern wafer-level packaging has a performance comparable to that of the chip-level packaging process, although the higher stress in the cover glass of the small pattern due to the closer proximity of the individual structures on the wafer results in reduced shear forces. The issue of applying the force individually for every single device on the wafer was resolved successfully for this basic pattern.

4.3.2 Wafer-scale Packaging with More Complex Pattern

After successfully demonstrating the basic principle of wafer-level bonding in laser-based processes by dint of the 5 sample pattern, the more complex pattern of 9 samples (see Figure 4.3b)) on the same wafer was investigated. The existing gaps in the previous pattern of 5 are filled in and the device in the centre is surrounded completely by neighbours. Once the feasibility of packaging this pattern has been shown it can easily be scaled up to a full wafer-level.

4.3.2.1 Bonding Experiments

As with the 5 sample pattern, two different spacings were used, a "small spacing" of 7 mm between the centres of adjacent samples, and a "large spacing" of 12.2 mm. To account for the greater flexibility demands of the cover glass of the more densely packaged pattern Borofloat glass substrates of thickness 200 µm were used. The total bonding force was restricted to a maximum of 25 N as forces greater than 30 N can result in cracking of the cover glass; thereby the force acting on every individual device is limited to around 2.7 N, which translates into a bonding pressure of 0.66 MPa.

In initial joining experiments with the large spacing successful bonding with good contact along the entire bond line could only be achieved for six of the nine BCB rings. Repetitions of the bonding experiments with different sequences, in which order the individual rings are scanned (cured), always resulted in the same three rings in the same positions not to be bonded (see Figure 4.10a)). Standard glass micro spheres with a variation in diameter of at least ±100 µm and limited sphericity were used to apply the pressure as a point load. In order to investigate whether the diameter variation significantly affects the bonding force applied individually to every sample on the chip the orientation of the glass wafer with the glass spheres attached to it was changed in

respect to the pattern to be bonded. A clockwise rotation of the glass wafer by 90° resulted in a 90° shift of the positions of the non-bonded rings as sketched in Figure 4.10b). The three remaining rings probably cannot be bonded because an insufficient force is applied during bonding due to a smaller diameter of the glass spheres in these particular positions.

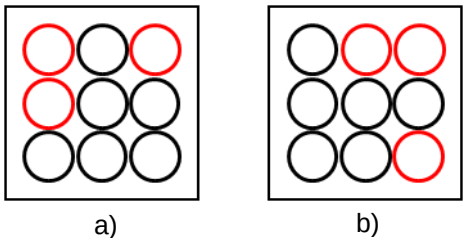

Figure 4.10: Sketch of BCB pattern indicating bonded rings (black) and structures with no contact of the bond interfaces (red)

To achieve a more even force distribution onto every individual ring structure and bonding of all nine samples further trials using micro-precision glass spheres (diameter 2 mm) were accomplished. These glass spheres feature a diameter tolerance of ±1 µm and spherical tolerance of $\leq \lambda/4$ at 587.6 nm. The bonding experiments showed that a slightly higher yield rate could be achieved. Successful bonding of seven to eight of the nine samples could be achieved with high repeatability, comparable to the yield rate of 87.5% achieved by Mohan et al. [99] who investigated wafer-level solder bonding in a laser-based process. The best bonding results could be achieved with the following laser parameters:

- for the small spacing a laser illumination of 32 W for 50 s for every individual ring and
- for the large spacing 37-39 W for 76-90 s.

In contrast to the pattern of 5, where a slightly higher energy was required to bond the sample in the centre, a different effect was observed for the pattern of 9, especially for the small spacing. At the closest point, there is a distance of only 200 µm between the BCB rings. Due to the close proximity the neighbouring rings were partly cured already by lateral heat flow while the ring next to them was illuminated. Hence, the ring in the centre did not require any additional heat input to be fully cured. Inspection of the structures which were not joined successfully showed that either they were only partly bonded along the sealing layer (compare Figure 4.7a)) or they had no contact of the bond interfaces at all. There was no significant difference in the yield of the joined

structures between the two different spacings, even though a lower success rate might have been expected for the small spacing pattern due to the higher stress in the cover glass caused by the closer proximity of the samples.

In some cases bonding of all 9 devices on the same wafer (see Figure 4.11) could be achieved demonstrating the feasibility of using this laser-based localised heating joining process in adhesive wafer-level packaging. First all BCB rings were scanned successively and then the force, which is applied during the bonding process, was released and re-applied again. This resulted in a slight shift of the wafer and the way the force is distributed on the cover glass. The rings which could not be bonded due to a lack of contact of the bond interfaces during the first attempt were scanned again with the laser and bonded successfully.

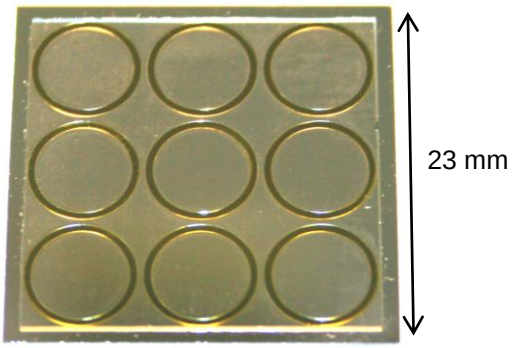

Figure 4.11: Photograph of bonded wafer with full contact of all samples along the entire bond line; small spacing pattern of 9

Closer investigation of the wafers with glass spheres attached to them for applying the force to every individual sample on the wafer showed that the spheres are set at slightly different heights (±50 µm); hence the force is not evenly distributed on all samples as intended. Substitution of the standard glass spheres with the micro-precision spheres did not resolve this issue entirely. The height difference does not only result from the variation in diameter of the glass spheres as previously assumed. As described in section 3.2.4, small recesses were laser-machined into the glass wafers to ensure a high positioning accuracy of the glass spheres. Inspection of these recesses under a microscope revealed that they vary slightly in depth and diameter. Refinement of this laser-machining process should overcome this issue and result in an even distribution of the force. For this reason it is this particular setup and not the actual bonding approach itself that is the limitation of this packaging process. This is underlined by the fact that

all structures can be bonded when the force is re-applied. If the setup were to be re-engineered with a particular focus on this bonding force issue, bonding of all nine structures on the same wafer with high repeatability is to be expected. An alternative approach to apply the bonding force individually would be the use of a spring loaded system. Such an approach was rejected due to the requirement for a very compact design, to avoid obstruction of the laser beam, as explained in section 3.2.4.

4.3.2.2 Shear Force Testing

The samples were subjected to shear force testing after dicing the wafers into individual samples. The testing was carried out by Optocap Ltd. As with the pattern of 5, the mechanical dicing process sometimes caused samples either to split apart or initiated partial delamination of the adhesive layer along the bond line. The shear forces were reduced in comparison with the chip-level packaged devices and the pattern of 5. This reduction was greater for the small spacing pattern, where shear forces averaged around 60 to 70 N, although with some samples achieving up to 95 N. Inspection of the shear force tested devices showed that the bond failure mostly occurred at the silicon interface. The close proximity of the neighbouring samples on the wafer and the reduced bonding force of 2.7 N due to the delicate cover glass resulted in reduced wetting during the bonding process. For the large spacing pattern slightly higher shear forces could be achieved; averaging around 80 to 90 N with a maximum of 150 N. All shear force test results are summarised in the plots shown in Figure 4.12.

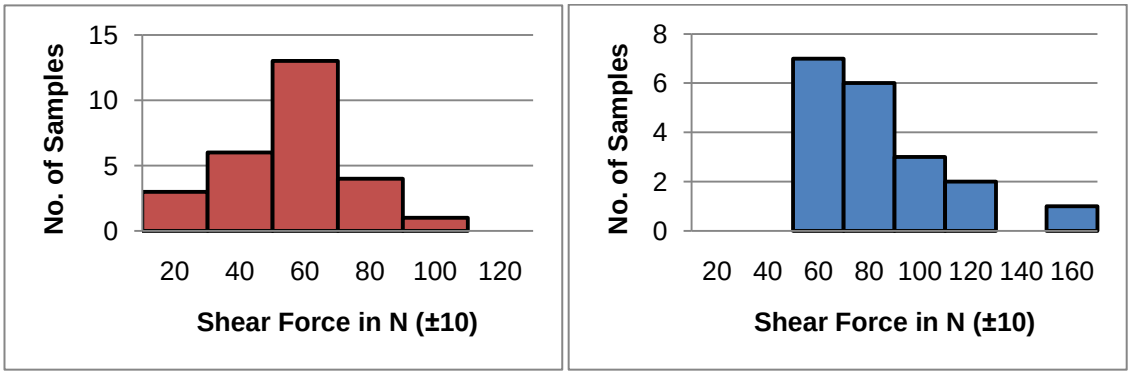

Figure 4.12: Plot of shear force test results for laser-bonded silicon to glass packages using pattern of 9. Left: small spacing; right: large spacing

Due to the wider distance between the neighbouring samples for the large spacing the stress in the cover glass can be greatly reduced and the wetting of the silicon surface during bonding is improved. The join failure mostly occurs at the glass interface or in the BCB adhesive layer. For shear forces above 100 N the cover glass started to crack;

in these cases the strength of the seal is exceeds the mechanical stability of the cover glass of thickness 200 µm. Even though the shear forces are lower for the pattern of 9, restricted by the mechanical stability of the cover glass and wetting of the silicon interface during bonding, this process benefits from a considerable reduction in production time and therefore costs. More importantly, the device to be packaged can be protected from dust and moisture ingress prior to dicing whilst still providing a reasonably high shear force.

In summary, a wafer-level packaging approach of silicon to glass with a BCB intermediate layer was demonstrated for two simplified patterns in a laser-based process. Additionally, the high temperatures were restricted greatly to the joining area only by active cooling. For a basic pattern of 5, successful bonding of all individual samples on the same wafer was achieved proving the feasibility of laser-based joining in such packaging processes. Average shear forces of around 165 N (large spacing) for an individual package after dicing were accomplished, comparable to results of chip-level packaging (typically ~170 N) and samples bonded using conventional flip-chip bonding (typically ~220 N) [56]. For the more complex pattern of 9 shear forces with an average of 80 to 90 N (large spacing) were achieved. Despite the reduced mechanical stability of these packages this process benefits from the two main advantages of wafer-level packaging – considerable reduction in process time and protection of the devices to be encapsulated prior to dicing.

4.4 Conclusions to Chapter 4

Adhesive layer bonding, in particular on a wafer-level, is a simple and robust process featuring the following key advantages: insensitivity to dust particles, surface roughness and non-planarization up to a few microns of the bond interfaces, thereby reducing process costs. Very few limitations exist for the choice of the materials to be bonded; and most importantly wafer-level packaging benefits from protection of the device to be packaged from dust and moisture ingress prior to dicing [3]. Traditionally these packaging processes are carried out using substrate bonders restricting the use of temperature sensitive materials within the package. In this chapter the combination of the benefits of laser-based joining – truly localised heating – and adhesive layer bonding was demonstrated in a novel localised heating packaging approach using the example of joining glass to silicon with a BCB intermediate layer. Due to the long time constant of the bonding process (tens of seconds) and the high thermal conductivity of the silicon

substrate (149 W m^{-1} K^{-1}) the heat flow to the sensitive device area in the centre was restricted further by active cooling. This novel bonding procedure was first demonstrated for single chip packaging and then a further development of this process to wafer-level packaging was shown. To assess the quality of the laser-sealed devices the bonding experiments were accompanied by shear force testing.

4.4.1 Chip-level Packaging

Successful chip-level packaging was demonstrated in a laser-based process where the temperature in the centre of the device was kept at least 120°C lower than in the bonding area. Optimisation of the bonding parameters has shown that there is a trade-off between the bonding speed and the quality of the seal. For bonding times down to 8 s, shear forces of 150 N on average with a maximum of 290 N were achieved. This is comparable and some cases even higher than results obtained by other researchers using conventional flip-chip bonding (typically ~200 N) [56] and the results (typically ~170 N) presented in the feasibility study on laser-based adhesive layer bonding here at Heriot-Watt University. The latter bonding techniques, however, both resulted in heating of the entire device during the bonding process unlike the localised heating process presented in this study. The comparison of the shear force test results shows that the selective laser heating and the heat sinking do not lower the mechanical stability of the seal provided that a full cure of the BCB adhesive layer has been achieved.

For further improvement of this bonding process control of the bonding temperature and laser power respectively (see chapter 3.3.1) would be highly desirable. Temperature measurements by pyrometry were identified as the only viable technique to accurately monitor the temperature in the joining area. For the experiments described above, the bonding parameters had to be obtained in experiments by judging the degree of cure of the BCB adhesive layer by its colour change. In some cases it turned out to be rather difficult to evaluate when exactly a full cure was achieved. Therefore, sometimes a range of bonding parameters, in particular for the samples bonded on a wafer-level, has been defined, rather than discrete optimal parameters. An alternative, more accurate method to determine the exact degree of cure is to monitor the change of certain peaks in the absorption spectrum of the BCB using FTIR spectroscopy. It is recommended that this method should be used in any future investigations.

4.4.2 Wafer-level Packaging

The feasibility of wafer-level packaging in laser-based joining was shown with successful bonding of simplified patterns of 5 or 9 samples on a single wafer. For the pattern of 5 successful bonding of all samples on the wafer was achieved for both spacings. The best bonding results were accomplished with the following parameters:

- a laser power of 30 W was applied for 50-70 s to each individual ring for the small pattern and
- 33 W for 57-77 s for the large pattern.

Comparison with devices packaged at chip-level showed that for the pattern of 5 with the large spacing the same quality of the seal with shear forces averaging around 165 N and a maximum of 285 N could be achieved. A reduction of the distance between the neighbouring samples resulted in a slightly reduced bond quality. A process such as this can be used in applications where high seal strengths and wafer-level packaging are required given the benefits of parallel processing out-weigh the waste of material (un-used silicon areas) due to the reduced sample density.

After successful packaging of this basic pattern a more densely packaged pattern of 9 samples on the same wafer was investigated. This pattern resembles full wafer-level bonding. The best bonding results were achieved for the following parameters:

- for the small spacing a laser power of 32 W for 50 s and
- for the large spacing 37-39 W for 76-90 s.

In some cases successful sealing of all nine samples on the same wafer was achieved proving the feasibility of wafer-level packaging using this localised heating bonding process. In most cases bonding of seven to eight of the nine samples could be achieved with high repeatability, comparable to the yield rate of 87.5% achieved by Mohan et al. [99] who investigated wafer-level solder bonding in a laser-based process. For the pattern of 9 with the small spacing, shear forces averaging around 60 to 70 N and a maximum up to 95 N were shown and for the large spacing an average of 80 to 90 N and a maximum of up to 150 N. The shear forces were considerably lower than for the devices packaged on a chip-level. They are restricted by the mechanical stability of the cover glass of thickness 200 µm and by the reduced wetting of the silicon interface during bonding due to the higher stress in the cover glass of the more densely packed

pattern. This process, however, is beneficial in applications where the device to be encapsulated needs to be packaged prior to dicing to protect it from dust and moisture ingress during the dicing process.

To improve this process and to achieve successful bonding of all nine samples on the same wafer with high repeatability the setup needs to be refined further with particular focus on applying the bonding force individually for every single device. Once this issue has been resolved this bonding method can easily be extended to larger numbers of individual samples on the same wafer.

5 Hermetic Packaging of LCC Packages Using Glass Frit Layer

This chapter presents an investigation of glass frit material as a sealing layer for hermetic packaging of Leadless Chip Carrier (LCC) devices in laser-based processes. There are well-documented [43, 44] advantages associated with glass frit packaging for the encapsulation of micro-devices, however, established processes require the entire package to be heated to the joining temperature of typically 300°C to 500°C. In this chapter the development of two laser-based glass frit packaging processes in both air and vacuum is presented. The process development focuses on the restriction of the high process temperatures to the joining area only. The development of a temperature monitoring method of the glass frit packaging process and quality testing of the packaged devices are also included in this chapter.

As described in chapter 2, glass frit packaging is a universal, simple and robust method and provides a very promising solution to the significant challenges in the encapsulation of micro-devices. One of the main advantages of glass frit bonding is the non-stringent requirements for the flatness of the surfaces to be bonded due to the high wetting abilities which even enable bonding of unpolished surfaces. Hermetic seals with high bonding strength can be achieved with most materials commonly used in manufacturing and packaging of micro-devices in high yield (>90%) processes and with good process repeatability. Conventional glass frit packaging processes are mostly furnace-based and hence, such processes do not allow temperature sensitive materials (e.g. polymer and magnetic materials) to be used within the package since the entire device is heated to the bonding temperature of several hundred degrees. These furnace based processes also generate problems in multi-step bonding processes where several bonding cycles need to be carried out in sequence where parts joined in an earlier heating step can disassemble in a later one.

An ideal solution here is to use a high power laser as a highly localised heat source to minimise the heat input into the bulk of the device. In this chapter the clear benefits of combining the merits of both glass frit packaging and localised laser heating to laser-based LCC packaging processes are demonstrated. Due to the long time constants (up to several minutes) of the bonding process, appropriate heat sinking was also introduced to further reduce the lateral heat flow from the bond line to the sensitive device area and thereby minimize the local temperature rise during the bonding process.

5.1 Packaging in Air

In this section hermetic glass frit packaging of LCC packages in air using glass frit material (supplied by Diemat) is investigated. The samples are joined according to the laser-based localised heating packaging process previously described in section 3.2.3.2. The pre-bonding preparations and deposition of the glass frit layer are presented followed by detailed temperature monitoring experiments, bonding experiments and finally quality testing of the seal. General characteristics for the glass frit material are given in section 2.5.2.

As mentioned before, the work of this PhD is a continuation of a project in laser-joining of micro-devices here at Heriot-Watt University which already began before the start of this PhD. Initial results on glass frit packaging of micro-devices were obtained by Q. Wu, who worked on the project at the time. During the first months of this PhD project, the author working in collaboration with Q. Wu presented a study [114] in which the feasibility of hermetic packaging of micro-devices in air using a glass frit intermediate layer in a laser-based process was demonstrated. The benefits of glass frit as sealant were highlighted; however in this case the heating was not properly localised. In this subsequent work the management of the heat flow within the package and the development of a truly localised heating process are described.

As discussed in chapter 2, the work presented in the paper [114] is a feasibility study on using laser heating in glass frit packaging. Hermetic packaging of a range of miniature packages and materials, which are all realistic packages used in actual device manufacture, was demonstrated. The main aim of the study was to show the ability of the laser to provide the required localised heating. The samples to be joined were placed on top of a thermal barrier (glass slide) for simplicity. As no measures were taken to prevent heating inside the devices due to lateral conduction, the whole sample was heated to a high temperature despite the localised heat input into the sample. To restrict the lateral heat flow to the sensitive device area in the centre of the package (substrate), the underside of the package must be placed in good thermal contact with an appropriate heat sink. From the range of packages investigated in the feasibility study the LCC package appeared to be the most suitable for further investigations in this study. With this type of package strong, hermetic seals were achieved. Shear forces of up to 600 N were required to split the samples open again. Even if the surface of the

substrate contained micro-machined grooves up to 100 µm deep, the glass frit was able to flow into these and so did not influence the hermeticity of the seal.

5.1.1 Bonding Experiments

5.1.1.1 Sample Preparation

The substrate used in all bonding experiments is the cavity style LCC (Figure 5.1), which is a standard off-the-shelf electronic package. It is commonly used to house micro-devices and electronic chips in commercial applications. It is manufactured by Kyocera and is made from a high temperature co-fired ceramic – mostly alumina (90%) together with some other glassy components for binding. The outer dimensions of the substrate are 14.2×14.2×1.5 mm with a cavity 8.9×8.9 mm by 1.02 mm deep in the centre. This substrate is originally intended for solder bonding. Metallised layers (nickel and gold) are deposited on top of the ceramic at the bond interface to improve the wetting of the solder. These layers have been removed from some of the substrates prior to bonding using a polishing process because they would not be used in a package specifically designed for sealing using glass frit. From now on such polished substrates are referred to as bare LCC substrates and the original ones simply as LCC substrates. A gold-plated Kovar™ lid (Figure 5.1) of dimensions 13.1×13.1×0.25 mm is used with these substrates. It is also intended for solder bonding. For this reason it is supplied with a solder preform attached along the edges of the bottom side of it. This preform is removed manually with a scalpel. Great care has to be taken that all solder is removed before the glass frit intermediate layer is applied.

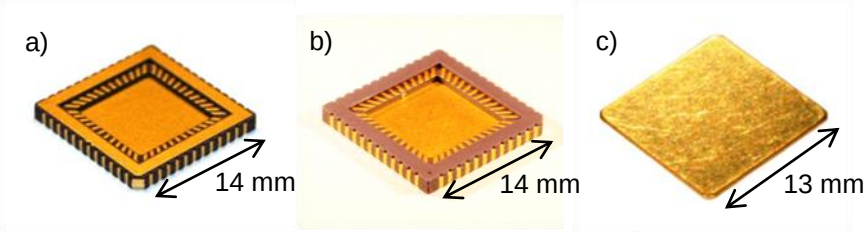

Figure 5.1: Photograph of a) LCC substrate b) bare LCC substrate – metallised layers removed in polishing process, glass frit bonded directly to bare ceramic – and c) gold-plated Kovar™ lid

The glass frit material used for the bonding experiments in air is the paste DM2700P/H848 from Diemat. It is particularly suitable for laser-based packaging processes for two main reasons: it has a short bonding time (only 60 s if bonded at 375°C) and it can tolerate the high temperature ramp rates possible in laser processes.

As the glass frit only needs to be applied onto one of the surfaces to be joined, the lid is always chosen, since for conditioning of the paste it needs to be heated up to the bonding temperature during the final glazing step. In packaging of real devices the substrate would contain the device to be packaged which should be exposed to as little heat possible. The glass paste can be screen printed or dispensed by syringe onto the lid. For initial experiments the paste was dispensed by syringe. To achieve a more reproducible thickness and width, together with a higher positioning accuracy of the layer on the lid, a simplified screen printing process was designed as shown in Figure 5.2. A sample holder for four lids was designed and machined from aluminium, and the screen printing mask was cut out of an aluminium sheet of thickness 300 µm using a nanosecond pulsed Nd:YVO_4 laser.

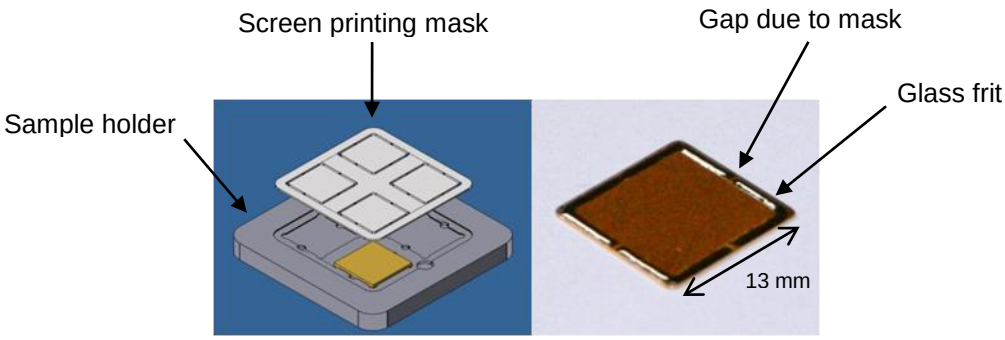

Figure 5.2: Sketch of screen printing and photograph of lid with glass frit layer

The lids are placed into the recesses in the sample holder and the screen printing mask is placed on top aligned by a further recess in the sample holder. The glass frit paste is screen printed onto the lid simply by forcing the paste through the slits in the mask with a razor blade. Afterwards the mask is removed and the lids with the glass frit layer on top are transferred onto a hot plate for the conditioning of the paste (organic burnout, glazing) as described in section 2.5.2. After glazing, the glass frit layer has a thickness of around 250 µm and a width of 700 µm. A photograph of such a lid with glass frit deposited on top is shown in Figure 5.2. Due to the design of the mask, small bars (fillets) are required to hold the centre pieces of the mask in position, and as a result there are four gaps of width around 500 µm as highlighted in Figure 5.2. These gaps reflow completely during the sealing process due to the very good wetting abilities of the glass frit and have no adverse effect on the hermeticity or strength of the seal.

5.1.1.2 Bonding Procedure

After the pre-bonding steps, the LCC packages are bonded according to the laser-based joining method described in section 3.2.3.2. In the feasibility study presented in [114] no heat sinking was provided which led to a significant temperature rise at the centre of the LCC package. In the experiments described in the following sections heat sinking has been introduced to restrict lateral heat flow into the centre of the device and to achieve truly localised heating. To remove the excess heat during the bonding process the substrate is placed in good thermal contact with the copper block. The gold-plated Kovar^{TM} lid with the glass frit layer is placed on top of the substrate.

To overcome the very limited absorption of gold at the laser wavelength of 940 nm a square piece of silicon is placed on top of the lid. A small amount of pressure is applied to the sample by applying a force from below via the pneumatic cylinder, pressing it against a glass sphere, and the sample is then bonded by scanning the laser beam at high speed (1000 mm s^{-1}) along the edges of the silicon piece. A photograph of the bonding setup and a schematic presentation of the bonding process are shown in Figure 5.3.

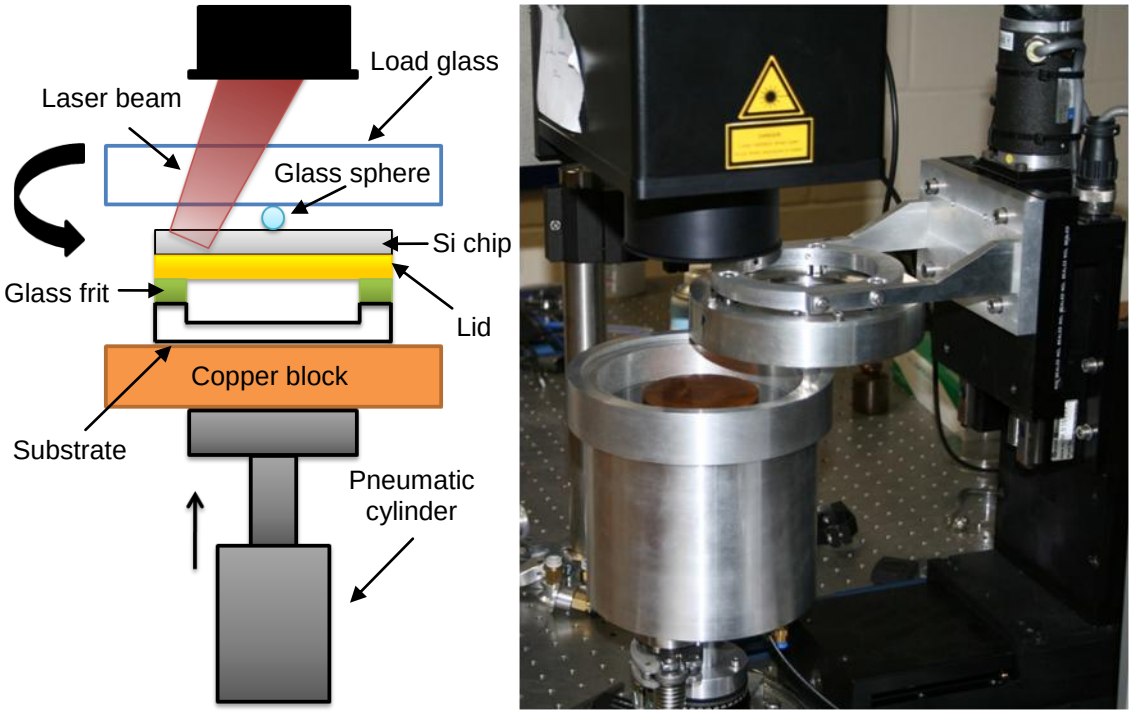

Figure 5.3: Sketch and photograph of bonding setup

5.1.1.3 Initial Bonding Experiments

Initial bonding trials using the new setup, and in particular introducing the concept of heat sinking, were carried out to test the potential of this novel bonding procedure. In

established processes glass frit packaging relies on heating in a furnace or substrate bonder where multiple samples can be bonded at the same time. With this laser-based process only one sample can be bonded at a time. A major advantage of laser heating is that in contrast to furnace heating no prolonged intervals for heating up and cool down are required. On switching the laser on or off, the full power (energy) is directly available or instantly stopped again. So the sample is only heated during the laser illumination (bonding time). Using this process scheme, the time for an entire bonding cycle, including warm up and cool down can be reduced considerably. Also, the time that the entire package is exposed to elevated temperatures is reduced greatly. This is beneficial in applications where temperature sensitive materials are packaged. According to the manufacturer's recommendation, reliable and hermetic seals can be achieved in as little as one minute with this type of glass frit material if sealing at a temperature of 375°C. Since this required temperature can be achieved in a very short interval, a short heating period of 60 s – the minimum bonding time – was selected. At this early stage of the project no method for temperature monitoring was available. The laser power, which is required to provide sufficient heating for bonding, was obtained by trial and error. A laser illumination power of 80 W for 60 s was found to be the optimum in order to fully reflow the glass frit sealing layer. Six samples were bonded using these parameters. A photograph of such a typical bonded LCC package is shown in Figure 5.4.

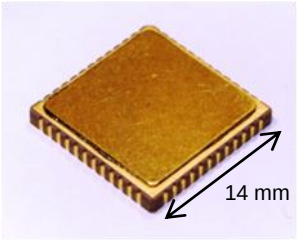

Figure 5.4: Photograph of laser-bonded LCC package

The samples manufactured in this initial trial were subjected to a simplified test routine to assess the quality of the seal. First they were inspected visually to check if the glass frit did reflow along the entire length of the seal, i.e. some glass frit escapes between the lid and the substrate due to compression of the sealing layer (Figure 5.5). For a basic gross leak test the packages are submerged in the test fluid FC-40, the higher boiling point test fluid (see section 2.6.1), at a temperature of 120°C and in case of a gross leak a stream of air bubbles will emerge from the sample. After a successful pass the sample

were subjected to helium leak testing according to MIL-STD-883G. Normally the fine leak test has to be carried out first as the liquids used in the gross leak test might shield smaller leaks. At this initial stage of the experiments, however, most samples already failed the gross leak test. The sequence of the test was reversed as the gross leak test is much simpler to accomplish. To test the mechanical stability of the seal, the samples were dropped twice from a height of around 2 m to a hard floor. If the packages remained bonded this was regarded as a pass otherwise not.

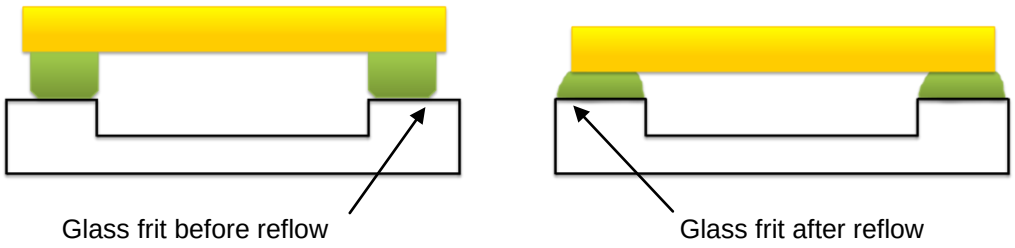

Figure 5.5: Sketch of LCC package before and after reflow of glass frit

From the six samples bonded at a laser power of 80 W one sample passed this simplified test routine, including the fine leak test. Prior to bonding a small quantity of thermo-chromatic paint was applied to the centre of the substrates to obtain an initial indication in of the temperature rise in the centre of the package. According to this method the temperature in the centre remained below 130°C throughout the entire bonding process.

These preliminary bonding experiments demonstrated for the first time that it is possible to achieve full hermetic seals in this laser-based glass frit packaging process where the temperature in the centre of the device is kept considerably lower than in the joining area. Knechtel [43, 44] states that temperature is the most important process parameter in glass frit packaging. Therefore, detailed temperature monitoring experiments are required to get a good understanding of the temperature cycle during the bonding process and especially to improve the yield of the process.

5.1.2 Temperature Monitoring

5.1.2.1 Introduction

In previous glass frit bonding experiments hermetic sealing could be achieved but the yield was only limited. A temperature monitoring method was developed to investigate the relationship between the temperature inside the bonding layer and the laser power in order to obtain a better understanding of the temperature cycle during the bonding process. A detailed description of the temperature monitoring method and the sample preparation is given in section 3.3.2.

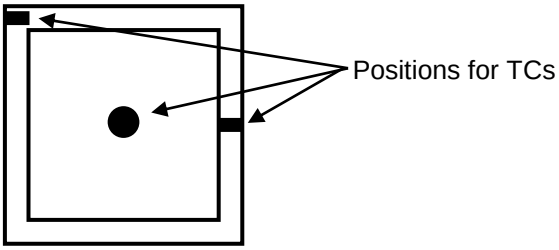

Figure 5.6: Sketch of LCC substrate for temperature monitoring with positions for thermocouples (TCs); two in joining area and one in the centre of the device.

Three miniature K-type thermocouples are integrated into the substrate at the positions shown in Figure 5.6. Two of these are placed along the bonding track – in the middle of one side and in one corner – to investigate the heat distribution and to ensure that the correct bonding temperature is used. A third thermocouple is integrated into the centre of the substrate to demonstrate the localised heating nature of this laser-based process and to quantify the likely temperature of any device mounted in the centre of the package.

5.1.2.2 Calibration of Laser Power to Bonding Temperature

A first set of temperature monitoring experiments was performed to determine the relationship between the laser power and the temperature inside the bonding layer. For these measurements it is only necessary to monitor the two thermocouples along the bonding track. According to the Diemat glass frit material datasheet, reliable and hermetic seals can be achieved if fired at a peak temperature of 375°C for 1 minute [52]. A series of measurements was taken for both types of substrates – LCC and bare LCC – in which the laser power was gradually increased and the steady-state temperature inside the joining layer recorded to determine the laser power required to achieve the optimum bonding temperature of 375°C. The results for the LCC substrate are plotted

in Figure 5.7. The laser power is plotted against the temperature inside the bonding layer once it has reached its steady-state.

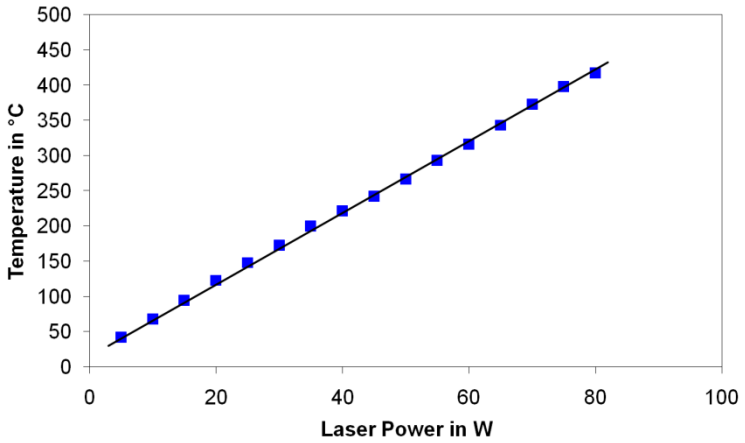

Figure 5.7: Temperature inside bonding layer vs. laser power (LCC substrate)

A linear dependency of the temperature on the laser power was observed. The graph of the bare LCC substrate looks very similar as shown in Figure 5.8. It has a slightly lower slope as a higher power is required to reach the same temperature within the bonding layer.

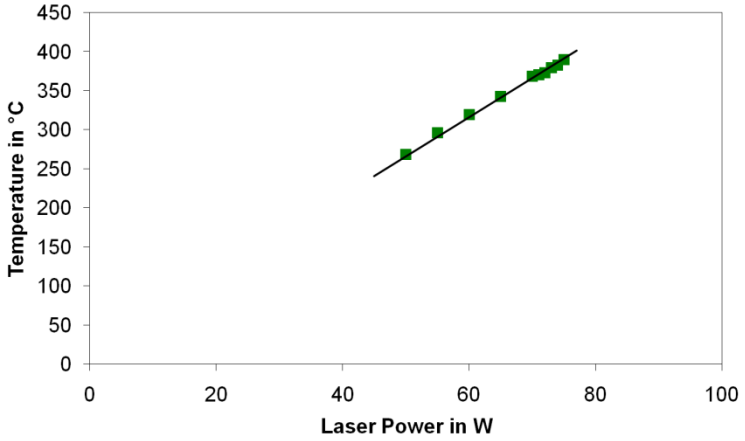

Figure 5.8: Temperature inside bonding layer vs. laser power (Bare LCC substrate)

For the LCC and bare LCC substrates laser powers of 70 W and 72 W respectively are required to heat the bonding layer to the required temperature of 375°C for the shortest possible bonding time of 1 minute.

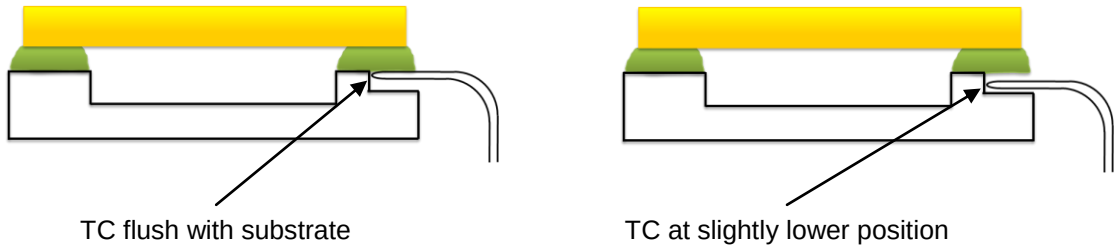

Figure 5.9: Sketch of vertical position of thermocouple (TC) in LCC substrate

During these initial temperature monitoring experiments it was noted that great care has to be taken when integrating the thermocouples into the LCC substrate. The vertical position of the thermocouple in the substrate (see Figure 5.9) is critical. It is important that the thermocouples are flush with the substrate surface to give a correct reading of the temperature inside the glass frit layer. Since the package is heated from the top whilst being cooled from the bottom, a steep temperature gradient exists within the substrate. A misalignment of the thermocouples can result in temperature readings reduced by 50-100°C. A typical example of such a temperature profile of a bonding process where one of the thermocouples is placed at a slightly lower position (~200 µm) is shown in Figure 5.10. In this particular example, at a laser illumination of 70 W the thermocouple positioned flush with the substrate gives a reading of 375°C whilst the other one only records a temperature of around 275°C.

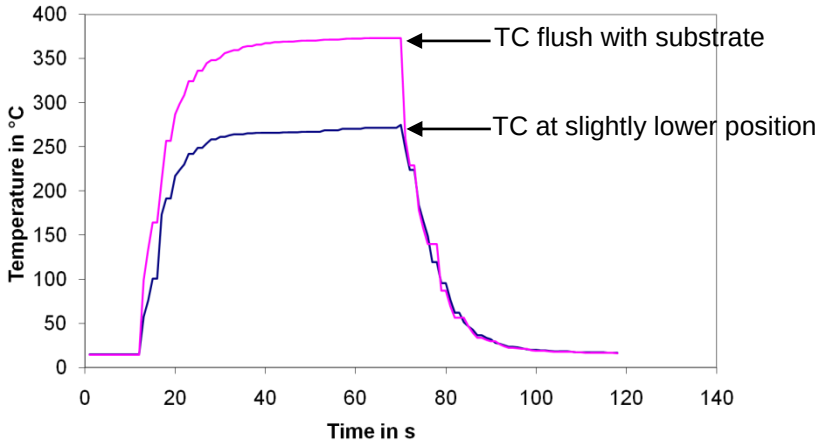

Figure 5.10: Temperature plotted as a function of time during the laser bonding process (laser power 70 W, time 60 s). Pink trace: TC flush with substrate surface; blue: TC at a slightly lower position (~200 µm).

5.1.2.3 Temperature Monitoring of LCC Packaging Process

In order to quantify the temperature reached in the centre of the package, the thermocouple in the centre of the substrate was also used. As described in section 3.3.2, the substrate is placed on a special cooling platform made from copper with a through-

hole in the centre for the thermocouple. Thereby it is guaranteed that the substrate is cooled in the same way during the temperature monitoring experiments as with the normal bonding process. Typical temperature profiles inside the bonding layer and in the centre of the device of such a LCC packaging process at a laser power of 70 W is shown in Figure 5.11.

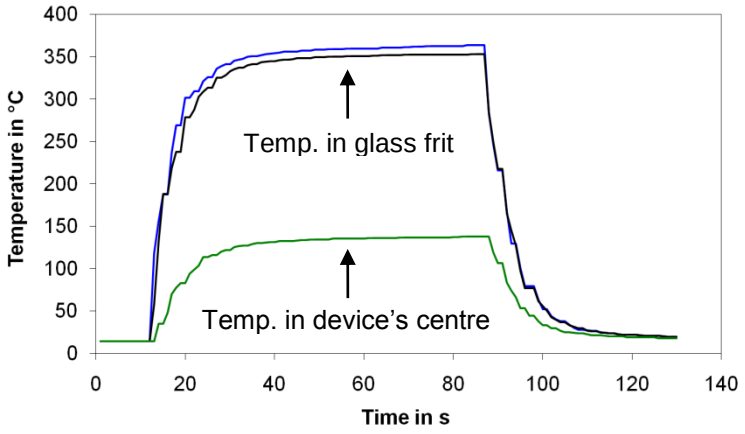

Figure 5.11: Temperature plotted as a function of time during the laser bonding process (laser power 70 W, time 75 s). Blue and black traces: inside bonding layer; green: on substrate in the centre of the device.

At switch-on of the laser, a steep increase in the temperature of the bonding layer is observed. After around 15 s the curve flattens and the temperature remains fairly stable at a value of around 375°C. The temperature has reached a steady-state where the rate of heat energy removal by the copper block equals the rate of laser energy being absorbed. Once the laser has been switched off, the sample cools down to room temperature again in less than 20 s. The two thermocouples in the different positions along the bonding track – in the middle of one side and in one corner – give almost the same reading, i.e. the heat is spread evenly along the bonding track. Due to the high speed scanning of the laser beam (1000 mm s^{-1}) along the edges of the lid the entire bonding track is heated up quasi simultaneously and the heat does not accumulate in the corners. The position of the thermocouple along the bonding track during temperature monitoring is not critical. This is in contrast to the vertical position, where it is important that the thermocouple is flush with the substrate surface, as explained above.

Most importantly, the temperature in the centre of the device always remains substantially lower than in the bonding area. The temperature is kept below 140°C throughout the entire bonding process despite the required temperature of 375°C in the joining region (see Figure 5.11). This demonstrates that the lateral heat flow in the

substrate is reduced considerably by the water-cooled copper block. Truly localised heating can indeed be achieved by this laser-based glass frit packaging process. Repetition of the temperature monitoring experiments with a number of samples showed that the results were very repeatable. Nearly identical temperature profiles within ±10°C could be achieved given the thermocouples along the bonding track were positioned flush with the surface of the substrate.

The manufacturer's shortest recommended bonding time for this material is 1 minute, if the glass frit is sealed at a temperature of 375°C. Since it takes around 15 s to reach a steady-state (sealing temperature) within the bonding layer the shortest bonding time (time of laser irradiation) possible with this setup is 75 s instead of 60 s, including the additional time for the temperature ramp. The total time for an entire bonding cycle, including the 20 s it takes the sample to cool down to room temperature again, only accounts for 95 s. Based on the temperature monitoring experiments the following optimum bonding parameters were obtained for this laser-based process: a laser illumination of power 70 W (LCC substrate) and 72 W (bare LCC substrate) respectively for a bonding time of 75 s. These optimised bonding parameters were used for all further glass frit bonding experiment of LCC packages in air.

5.1.2.4 Temperature Monitoring with Heat Conductive Material

Additional temperature monitoring experiments were performed to determine whether the temperature in the centre of the device can be reduced any further. A heat conductive material is placed between the bottom of the LCC substrate and the copper platform to increase the rate of thermal transfer. The material under investigation is a soft, silvery metal sheet (Liquid MetalPad^{TM}, Coollaboratory) of thickness around 50 µm. It has a high thermal conductivity of 126 W m^{-1} K^{-1} and consists mainly of indium, bismuth, tin and copper. The material is soft enough to fill any insulating air gaps between the surfaces of the copper block and the substrate caused by their inherent surface roughness. A graph of the temperature profile of such a bonding process using the heat conductive material is shown in Figure 5.12. In this case, a LCC substrate was bonded at a laser power of 70 W. For ease of comparison the typical temperature evolution curve within the bonding layer at the same power level but without the heat conductive material is included in the figure (blue trace).

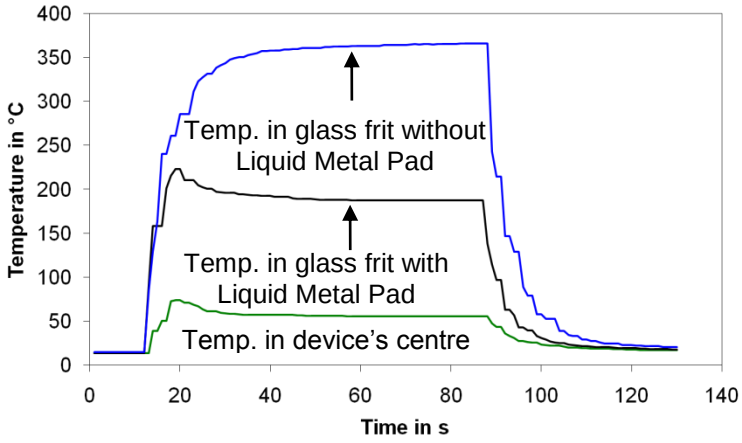

Figure 5.12: Temperature plotted as a function of time during the laser bonding process (laser power 70 W, time 75 s). Blue trace: inside bonding layer without Liquid Metal Pad; black trace: inside bonding layer with Liquid Metal Pad; green trace: on substrate in the centre of the device with Liquid Metal Pad.

Figure 5.12 shows that the Liquid Metal Pad results in much lower temperatures in the joining area (around 200°C instead of 375°C) and in the centre of the package (around 55°C). The heat transfer between the bottom of the substrate and the copper block is greatly improved by the Liquid Metal Pad. Further experiments demonstrated that significantly higher laser powers (around 125 W) are required to achieve the desired temperature of 375°C in the bonding layer. In this case the temperature in the centre of the substrate rises to just below 140°C, as before. Although the heat conductive material clearly increases the heat exchange rate between the substrate and the cooling block, it has no beneficial effect with regard to restriction of the lateral heat flow in the substrate. An alternative approach, which may be more effective, is to place the Liquid Metal Pad material only below the centre of the substrate to cool it locally. This is a promising alternative which could be investigated in the future.

5.1.3 Quality Testing, Results and Discussion

In this subsection quality testing of the LCC packages, which were sealed using the laser-based localised heating glass frit packaging process in air, will be discussed. These results will be compared to the results reported in the feasibility study on laser-based glass frit packaging [114] obtained in collaboration with Q. Wu to investigate the influence of the localised heating packaging approach on the quality of the seal. For better comparison, the samples are investigated using standardised test methods described in MIL-STD-883G, namely leak testing (TM1014), temperature cycling (TM1010), constant acceleration (TM2001), and shear force testing (TM2019.7). As

most of the equipment required for these test methods is not available at Heriot-Watt University the testing was mainly carried out by certified companies.

In total 23 LCC packages were bonded successfully using the optimised bonding parameters based on the experiences from the temperature monitoring experiments.

For packaging of:

- standard LCC substrates a laser power of 70 W for 75 s was used (12 samples)
- bare LCC substrates a slightly higher power of 72 W was required (11 samples)

for successful joining.

A bonding force of around 8 N was applied to an individual sample in all experiments to ensure sufficient wetting of the bond interfaces during the bonding process. After bonding the samples were inspected visually to ensure the samples are bonded and the glass frit layer is probably reflowed.

5.1.3.1 Leak Testing (TM1014)

One of the most common and crucial test methods is hermeticity testing. A hermetic seal keeps gases and moisture out of a package thus avoiding failure of the device due to condensing water and maintaining its protective atmosphere to ensure a proper functionality of the device for an extended period. Hence, it is a minimum requirement that the packages pass the hermeticity test according to test method 1014 of MIL-STD-883G for this newly developed glass frit packaging process to be of viable significance in commercial applications (micro-systems production). The samples were first tested in-house. The helium leak testing was carried out by Suzanne Millar. The gross leak testing was accomplished following the test procedure described in section 2.6.1. For validation of these results the samples were tested again by the 'Test House for the environmental testing' (ISO 17025 accredited) of C-MAC MicroTechnology, an industrial collaborator specialising in electronics for the automotive, aerospace and defence industries.

All samples were tested for fine and gross leaks in a two-step process. First the samples were checked for fine leaks using helium leak testing followed by bubble testing for gross leaks. 21 of the 23 samples passed both leak tests demonstrating that a reliable

joining process with a high yield of more than 90% has been developed. The test results obtained in-house agreed with the results of C-MAC in most cases proofing the validity of the testing capabilities at Heriot-Watt University.

The two samples which failed the leak test were investigated further. The lid was levered off with a scalpel. An inspection of the bond interfaces showed that the failure of the bond of one of the samples occurred due to overheating of the glass frit layer during bonding. In this case, a slight burnt smell was noticed directly after the bonding process when opening the bonding chamber. Most likely dirt particles between the bottom of the substrate and the copper block disrupted the heat exchange between the interfaces and caused a higher temperature (overheating) in the joining region. Hence, great care has to be taken when assembling the samples before bonding on the copper block that both interfaces – the bottom of substrate and the copper block – are dust (particle-free) to guarantee a reliable and constant thermal transfer. The bond failure of the second sample occurred due to insufficient reflow of the glass frit sealing layer. In this particular case some of the material must have remained stuck in the mask (close to the support structure of the central piece of the mask) during screen printing of the glass frit onto the lid. This resulted in a wider gap of the sealing layer and insufficient material to fill the gap during the reflow.

5.1.3.2 Shear Force Testing (TM2019.7)

Shear force testing is a test method to determine the mechanical durability of the seal; i.e. the force required to break the package open along the bond line is investigated. Ten of the sealed samples, five packages bonded to the LCC substrate and five to the bare LCC substrate, respectively, were additionally subjected to shear force testing after the leak testing. This testing was carried out by Optocap Ltd., a service provider specialised in packaging and assembly in microelectronics and optoelectronics. The failure of the join occurred exclusively in the joining layer itself. Excellent wetting of the bond interfaces is achieved using this laser-based glass frit packaging process. The strength of the seal is only limited by the mechanical strength of the glass frit layer itself. A typical photograph of such a split package is shown in Figure 5.13.

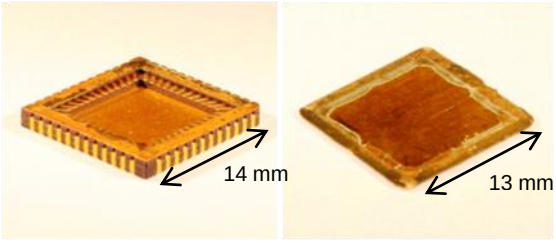

Figure 5.13: Photograph of split LCC package after shear force testing

Shear forces ranging from 232 N to as high as 855 N were required to displace the lid with these samples. All the shear force test results are given in Table 5.1.

Table 5.1: List of shear force testing results of laser-bonded LCC packages in air

Sample No.:	Substrate type:	Shear force (N):
1	LCC	500
2	LCC	293
3	LCC	293
4	LCC	232
5	LCC	482
1	Bare LCC	613
2	Bare LCC	407
3	Bare LCC	343
4	Bare LCC	855
5	Bare LCC	698

In the feasibility study on using laser heating in glass frit packaging [114], where the samples to be joined were placed on top of a thermal barrier (glass slide), shear forces up to 610 N were achieved for the packages with the glass frit bonded directly to the bare ceramic of the LCC substrate. The results in Table 5.1 show that three of the five samples bonded using this novel localised heating packaging process clearly exceed this value. This indicates that the active cooling of the substrate during the bonding process does not have any adverse effect on the quality (strength) of the seal despite the thermal stress which is generated within the package. For the ease of comparison of the shear forces achieved with the LCC substrate relative to the bare LCC substrate all shear force test results are illustrated in the plots shown in Figure 5.14.

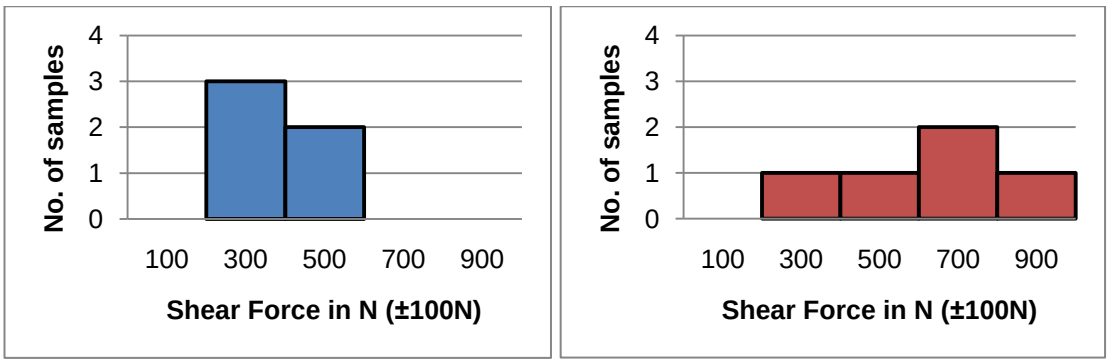

Figure 5.14: Plot of shear force test results for laser-bonded LCC packages in air. Left: LCC substrate; right: Bare LCC substrate

The tests indicated that the shear strength of the packages with the glass frit bonded directly to the bare ceramic of the LCC substrate tended to be higher than the one to the LCC substrate with the metallised surface. The reason for this is unclear as the failure of the join occurred in the sealing layer itself and not at the bond interface to the substrate. However, it may simply be a reflection of statistical variation across a small number of samples. The Diemat glass frit material appears to show good adhesion to both the locally rough bare ceramic and the comparatively smooth surface of the metallised layers (gold).

5.1.3.3 Cross Sectioning

Sectioning and polishing of both types of samples were carried out and the quality of the joints was assessed under a microscope. A typical micrograph of such a sectioned sample in Figure 5.15 shows the excellent wetting of the glass frit bonding layer with both interfaces (lid and substrate) without any voids. The darker areas in the sealing layer are not voids but rather the inorganic fillers contained in the glass frit material to match the coefficient of thermal expansion (see section 2.3.2). This micrograph also shows that the glass frit layer thickness is reduced from around 250 µm to 100 µm during the bonding process.

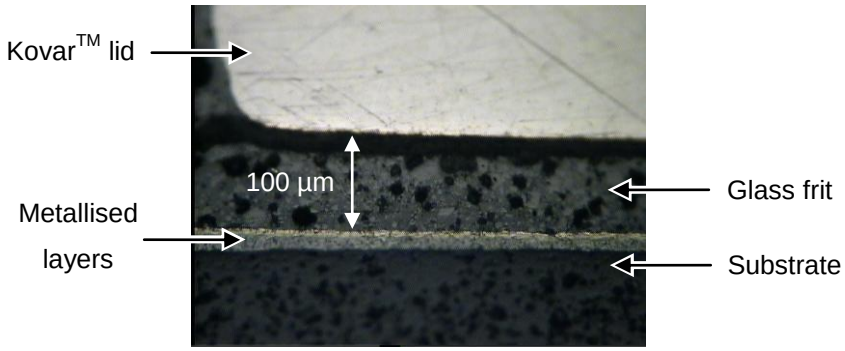

Figure 5.15: Micrograph of cross sectioned LCC package viewed under a microscope

5.1.3.4 Temperature Cycling and Constant Acceleration Testing

Temperature cycling (TM1010) and the constant acceleration testing (TM2001) were also carried out by the 'Test House for environmental testing' of C-MAC MicroTechnology. Five samples were submitted to the following test routine: temperature cycling from -65°C to 150°C (10 test cycles) followed by constant acceleration testing at 5000 g for 60 s. To determine whether the samples survived these test conditions they were leak tested again. After a successful pass, all five samples were subjected to a further 90 temperature cycles which was again followed by successful hermeticity testing. These extensive test methods have shown that this laser-based glass frit packaging process complies with a major part of the qualification process for military and space grade products.

In summary, the quality testing of the LCC devices packaged using the laser-based glass frit packaging process in air shows the well-known benefits of glass frit as a bonding material, i.e. it is capable of providing strong and hermetic seals and a high process yield. The main benefit of this novel bonding procedure is that the required high bonding temperature is strongly localised which enables packaging of temperature sensitive materials. By active cooling of the substrate, the temperature in the centre of the LCC package is kept below 140°C despite a temperature of 375°C over a period of 60 seconds in the joining area. A comparison with laser-bonded samples where the centre of the device was not actively cooled by using a thermal barrier below the substrate to eliminate contact with the heat sink showed that the active cooling of the substrate during the bonding process has no negative effect on the quality of the seal.

5.2 Packaging in Vacuum

In this section hermetic glass frit packaging of LCC packages in vacuum using the glass frit material supplied by Asahi Glass Company (AGC) is investigated. This is a further development of the previously described glass frit packaging process in air, requiring a different glass frit material and more careful thermal management. The samples are joined according to the laser-based localised heating packaging process previously described in section 3.2.3.2. Slight adaptations of the procedure are necessary to meet the special challenges in vacuum packaging. The development of the vacuum packaging process, including detailed temperature monitoring experiments is presented, followed by bonding experiments, and quality testing of the seal. Finally the packaging of miniature pressure gauges is demonstrated.

As mentioned before, applications in microsystems technologies often require a controlled atmosphere (e.g. low moisture content, no dust ingress) to ensure a reliable functionality of the device. Hermetic packaging is necessary to maintain this controlled atmosphere stable over the life-time of such packaged devices. Numerous applications such as resonant and tunnelling devices, pressure sensors, infrared detectors, vacuum displays and voltage controlled oscillators require a vacuum within the package for improved functionality [12]. In these applications, of course, hermetic seals with long-term stability are essential to ensure the same level of vacuum throughout the life-time of the device posing even higher requirements on the packaging process. Alternative vacuum packaging techniques have been developed; however, in general these require the entire package to be heated to the elevated joining temperature. Therefore, the further development of the previously described laser-based glass frit packaging process in air to vacuum packaging using localised heating will be presented.

5.2.1 Vacuum Packaging Process and Challenges

The vacuum packaging process is a further development of the laser-based glass frit packaging process in air described in detail in section 5.1. The glass frit material DM2700P/H848 (Diemat), used for the bonding experiments in air, is according to the manufacturer's recommendation not suitable for sealing in vacuum. The glass frit paste 5115HT1 (AGC) has however been specifically developed for vacuum packaging. Since the glass used in this paste is lead-free it requires a higher sealing temperature compared with the Diemat paste. The manufacturers recommend heating to 440°C for at least 10 minutes, so appropriate heat sinking is even more important if the centre of the package is to be kept cool. In addition, a maximum cooling rate of only 10°C min^{-1} is recommended.

Traditionally glass frit packaging is based on furnace heating which has far lower temperature ramp rates for heating and cooling cycles compared to the rapid temperature cycles possible with laser heating. In contrast, when the laser is switched on the temperature rises rapidly and drops almost instantly after switching off. The recommended firing profile of the glass frit paste is given for furnace based processing since a cool down rate of 10°C min^{-1} is recommended. In order to follow this guideline at the end of the bonding process the laser power has to be is gradually reduced to create a cool down rate of around 10°C min^{-1}.

5.2.1.1 Heat Transfer Mechanism in Vacuum

Initial temperature monitoring experiments in vacuum highlighted the significant thermal transfer issues (between the base of the substrate and the heat sink) that occur when the bonding atmosphere is changed from an air environment to a moderate vacuum. At atmospheric pressure, a temperature monitoring experiment with a number of samples proved that very repeatable results with nearly identical temperature profiles within ± 10°C are achieved (see section 5.1.2.3). Conversely under vacuum considerable fluctuations are typically observed. The laser power required to reach the desired bonding temperature fluctuates by up to ± 50%. Such a change in the required laser power can simply result from repositioning of the same sample on the copper cooling platform. This means that in a vacuum the thermal transfer between the base of the sample and the copper block is highly variable. The laser power, required to achieve the desired bonding temperature, is highly unpredictable resulting in a low process yield. Additionally an overall reduction of the thermal transfer rate from the device to the copper block is noted.

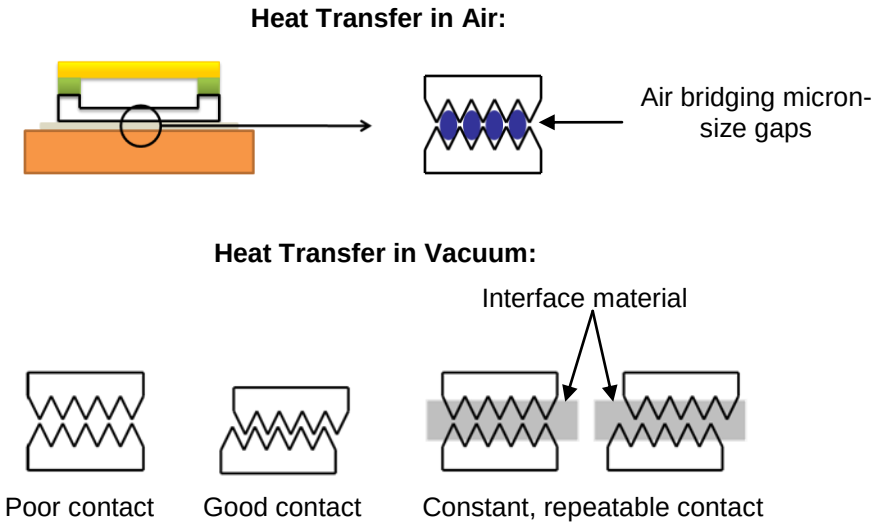

Figure 5.16: Sketch of thermal transfer between copper block and LCC substrate in air and vacuum

These phenomena can be explained by the inherent surface roughness of the contacting interfaces. Depending on how two surfaces are orientated to each other, the physical contact and therefore the thermal transfer by conduction varies, as shown in Figure 5.16. Under atmospheric pressure the thermal contact of these micron-sized gaps between the two interfaces is bridged by air despite its relatively low thermal conductivity of 1 W m^{-1} K^{-1}. In vacuum, however, the heat transfer between the base of the substrate

and the copper block relies mostly on conduction by contact only. The heat conduction varies greatly with the area of physical contact (see Figure 5.16). To resolve this issue, a soft thermally conductive material is placed between the contacting interfaces, which ensures a constant thermal transfer rate with high repeatability between the substrate and the copper block. This is essential for the precise temperature control required in this glass frit packaging process.

5.2.1.2 Vacuum Packaging Process

The sample used in all bonding experiments is the cavity style LCC substrate and the gold-plated Kovar™ lid (Figure 5.17), which were also used for the glass frit packaging in air. Only packaging of the LCC substrate in its original state with the metallised layers on top of the ceramic at the bond interface, which are required for proper wetting in solder bonding, was investigated. The previous experiments in air did not show any significant influence of the presence of these layers on the quality of the bond if glass frit is used as sealant. The glass frit paste 51115HT1 (AGC) is dispersed by syringe along the edges of the lid as it is insufficiently viscous to be screen printed. After deposition onto the lids, the paste is conditioned (organic burnout, glazing) as described in section 2.5.2. The glass frit layer has a thickness of 200-300 µm and a width of 1.0-1.2 mm after glazing. The greater variations in thickness and width of the layer compared to the Diemat material are due to the more inaccurate deposition by syringe. A photograph of such a lid with glass frit is shown in Figure 5.17.

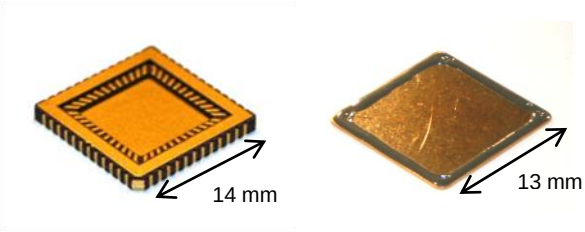

Figure 5.17: Photograph of LCC substrate and Kovar™ lid with glass frit layer

In principle the LCC packaging process in vacuum is the same as the laser-based process described in detail in section 3.2.3.2. Due to the higher bonding temperature and longer bonding time (440°C for 10 min) appropriate heat sinking is even more important if the centre of the package is to be kept cool. As with bonding in air, the substrate is placed on top of the copper block to remove the excess heat during the bonding process. In vacuum a soft thermally conductive material is placed between the

contacting interfaces to ensure a constant thermal transfer rate, as explained above. The Kovar^{TM} lid with the glass frit and the silicon chip for increased absorption at the laser wavelength at 940 nm are placed on top of the substrate (see Figure 5.18). The bonding chamber is closed and a force of around 10 N is applied onto the sample by pressing it against the glass sphere via the pneumatic cylinder. Prior to bonding the chamber is evacuated to a moderate vacuum (~5×10^{-2} mbar). For the actual bonding process the laser beam is scanned at high speed (1000 mm s^{-1}) along the edges of the silicon piece followed by a controlled cool down. The laser power is reduced step-wise in equally spaced power and time intervals over a time period of 40 minutes to allow for a gradual cool down with a rate of around 10°C min^{-1}. A schematic presentation of the bonding process is shown in Figure 5.18. This is the same as Figure 5.3 with addition of the conformable conductive material between the substrate and the copper block.

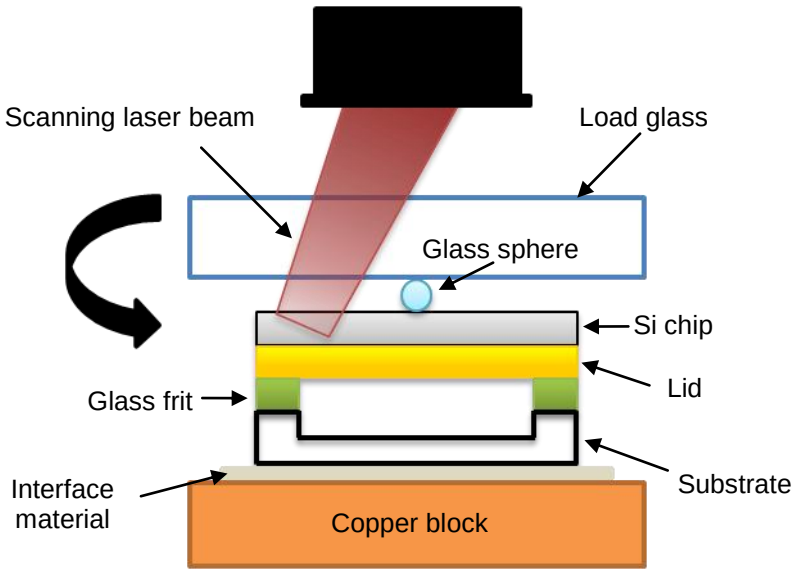

Figure 5.18: Sketch of bonding procedure in vacuum with interface material between copper block and substrate

5.2.2 Temperature Monitoring

As with the glass frit packaging in air, temperature monitoring experiments in vacuum were carried out to investigate the relationship between the temperature inside the bonding layer and the laser power, and to demonstrate the localised heating nature of this laser-based process. A detailed description of the temperature monitoring method and the sample preparation is given in section 3.3.2. The temperature is monitored by thermocouples in three positions across the LCC substrate as shown in Figure 5.6. Two thermocouples are placed along the bonding track to ensure the correct bonding

temperature is used whilst the third is placed in the centre of the substrate to determine the extent to which the heat is restricted to the joining area.

As described in section 3.3.2, the substrate is placed on a special copper cooling platform with a through-hole to accommodate the thermocouple for temperature monitoring in the centre of the substrate, to ensure that the substrate is cooled in the same way as during the normal bonding process. To overcome the issue of the unreliable thermal transfer rate a soft thermally conductive material must be placed between the substrate and the heat sink. Polytetrafluoroethylene (PTFE) proved to be an appropriate solution to this problem due to its high melting point (327°C), high conformability and easy handling as relatively thin (0.26 mm) sheet material. Its thermal conductivity is however only 0.25 W m^{-1} K^{-1}, which is four times lower than that of air. Nonetheless, with a PTFE sheet of thickness 0.26 mm it was found that the temperature in the centre of the device is kept below 250°C during the 10 minute bonding process, with the required temperature of 440°C in the joining area. A typical temperature profile of such a bonding process in vacuum at a laser power of 13 W can be seen in Figure 5.19.

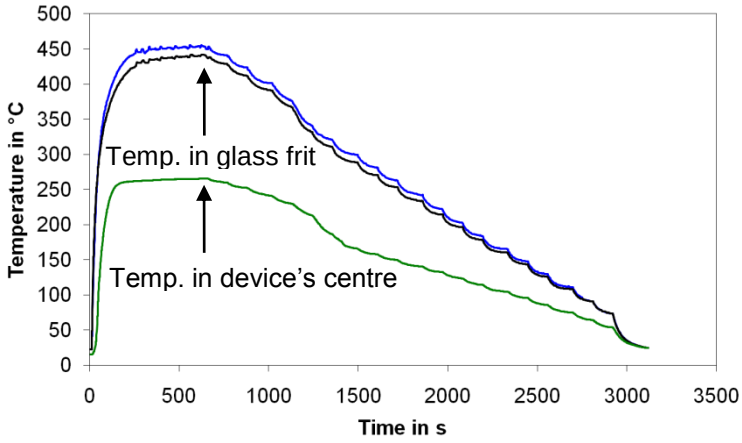

Figure 5.19: Temperature plotted as a function of time during the laser bonding process in vacuum (power 13 W, sealing time 10 min, cool down 40 min). Blue and black traces: inside bonding layer; green: on substrate in the centre of the device.

As explained in section 5.2.1.2, after bonding the laser power is gradually reduced in 86 equally spaced power (~0.15 W) and time (~28 s) intervals to achieve a cool down rate of around 10°C min^{-1}. As can be seen in Figure 5.19 using this technique, a gradual cool down of the glass frit in the joining area to a temperature of around 70°C can be achieved. Below 70°C, after 38 minutes of cool down, the temperature drops more

rapidly since at this point the required output power of <0.7 W falls below the lasing threshold i.e. the sample is not heated any more although it is expected that at these comparatively low temperatures this should not have any significant adverse effects.

Most importantly, the lateral heat flow within the substrate is reduced considerably and truly localised heating is achieved – maximum temperature of 250°C in the centre despite a bonding temperature of 440°C – using this laser-based glass frit packaging process in a vacuum. Repetitions of the thermal monitoring experiments with a number of samples have shown that temperature profiles with high repeatability are achieved (repeatability similar to that in air, ±10°C).

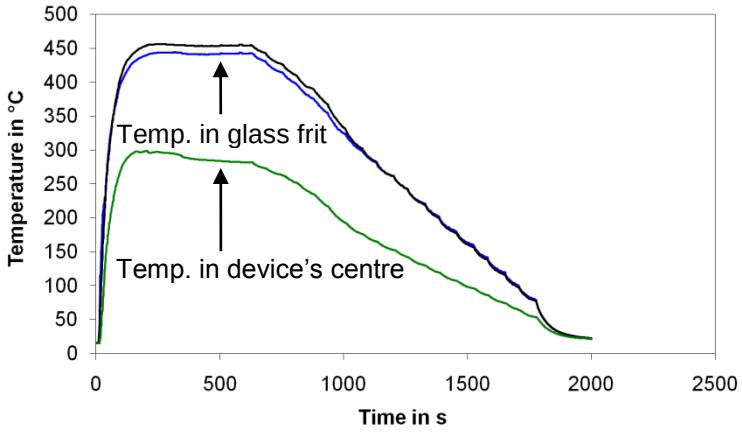

Figure 5.20: Temperature plotted as a function of time during the laser bonding process in vacuum (power 13 W, sealing time 10 min, cool down 20 min). Blue and black traces: inside bonding layer; green: on substrate in the centre of the device

The total time for a single bonding cycle, including the 15 s for the temperature to reach the sealing temperature, the 10 minutes holding time at bonding temperature plus the additional 40 minutes for the controlled cool down, accounts for slightly more than 50 minutes. Since the laser process must be carried out in series rather than in parallel, this long heating and cooling time would make the laser process rather expensive. A series of experiments was therefore carried out to investigate the impact of shortening the cool-down period. A typical temperature profile of such a LCC packaging process, where the length of the time intervals (~14 s) has been halved to achieve a total cool down time of 20 minutes, is shown in Figure 5.20. Ultimately it was found that simply switching the laser off at the end of the bonding period, giving a cool down time of 2 minutes, was sufficient (see Figure 5.21).

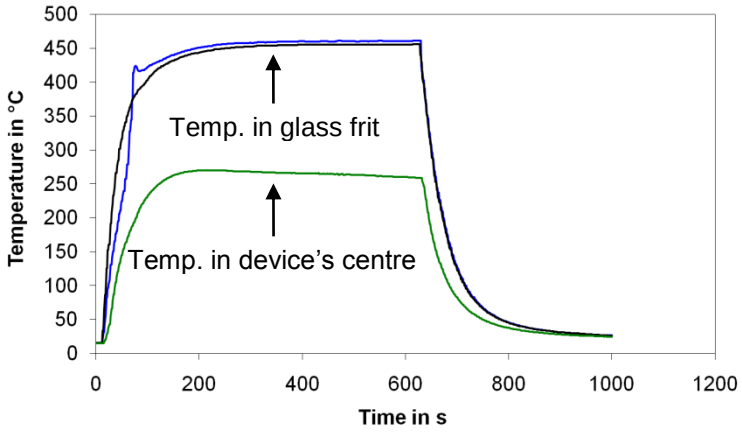

Figure 5.21: Temperature plotted as a function of time during the laser bonding process in vacuum (power 13 W, sealing time 10 min, cool down 2 min). Blue and black traces: inside bonding layer; green: on substrate in the centre of the device

Although PTFE provides highly repeatable results, it would be preferably to further reduce the temperature in the centre of the LCC substrate. PTFE has a thermal conductivity of only 0.25 W m^{-1} K^{-1}, so alternative, deformable materials with a significantly higher thermal conductivity were investigated as interface layers. The choice of these materials is rather limited as they both need to withstand relatively high temperatures above 200°C and are suitable for applications in a vacuum. The range of materials tested, e.g. silver paste, graphite sheet material and thermal interface compound, have thermal conductivities in the range of 3 to 33 W m^{-1} K^{-1}. Unfortunately this means that the region of highest thermal resistance is the glass frit itself giving rise to a very steep thermal gradient within this frit layer. As a result, when sufficient laser power is absorbed to raise the temperature at the lid to glass frit interface to the bonding temperature, the temperature at the glass frit to substrate interface stays well below the melting point. Therefore, the glass frit reflows only partly and no reliable seal can be achieved. One possible solution would be to engineer a conformable material with a thermal conductivity of approximately 1 W m^{-1} K^{-1} which can withstand temperatures above 200°C in a vacuum environment to create conditions similar to bonding in an air atmosphere. A different approach, which will be described in chapter 5.2.5, is to use one of the higher conductivity materials but to reduce the area which is cooled.

5.2.3 Bonding Experiments

The bonding experiments described in this section are carried out according to the laser-based vacuum packaging procedure described in section 5.2.1.2. A PTFE sheet of dimensions 16 mm×16 mm by 0.26 mm thick was used between the substrate and the

copper block. In some cases, after the bonding procedure, the PTFE layer stuck slightly to the base along the edges of the LCC substrate due to softening of the PTFE upon heating. The PTFE sheet, therefore, was replaced before each bonding process to always ensure a constant, repeatable thermal transfer between the contacting interfaces. Prior to bonding the bonding chamber was evacuated to a moderate vacuum ($\sim 5 \times 10^{-2}$ mbar). Based on the experience gained during the temperature monitoring experiments six samples were bonded successfully at a laser power of 13 W for 10 minutes followed by a stepped cool down for 40 minutes. During the bonding process a slight force of around 10 N was applied to the sample to ensure sufficient wetting of the bond interfaces. A photograph of such a typical laser-bonded LCC package is shown in Figure 5.4.

As mentioned previously, the recommendations for the firing profile appear to be based on heating cycles common in furnace heating. In order to make full benefit of the rapid temperature ramp rates possible in laser joining it would be beneficial to use much higher cool down rates provided the quality of the seal is not affected significantly. Furthermore, it would be desirable to reduce the overall bonding time at peak temperature to minimise the heat input into the device's centre. During sealing the thermal load on the package is at its highest and hence the strain on the device to be packaged. A series of samples was bonded where the time at peak temperature and the cool down time were greatly reduced.

For closer investigation of the influence of the cool down rate and the sealing time on the quality of the bond (hermeticity and shear force) a number of samples were bonded using the following parameters. To check for the effect of the cool down rate on the bond quality, samples were sealed for 10 minutes followed by a 20 minutes long controlled, gradual cool down (3 samples) or by simply switching the laser off at the end of the sealing period, resulting in a cool down of 2 minutes (6 samples). A further three samples each were bonded with a sealing time of 7.5 minutes and three with a sealing time of 5 minutes, to investigate the influence of time at sealing (peak) temperature on the quality of the seal. To achieve the shortest possible overall time for an entire bonding cycle the laser was switched off directly at the end of the sealing period. As with the previous bonding experiments following the recommended firing profile, the samples were bonded at a laser power of 13 W in a moderate vacuum

(~5×10^{-2} mbar) with a PTFE layer as interface material. A list of all bonded samples and the bonding parameters are summarised in Table 5.2.

Table 5.2: List of LCC packages bonded in vacuum

No. of samples:	Bonding Time:	Cool Down:	Comment:
6	10 min	40 min	Gradual, stepped cool down
3	10 min	20 min	Gradual, stepped cool down
6	10 min	2 min	Laser switched off directly
3	7½ min	2 min	Laser switched off directly
3	5 min	2 min	Laser switched off directly

Visual assessment of all the bonded samples did not indicate any adverse effects of the shorter bonding time and higher cool down rate on the quality of the seal. An overall reduction of the time for a full bonding cycle – sealing at peak temperature plus cool down phase – from 50 minutes based on the suppliers recommendation to only 7 minutes was achieved. Additional bonding trials have shown that a further reduction of the bonding time much shorter than 5 minutes is not recommended as a proper reflow of the glass frit sealing layer and bond formation might be affected.

A further six LCC packages were bonded and then subjected to residual gas analysis (RGA) – TM1018.5 in MIL-STD-883G – to determine the level of vacuum inside the packages after sealing. Before sealing the bonding chamber was evacuated for half an hour to achieve a vacuum of around 4×10^{-2} mbar – measured at the position of the Pirani gauge which is attached directly to the vacuum pump. These samples were bonded for 5 minutes; after the sealing period the laser was simply switched off. The pressure inside the bonding chamber is monitored by the Pirani gauge but the pressure inside the package after sealing is unknown. The vacuum inside the cavity might be partially destroyed due to out-gassing of the glass frit layer during the bonding process.

In total 21 LCC packages were bonded using this laser-based glass frit packaging process in vacuum which are subjected to hermeticity and shear force testing. A further six samples were sealed for RGA to determine the actual level of vacuum inside the cavity.

5.2.4 Packaging of Miniature Pressure Gauges

As mentioned in the previous section the level of vacuum inside the LCC packages after sealing using this laser-based glass frit packaging process is unknown. To determine this, one option is to subject the sealed LCC packages to RGA; however this is a destructive test method. The samples cannot be used in repetitive measurements to investigate the long term stability of the vacuum inside the package. In an attempt to measure the actual level of vacuum inside the LCC packages after sealing packaging of miniature pressure gauges, which are sufficiently small to fit into the cavity of the LCC substrate, was investigated. Such miniature pressure gauges are manufactured by INO; some typical, selected specifications of these particular sensors are listed in Table 5.3.

Table 5.3: Selected specifications of micro-Pirani gauges from INO [122]

Specifications of miniature pressure gauge:	
Sensors type	MEMS micro-Pirani
Measurement range	4×10^{-3} mbar to 1013 mbar
Accuracy (typical)	±5% of reading from 4×10^{-3} mbar to 1.3×10^{-2} mbar ±2% of reading from 1.3×10^{-2} mbar to 1013 mbar
Repeatability	±0.7%/°C from 6.7×10^{-3} mbar to 53 mbar
Bake-out temperature	300°C maximum
Response time	<100 ms
Chip size	Down to 1 mm×1 mm

These Pirani-style micro sensors are of very compact architecture (2×2×0.7 mm) and fit into the cavity of the LCC substrate, which is 8.9×8.9 mm by 1.02 mm deep. They have a measurement range from 4×10^{-3} mbar up to atmospheric pressure, which is sufficient for this vacuum packaging process. According to the Pirani gauge which is integrated into the bonding setup a maximum level of vacuum around 3×10^{-2} mbar can be achieved with this system. In the range from 1.3×10^{-2} mbar to atmospheric pressure the sensors have a very high accuracy of ±2% of the reading. This overlaps with the pressure range the sensors will be operated at in this particular application. Long term observations of the level of vacuum within the glass frit packaged LCC devices and also monitoring of a slight, gradual decline of the vacuum should be possible with this sensor. The miniature pressure gauges can only withstand a maximum temperature of 300°C (bake-out temperature), so packaging of these sensors is an ideal demonstration of the main benefit of this laser-based packaging process.

The miniature pressure gauge from INO is a sensor based on the principle of the Pirani gauge: the pressure of a gas surrounding a hot body influences the heat exchange between the hot body and its environment [123]. The micro-sensor mainly consists of a suspended platform which is attached to the substrate by zigzag shaped legs as shown in Figure 5.22. If a current is applied to the sensor, the thermal transfer between the platform and its environment changes when the surrounding pressure is altered resulting in a change of the electrical resistance of the sensor. This change in resistance can be measured and translated to the pressure surrounding the sensor. A detailed description of these miniature pressure gauges and their functional principle is reported on in [123].

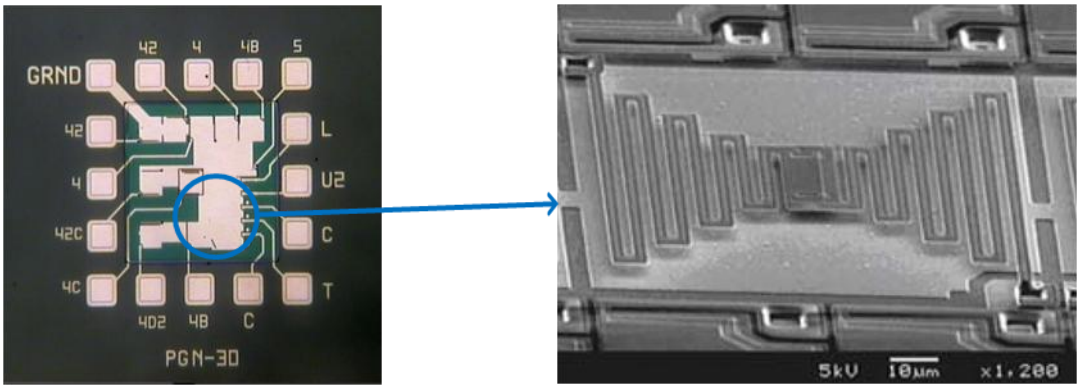

Figure 5.22: Microscope picture of sensor array and SEM picture of suspended micro-sensor platform [122]

INO offered to supply ten of these miniature pressure gauges free of charge. However, they were not calibrated since the calibration is the most time consuming and expensive step during production. In order to achieve such a high accuracy as stated in Table 5.3 the sensors must be calibrated according to an elaborate procedure as reported in [123]. Two essential items of equipment for this calibration process are a vacuum pump with integrated pressure control and a thermoelectric cooler, neither of which were available in the research group at that time. However, a simplified procedure can be used with an accuracy of ±4% of the reading, sufficient to provide useful information about the vacuum sealing process.

The chip containing the miniature pressure gauge is attached to the LCC substrate using a high temperature adhesive (Permabond 820) which withstands temperatures in excess of 200°C; during the laser sealing process the centre of the package is heated to a temperature of around 250°C. The contact pads “GRND” (ground) and “T” (see Figure 5.22) were wire-bonded to the input and output ports of the chip carrier to be able to establish the necessary electrical connections with the sensor also after packaging. This

work (integration of the sensors and wire-bonding) was carried out by Suzanne Millar. A photograph of such a miniature pressure gauge integrated into a LCC substrate is shown in Figure 5.23.

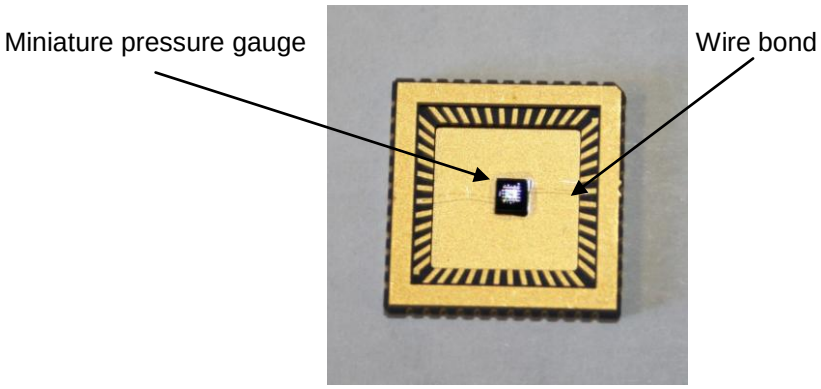

Figure 5.23: Photograph of LCC substrate with wire-bonded miniature pressure gauge in centre

For the simplified calibration of the miniature pressure gauges only the change of electrical resistance of the sensor with the pressure of its environment was taken into consideration. A constant current was applied to the sensor and the change in voltage with pressure was measured. The calibration was accomplished in a custom-made test stand which is shown in Figure 5.24. The sensor inside the chip carrier is placed into the test chamber and connected to the current source via vacuum feedthroughs. The test chamber is connected directly to a rotary vacuum pump (Trivac 2,5E, Leybold Vakuum). With this setup a final pressure of around 1×10^{-2} mbar can be achieved given the pump is constantly switched on. The pressure inside the test chamber is monitored with a Pirani gauge (APG100-XLC, Edwards) and the level of vacuum is adjusted by using a needle valve to introduce a controlled leak. As current source a multifunction calibrator (5021-100 PPM, Time Electronics) with a resolution of 20 nA and for voltage measurements a multimeter (1906 Computing Multimeter, TTi) of resolution of ±0.019% of reading were used. Experiments have shown that the resolution of this calibration procedure is limited by the resolution of the Pirani gauge (±4% of reading) used as a reference.

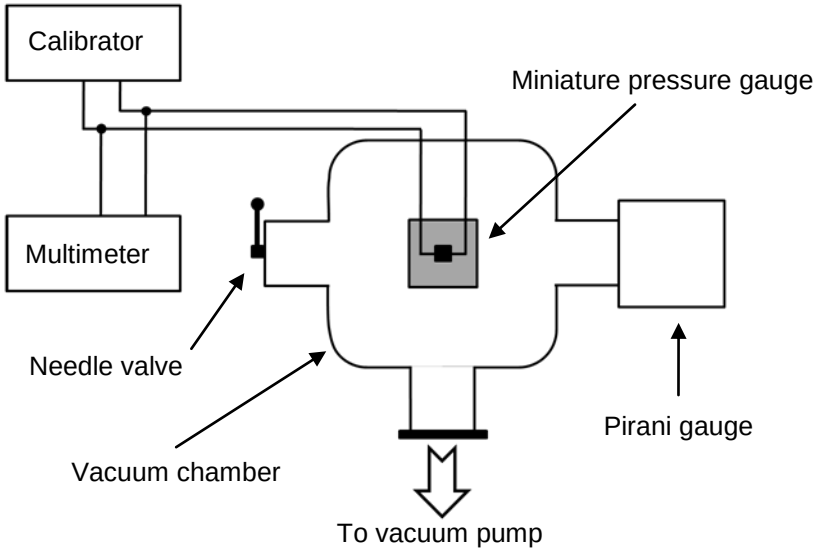

Figure 5.24: Sketch of setup for calibration of miniature pressure gauges

The calibration of the miniature pressure gauges was carried out at room temperature without additional temperature control. After the current (typically ~50µA) was applied to the sensor it was left for 10 minutes to heat up till it reached a steady state to ensure the temperature remains fairly constant during the series of measurement. Subsequently the pressure inside the test chamber was adjusted using the needle valve and the change of the measured voltage was noted. Such a typical calibration curve is shown in Figure 5.25.

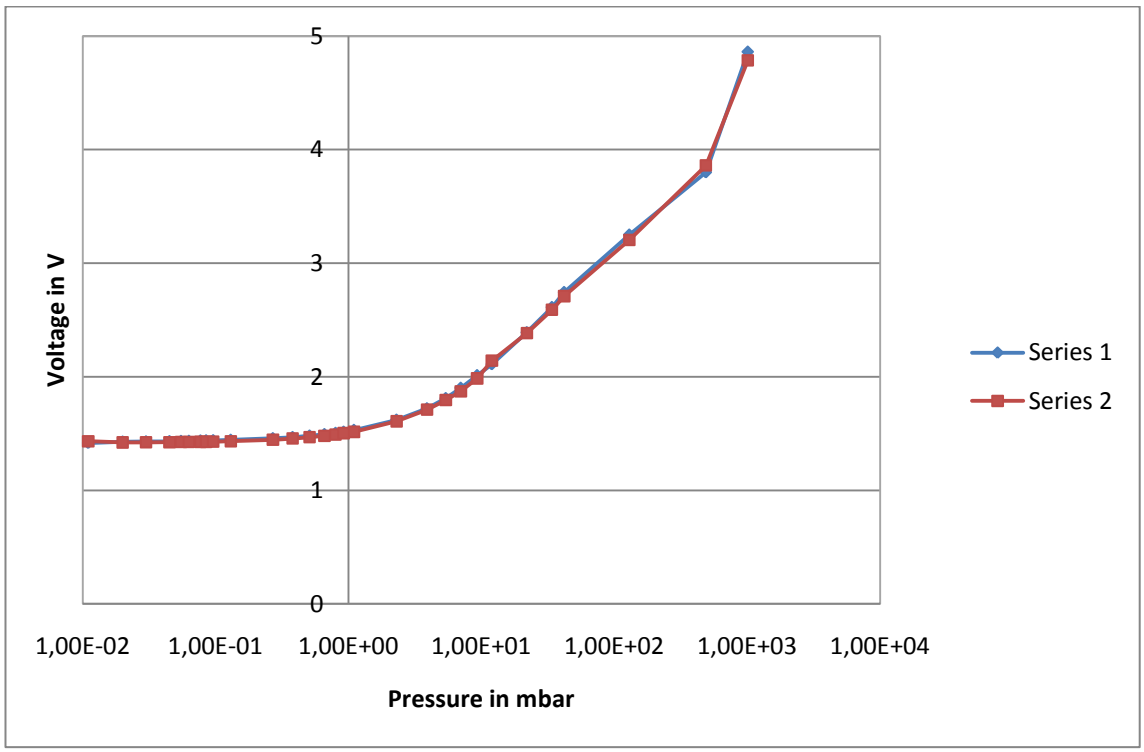

Figure 5.25: Calibration curve of miniature pressure gauge (I = 50 µA)

Repeating of the calibration procedure with the same sensor showed that the results of the measured voltage are very consistent (compare Figure 5.25). For different sensors, however, slightly different voltage levels were obtained. For each miniature pressure gauge an individual calibration curve must be recorded. To investigate the influence of the elevated temperatures during the packaging process on the calibration and the functionality of the device, one of the sensors was heated after calibration to a temperature of 250°C for 5 minutes on a hot plate – this resembles the thermal load the sensor will be exposed to during the bonding process. A repetition of the calibration procedure after cool down to room temperature did not show any influence of the heating cycle on the measurement results.

Six of the miniature pressure gauges were packaged using the laser-based vacuum packaging process described in section 5.2.3 where the entire bottom area of the substrate is in contact with the heat sink through a PTFE sheet. The samples were bonded for 5 minutes and the laser was switched off directly after sealing. Prior to bonding the setup was evacuated for half an hour to achieve a final pressure of around 4×10^{-2} mbar inside the system. To measure the actual level of vacuum inside the cavity of the LCC package after sealing, the same current as during calibration was applied to the packaged sensors and the voltage was measured. Using the particular calibration curve for each sensor the pressure inside every package was estimated. These results including a comparison with the measured values obtained with the Pirani gauge are summarised in Table 5.4.

Table 5.4: Comparison of level of vacuum measured using Pirani gauge and miniature pressure gauges inside the cavity of the LCC packages

Sample	Level of vacuum (mbar)	
	Measured with Pirani gauge:	Miniature pressure gauge:
A	3.9×10^{-2}	~4.4×10^{-2}
B	3.9×10^{-2}	~7.0×10^{-2}
C	3.2×10^{-2}	~1.2
D	3.7×10^{-2}	~1013
E	3.6×10^{-2}	———
F	3.5×10^{-2}	~1

According to the sensors sealed in packages A and B a similar level of vacuum ($4 – 7\times10^{-2}$ mbar) can be achieved inside the cavity of the LCC packages as measured with the Pirani gauge. The sensors in packages C and F give a reading of around

1 mbar and D a reading of around 1013 mbar close to atmospheric pressure. Package D might have a leak or the sensor was slightly damaged during the packaging process and gives a false reading. From the pressure gauge in package E no reading could be obtained. Either the wire-bond (electrical connection) broke or the sensor was damaged during the packaging process. As these results gave no clear indication of the level of vacuum inside the cavity of the laser sealed LCC packages these samples were also subjected to residual gas analysis (RGA) for verification of the results. A discussion of these test results including a comparison with the values in Table 5.4 will be given in section 5.2.6.3.

5.2.5 Cooling Sandwich Structure / Bonding Experiments on Copper Boss

In an attempt to further reduce the temperature in the centre of the device whilst still maintaining sufficiently high temperatures in the bonding region, alternative heat sinking arrangements were tested. As explained in section 5.2.2, if one of the materials with higher thermal conductivity (3 to 33 W m^{-1} K^{-1}) is used as deformable interface layer between the LCC substrate and the heat sink, successful bonding cannot be achieved due to a very steep thermal gradient within the sealing layer. To resolve this issue localised cooling, i.e. the area which is in direct contact with the heat sink is reduced, was investigated. A specialised cooling platform was designed which is only in direct contact with the centre of the substrate where the temperature sensitive device would be situated in real applications. The cooling platform has a raised square boss in the centre of side-length 7 mm×7 mm. The substrate to be bonded is centred on this boss. To ensure a constant thermal transfer with high repeatability, the same interface materials (3 to 33 W m^{-1} K^{-1}) were tested as previously. A sketch of this heat sinking arrangement is shown in Figure 5.26.

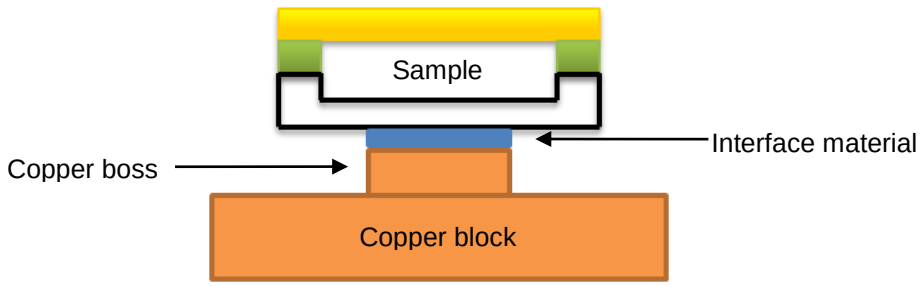

Figure 5.26: Sketch of localised heat sinking arrangement

By introducing the localised cooling the area being cooled was reduced by a factor of four in comparison to placing the substrate in direct contact with the copper block.

Nevertheless, the use of the interface material with the lowest thermal conductivity of 3 W m^{-1} K^{-1}, a thermal interface compound (Thermstrate 2000, Loctite), still resulted in a too high thermal transfer rate to achieve the required bonding temperature inside the joining area. A further reduction of the size of the cooling area is not advisable as it would restrict the area in the centre of the package, which is protected from high temperatures, too greatly.

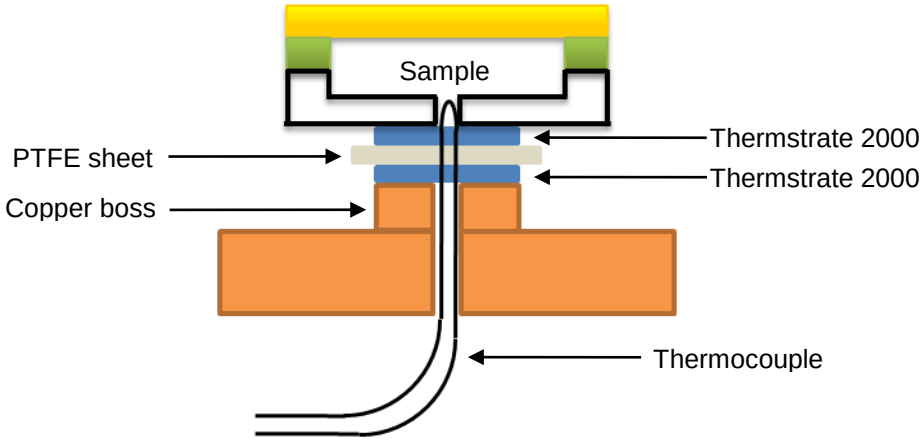

Figure 5.27: Sketch of localised heat sinking arrangement with "sandwich structure" and thermocouple for temperature monitoring in the centre of the LCC substrate

Instead a "sandwich structure" was introduced at the interface, where a PTFE sheet of thickness 0.26 mm was placed between two layers of Thermstrate 2000, the thermal interface compound, to tailor the thermal transfer to the copper boss. A thin layer of the thermal compound was applied to the copper boss and to the central area of the substrate base of dimensions around 7 mm×7 mm using a scalpel. In between these two layers a PTFE sheet was placed as thermal barrier. The dimensions of the sheet were chosen to be considerably larger (10 mm×10 mm) than the thermal compound layer to ensure that there is no direct contact between those layers and, hence, a true thermal barrier is created. A cross sectional view of this cooling arrangement including the "sandwich structure" is sketched in Figure 5.27. Temperature monitoring experiments showed that this cooling arrangement provided a suitable thermal transfer rate to enable the required bonding temperature to be maintained within the joining area. A typical profile of the temperature in the sealing layer of such a bonding process at a laser power of 24 W (sealing time 10 min) is shown in Figure 5.28.

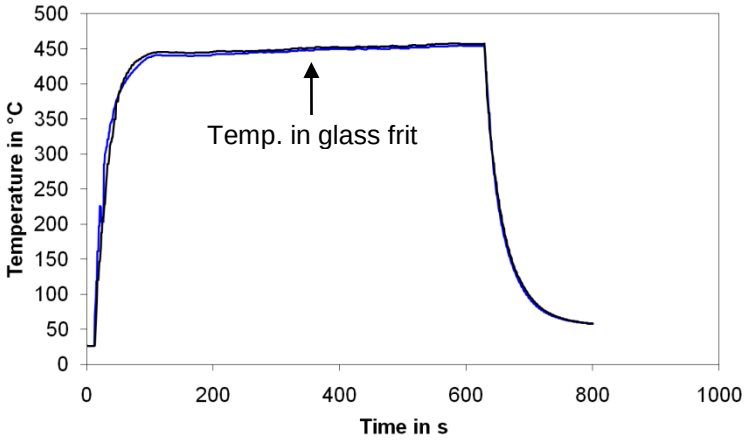

Figure 5.28: Temperature plotted as a function of time during the laser bonding process in vacuum with cooling sandwich structure (power 24 W, sealing time 10 min). Blue and black traces: inside bonding layer.

The temperature profile resembles that of the "normal" bonding process, where only a single layer of PTFE is used as interface material, shown in Figure 5.21. However, a higher laser power of 24 W instead of the previously used 13 W is required to achieve the required bonding temperature of 440°C inside the sealing layer. This indicates that by this "sandwich structure" cooling arrangement the overall thermal transfer between the substrate and the heat sink is nearly doubled.

For the initial temperature monitoring experiments using this "sandwich structure", as described above, only the temperature in the sealing layer was investigated. Repeatable results could be achieved with only these two thermocouples. The integration of the third one into the centre of the substrate proved to be more demanding. To monitor the temperature in this position the thermocouple must penetrate through the cooling platform and the sandwich structure as demonstrated in Figure 5.27. A small hole was punched into the centre of the PTFE sheet to accommodate the thermocouple. Great care has to be taken to ensure a tight fit otherwise the functionality of the PTFE layer as thermal barrier is not ensured any more. If the two layers of thermal compound are in direct contact in the proximity of the thermocouple the main heat flow would be along this path of lowest thermal resistance. Otherwise, a true representation of the natural heat flow as in the real bonding experiments would not be guaranteed in the temperature monitoring experiments. A typical temperature profile in the joining area and in the substrate centre of such a glass frit bonding process in vacuum using the "sandwich structure" heat sinking arrangement can be seen in Figure 5.29.

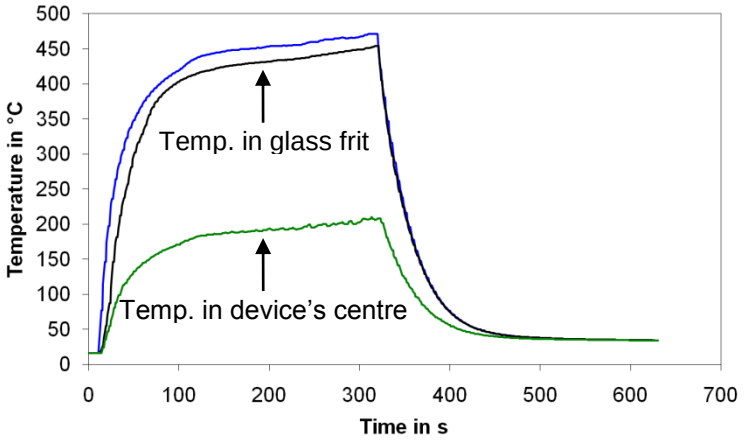

Figure 5.29: Temperature plotted as a function of time during the laser bonding process in vacuum with cooling sandwich structure (power 22 W, sealing time 5 min). Blue and black traces: inside bonding layer; green: on substrate in the centre of the device.

A suitable thermal transfer rate is provided to enable the required bonding temperature (440°C) to be maintained whilst keeping the temperature in the centre of the device below 250°C during the 5 minutes of laser irradiation (bonding time). If the sealing time at the peak temperature of 440°C is restricted to 4 minutes the temperature in the centre of the package actually remains below 200°C. It was noted that a slightly lower laser power of 22 W was necessary to achieve the required bonding temperature after the third thermocouple was integrated into the substrate. In comparison, a laser power of 24 W is required if only the two thermocouples are integrated into the sealing layer. The thermocouple in the centre of the substrate base seems to lower the rate of thermal transfer between the substrate and the heat sink. Nevertheless, the measured values of the temperature in the substrate centre should give a good representation of the natural temperature profile (heat flow) in the real bonding process.

Based on the experience gained in the temperature monitoring experiments five samples were bonded successfully at a laser power of 24 W for 4 minutes.

5.2.6 Quality Testing, Results and Discussion

In this subsection, quality testing of the LCC packages, which were sealed using the laser-based localised heating glass frit packaging process in vacuum, will be discussed. To test the quality of the seal of the vacuum packaged devices and in particular the influence of the reduced bonding time, shortened cool down phase and localised cooling, the samples were leak and shear force tested according to MIL-STD-883G. A

list of all the bonded samples which were subjected to hermeticity and shear force testing including the results is summarised in Table 5.5.

Table 5.5: List of vacuum packaged LCC devices including bonding parameters, hermeticity and shear force test results

Sample No.:	Bonding Time:	Cool Down:	Leak Test:	Shear Force:
1	10 min	40 min	PASS	>990 N
2	10 min	40 min	PASS	725 N
3	10 min	40 min	PASS	622 N
4	10 min	40 min	PASS	868 N
5	10 min	40 min	PASS	769 N
6	10 min	40 min	PASS	541 N
7	10 min	20 min	PASS	>990 N
8	10 min	20 min	PASS	778 N
9	10 min	20 min	FAIL	Not tested
10	10 min	2 min	PASS	815 N
11	10 min	2 min	PASS	580 N
12	10 min	2 min	PASS	332 N
13	10 min	2 min	PASS	744 N
14	10 min	2 min	PASS	598 N
15	10 min	2 min	PASS	689 N
16	7½ min	2 min	PASS	806 N
17	7½ min	2 min	PASS	792 N
18	7½ min	2 min	PASS	981 N
19	5 min	2 min	PASS	608 N
20	5 min	2 min	PASS	915 N
21	5 min	2 min	PASS	808 N
22	4 min	2 min	PASS	>990 N
23	4 min	2 min	PASS	>990 N
24	4 min	2 min	FAIL	162 N
25	4 min	2 min	PASS	890 N
26	4 min	2 min	FAIL	480 N

Additionally, some samples were subjected to residual gas analysis (RGA) – TM1018.5 in MIL-STD-883G – to determine the level of vacuum inside the packages after sealing.

5.2.6.1 Leak Testing (TM1014)

Leak testing by C-MAC MicroTechnology of the LCC devices packaged in air had demonstrated the validity of the tests carried out within the university. The vacuum packaged devices were therefore only tested in-house. The helium fine leak testing was carried out by Suzanne Millar as before. 20 of the 21 LCC packages which were sealed using the "standard" process, where the entire bottom area of the substrate is in contact with the PTFE sheet (heat sink), passed both the fine and gross leak tests. Using PTFE as interface material between the bottom of the substrate and the copper block has

solved the initial issue of unreliable, unrepeatable thermal transfer in vacuum. A process yield of more than 95% has been demonstrated. For the devices packaged with the cooling sandwich structure in combination with localised cooling three of the five samples passed both the fine and gross leak test. Closer inspection of the samples which failed the leak test showed that the failure of the seal was due to insufficient reflow of the glass frit sealing layer.

5.2.6.2 Shear Force Testing (TM2019.7)

The 20 hermetic samples which were sealed using the "standard" process (entire substrate in contact with heat sink) were subjected to shear force testing to determine the physical strength of the seal. Again, the shear force testing was carried out by Optocap Ltd. Only two devices – sample 9 and 13 – split open during testing, for the remaining samples the lid stayed attached to the substrate. Shear forces of 868 N (sample 4) and 598 N (sample 14), respectively, were required to break the two samples open, and in each case the failure of the join occurred inside the glass frit sealing layer (see Figure 5.30).

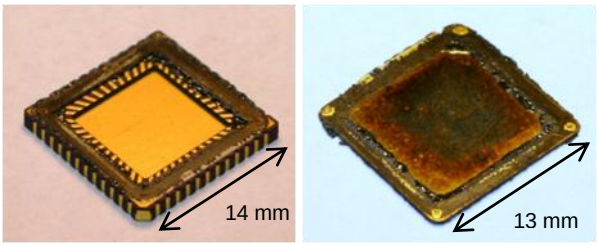

Figure 5.30: Photograph of split vacuum packaged LCC device after shear force testing

In two cases the strength of the packaged devices exceeded the maximum load (>990 N) of the shear force testing machine. In most cases the shear tool, which is aligned against one side of the Kovar^{TM} lid, started to slip and shear off the edge of the lid. Closer inspection of these samples showed that the shear tool started to slip because some glass frit material had been squeezed out between the lid and substrate during bonding. This means that instead of lying flush against the lid the shear tool is positioned against a slight slope – the reflown glass frit outside the lid. This causes the shear tool to slip more easily and shear off the edge of the lid instead of splitting the package open as illustrated in Figure 5.31.

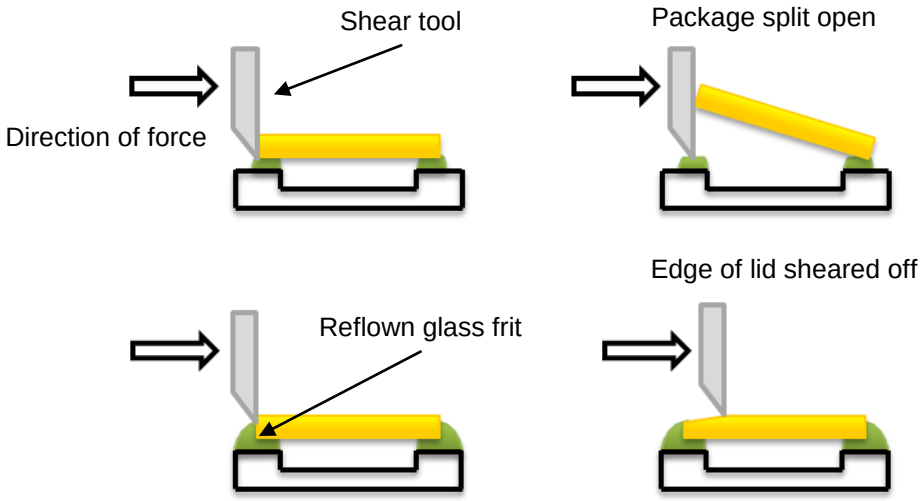

Figure 5.31: Sketch of shear force test produce. Top: Package is split open during testing; bottom: shear tool slipping and shearing off edge of lid due to reflown glass frit.

Most of the time this happened at shear forces above 600 N and hence it was concluded that all seals withstand shear forces of at least 600 N. No influence of the bonding time or the cool down rate on either the hermeticity or the mechanical strength of the bond was observed. A comparison with the shear force testing results of the LCC devices packaged in air (maximum shear force of 855 N) presented in Table 5.1 shows that even higher shear forces (>1 kN) are achieved with the vacuum packaged devices. This is probably due to the individual properties of the two different glass frit materials used – Diemat material for packaging in air and AGC material for vacuum. All shear force test results of the vacuum packaged samples are illustrated again in the plots shown in Figure 5.32.

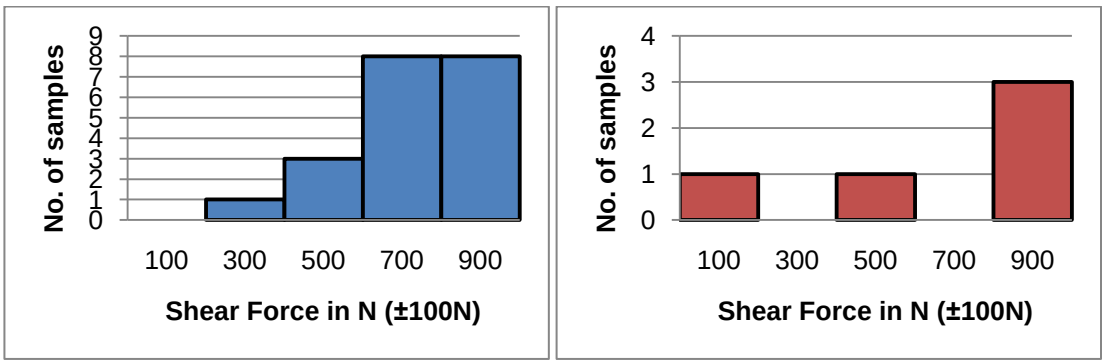

Figure 5.32: Plot of shear force test results for laser-bonded LCC packages in vacuum. Left: LCC devices packaged using "standard" process (entire substrate in contact with heat sink); right: LCC devices packaged using cooling sandwich structure and localised cooling.

For the devices packaged using the cooling sandwich structure in combination with localised cooling all five samples were subjected to shear force testing regardless

whether they passed the hermeticity test. For the two samples which failed the leak test shear forces of only 162 N and 480 N were achieved. The hermetically sealed samples withstood far higher shear forces (see Figure 5.32). Two samples exceeded the test limit whilst the third split open at a shear force of 890 N. The localised cooling appears to have no negative influence on the quality of the seal, provided a proper reflow of the glass frit sealing layer is achieved during bonding. Vacuum packaging, therefore, was demonstrated in a process where the temperature in the centre of the device is kept below 200°C despite a joining temperature of 440°C. In addition, a further reduction of the bonding time to four minutes was shown resulting in an overall process time for the full bonding cycle of six minutes (4 min bonding + 2 min cool-down). It is expected that further refinements of this process would provide a yield similar to that obtained with the earlier heat sinking arrangement.

5.2.6.3 Residual Gas Analysis (TM1018.5)

To measure the actual level of vacuum inside the LCC packages after sealing six samples without anything attached to the cavity were subjected to the destructive testing technique of residual gas analysis (RGA). Additionally, the LCC devices with the packaged miniature pressure gauges inside were also tested for validation of the measurements provided by the packaged sensors. Originally the packaged devices were intended for long-term monitoring of the level of vacuum inside the LCC packages; however the results obtained with the different sensors varied significantly as reported in section 5.2.4. The RGA testing was accomplished by Mead Testing Ltd., an external company. The results of the RGA testing including a comparison with results of the packaged miniature sensors are illustrated in Table 5.6.

Table 5.6: Comparison of level of vacuum measured using residual gas analysis, Pirani gauge and miniature pressure gauges inside the cavity of the LCC packages

Sample	Level of vacuum (mbar)		
	Measured with Pirani gauge:	RGA:	Miniature pressure gauge:
1	5.4×10^{-2}	3	———
2	4.1×10^{-2}	4	———
3	4.0×10^{-2}	5	———
4	3.9×10^{-2}	5	———
5	4.0×10^{-2}	8	———
6	4.0×10^{-2}	15	———
A	3.9×10^{-2}	71	$\sim4.4\times10^{-2}$
B	3.9×10^{-2}	20	$\sim7.0\times10^{-2}$
C	3.2×10^{-2}	104	~1.2
D	3.7×10^{-2}	———	~1013
E	3.6×10^{-2}	100	———
F	3.5×10^{-2}	20	~1

The results of the RGA testing showed that a moderate vacuum of around 5 mbar is achieved inside the packages without the miniature pressure gauges inside; this compares well to the results reported by Knechtel et al in [44]. Such a level of vacuum is sufficient for applications such as accelerometers where the vacuum simply needs to be sufficient to provide the required minimal air-resistance inside the cavity. If higher levels of vacuum are required the samples could be baked and stored inside a nitrogen environment prior to bonding to minimise the moisture content inside the package. Indeed, the entire bonding setup could be transferred into a nitrogen glove box, using a fibre-delivered laser beam. A further reduction of the pressure inside the cavity of the LCC package could be achieved by the use of getters attached to the inside of the lid as demonstrated in [47]. The getters would be thermally activated during the bonding process and trap any gases inside the cavity; overcoming the issue of out-gassing of water and organic residuals upon heating. The great difference of around two orders of magnitude between the measured values of vacuum of the Pirani gauge and the results of the RGA can be explained by two reasons: (i) out-gassing of the glass frit on heating and (ii) the position of the Pirani gauge in the bonding setup. The Pirani gauge is attached directly to the vacuum pump where the pressure is lowest. For more accurate results it would be best if the gauge could be moved inside the bonding chamber to give a more likely reading of the actual pressure inside the device to be packaged.

The residual gas analysis of the LCC devices with the packaged miniature pressure gauges has shown that the actual pressures inside these devices ranges from 20 mbar to

104 mbar (see Table 5.6). For sample D no measurement result could be obtained due to a failure of the measurement procedure. In general a slightly lower level of vacuum was observed with these samples than with the samples with the empty cavity. The reason for this is the integration of the sensor into the package itself. Due to the miniature pressure gauge the overall surface area inside the LCC package is increased providing a larger area where water molecules can adhere to. Water molecules are the most difficult particles to extract when trying to achieve a vacuum inside a confined volume. Hence, a larger surface area inside the cavity results (in most cases) in a higher final pressure (lower level of vacuum). Additionally, the sensors are attached to the centre of the substrate using glue. Therefore, some air gets enclosed between the substrate and the bottom of the sensors. After packaging this air slowly escapes partly destroying the vacuum.

The large discrepancy between the results obtained by the miniature pressure gauges and RGA (see Table 5.6) remained unclear. During the RGA the miniature pressure gauges were destroyed, so it was not feasible to investigate whether the sensor were already damaged by the packaging process. The data of the RGA is considered as genuine rather than the results measured with the miniature pressure gauges as Mead Testing Ltd. is an UKAS accredited test house. To achieve more accurate results the sensors must be calibrated according to the full procedure as described in [123]. Nevertheless, successful packaging of miniature pressure gauges was demonstrated which would not have been possible using conventional glass frit packaging technologies. The laser-based packaging process enables packaging of these temperature sensitive devices (T_{max} = 300°C) where the temperature in the centre of the LCC substrate is kept below 250°C despite a temperature of 440°C in the joining area.

In summary, a laser-based localised bonding process suitable for vacuum packaging has been developed and demonstrated, with a yield rate of approximately 95%. The temperature in the centre of the device can be kept below 250°C (and with additional tailoring of the heat sinking below 200°C) despite a temperature of 440°C in the joining region. Shear force testing has shown that superior bonding strengths are achieved. In some cases the vacuum packaged LCC devices withstand shear forces in excess of 1kN – the limit of the testing machine. RGA has shown that indeed a vacuum of around 5 mbar is accomplished within the LCC packages. Furthermore, successful packaging of an application – miniature pressure gauges – using this localised heating bonding

process was demonstrated. Packaging of these devices would not been possible using conventional glass frit bonding techniques where the entire package is heated to the required sealing temperature of 440°C. The sensors only withstand a maximum temperature of 300°C underlining the advantages of this innovative localised heating packaging process.

5.3 Conclusions to Chapter 5

Glass frit packaging is a simple and robust process where strong and hermetic seals can be achieved in high yield processes. Conventional, furnace-based glass frit packaging requires the entire package to be heated to the bonding temperature of several hundred degrees. In this chapter the development of two laser-based glass frit packaging processes in both air and vacuum has been investigated. Due to the localised heat input of the laser beam and active cooling of the substrate of the device the heat is restricted to the joining area. This enables the use of temperature sensitive materials within the package. The combination of the key advantages of glass frit packaging and localised heating using a laser as the heat source was demonstrated. Temperature monitoring experiments for an in-depth understanding of the temperature profile during the bonding procedure and process optimisation and quality testing of the packaged devices were also presented in this chapter.

5.3.1 Packaging in Air

A laser-based glass frit packaging process of LCC devices in air has been demonstrated using the glass frit material DM2700P/H848 from Diemat. Temperature monitoring experiments have shown that for packaging of the standard LCC substrate and the bare LCC substrate laser powers of 70 W and 72 W respectively, are required for 75 s to achieve successful bonding. Furthermore, it was demonstrated that by active cooling of the substrate the temperature in the centre of the device is kept below 140°C despite a temperature of 375°C in the joining region. Through a combination of localised laser heating and thermal management using heat sinking a localised heating glass frit packaging process has been created which enables packaging of temperature sensitive materials whilst still benefiting from the well-known advantages of glass frit as sealant material. Extensive testing of the packaged devices to assess the quality of seal according to MIL-STD-883G was accomplished. Leak testing showed that hermetic seals were achieved in a high yield process (>90%). Shear forces as high as 855 N were required to split apart these samples, which were bonded using localised heating; even

exceeding the strength of devices (610 N) where the lateral heat flow during bonding was not restricted [114]. Additional temperature cycling and acceleration testing showed that the LCC packages even pass a major part of the qualification process required in military and space grade products. In summary, a localised heating glass frit packaging process in air was developed which shows all the benefits of glass frit packaging without any negative effect of the thermal management on the quality of the seal.

5.3.2 Packaging in Vacuum

For the development of a laser-based glass frit packaging process of LCC devices in vacuum the paste 5115HT1 from AGC was used which is specially developed for vacuum applications. Initial temperature monitoring experiments in vacuum showed that a PTFE sheet of thickness 0.26 mm must be placed as an interface material between the bottom of the LCC substrate and the copper block to ensure a constant, repeatable thermal transfer required for successful bonding. Hermeticity testing confirmed that a very reliable joining process (yield rate ~95%) had been developed. The temperature in the centre of the device was kept below 250°C despite a temperature of 440°C in the joining region. Using a special cooling sandwich structure the heat flow was tailored additionally to reduce the temperature in the centre of the device below 200°C. Hermeticity and shear force testing demonstrated that the overall process time for a single bonding cycle was reduced from 50 minutes to 7 minutes without any adverse effect on the quality of the seal. Shear force testing underlined the excellent of properties of glass frit as sealant; the packages withstood shear forces in excess of 1 kN (limit of the test machine). Residual gas analysis has shown that a moderate vacuum of around 5 mbar was achieved inside the vacuum packaged LCC devices. Miniature pressure gauges were packaged successfully to emphasise the main advantage of this laser-based localised heating glass frit packaging process in vacuum. The sensors can only withstand a temperature of maximum 300°C and would be destroyed if heated to the bonding temperature (440°C) of the glass frit material. Using this laser-based packaging process in combination with active cooling the temperature in the centre of the LCC substrate was kept below 250°C enabling packaging of temperature sensitive materials.

6 Conclusions and Future Work

The project, on which this thesis has been based, set out to develop a technology to provide a solution to a problem of critical importance in the area of packaging of temperature sensitive micro-devices. The successful development of a range of solutions which address this need has been demonstrated. Two novel laser-based packaging processes for applications in device manufacture in microsystems technologies are presented in this PhD thesis.

Silicon to glass joining, a typical MEMS application, with a Benzocyclobutene (BCB) adhesive layer and hermetic glass frit packaging of Leadless Chip Carrier (LCC) devices, a standard off-the-shelf electronic package, were investigated. These packaging techniques are already established in industry for their robustness and simplicity. However, conventional techniques in general require the entire package to be heated to the bonding temperature thereby limiting the use of temperature sensitive materials within such devices. Here a high power laser is an ideal solution. Due to its high focusability and very flexible, remote positioning of the focal spot the laser can be used to heat the joining area highly localised. To additionally confine the high temperatures to the bonding area only, active cooling is applied to the substrate of the device. The lateral heat flow to the centre of the package, the sensitive device area, is restricted. In comparison to the joining area the temperature in the centre is reduced considerably. It was demonstrated that it is possible to use thermosetting polymers (BCB) and glass frit materials for packaging of micro-devices whilst maintaining low temperatures at the centre of packages during these processes. This allows for the first time the use of highly temperature sensitive devices in packaged devices using these sealing materials. By combining the advantages of intermediate layer bonding and localised laser heating, simple, robust and highly versatile packaging processes have been accomplished.

A multi-purpose bonding setup has been developed to fulfil the numerous requirements of these bonding processes. Bonding experiments have shown that the application of the bonding force is a critical process step. It must be applied uniformly and spread evenly to ensure sufficient contact of the bond interfaces along the entire bond line. The design considerations were focused on this issue in particular to ensure the high process yields required in commercial applications. The bonding processes under investigation

have been developed to such extend that they can be applied quite readily to packaging in device manufacture in industry. The industrial collaborators, who have partly driven the research interest of the work of this PhD thesis, are looking at the exploitation of this technology for their purposes.

In the following the key findings of the three main experimental research areas are discussed and recommendations for future investigations are highlighted.

The three areas are:

- development of the bonding setup,
- silicon to glass joining with a BCB adhesive layer, and
- hermetic glass frit packaging of LCC devices.

6.1 Bonding Setup

In microsystems technologies packaging is often application specific and hence accounts for a major part of the overall production costs of such a device. In order to achieve a considerable reduction of the packaging costs a generic packaging process is required. To provide for such a process a multi-purpose bonding setup has been developed which can be used for a range of intermediate layer bonding processes with only minimal adaptations required to change between the processes, as described in chapter 3.

Typical requirements (section 3.1) of the bonding process and the setup, respectively, are:

- packaging in a vacuum or inert gas atmosphere,
- application of a bonding force
- suitability for wafer-level packaging
- active cooling of the device substrate during bonding to keep the thermal load on the bulk of the package as low as possible is an additional requirement for this particular setup.

A design (see section 3.2) has been chosen where all required components are integrated inside a bonding chamber to provide for a controlled atmosphere during the bonding process since often a vacuum or an inert gas environment are required for bonding. A

water-cooled copper block is used as heat sink. The required bonding force is provided by a pneumatic cylinder. Since these components are required to work inside the bonding chamber, the feed-lines and couplings had to be designed carefully to avoid leakage.

Any adaptations of the bonding setup to a particular process were restricted to modules which could be exchanged within minutes without the need for re-alignment of the entire bonding setup afterwards. A camera was integrated into the setup to allow for precise alignment of the beam path of the laser, i.e. area of localised heat input, to the bonding track of the sample.

For the silicon to glass joining process there are two major challenges; especially if this process is expanded to a wafer-level:

- the required bonding force needs to be applied individually for every single device on the wafer (section 3.2.4) and
- localised heat sinking of the centre of the substrate only to ensure sufficient high process temperatures in the bonding area (section 3.2.5).

Special, exchangeable slide-on cooling platforms, which correspond to the design of pattern to be bonded, were designed to introduce localised cooling. A method to apply the bonding force individually, by means of a single contact point for every sample was developed using precision glass spheres.

As for most bonding processes, temperature control is one of the most important process parameters for glass frit packaging. A temperature monitoring method was developed, as described in section 3.3.2. Using thermocouples the temperature within the bonding layer can be controlled to within $\pm 10°C$ of the required process temperature. Furthermore, a technique was developed to monitor the temperature in the centre of the package without significant influence on the natural heat flow within the sample.

The bonding setup has shown its great flexibility and capabilities throughout the experimental work of this PhD. However, three possible upgrades have been identified: (i) For example, at present the samples are aligned by hand which is undesirable for

industrial applications. The integration of a fully automated pick and place robot should be considered.

(ii) Online process control of the laser power by monitoring the bonding temperature using a pyrometer integrated into the beam path of the laser has been shown to improve the process yield in other laser-based joining techniques. Integration of such a system is highly desirable as it would overcome the shortcoming that currently the bonding temperature for the silicon to glass joining process cannot be measured; however, considerable costs are required for such an upgrade.

(iii) The process speed of the wafer-level packaging process is limited by the fact that each sample needs to be bonded individually and in sequence. Introduction of a multiple-beam approach would result in parallel processing and a considerable reduction of the overall process time.

6.2 Silicon to Glass Joining with BCB Adhesive Layer

In chapter 4, successful silicon to glass joining with a BCB adhesive layer was demonstrated in a novel laser-based process where the lateral heat flow to the centre of the package was reduced considerably by active cooling of the substrate. This process was first demonstrated for single chip packaging and then a further development of this process to wafer-level packaging was shown. The combination of the benefits of localised laser heating with a simple and robust adhesive layer bonding process was clearly shown.

For single chip packaging (section 4.2) a considerable reduction of the bonding time was achieved (8 s instead of 20 min) in comparison to conventional single chip packaging where the entire device is heated up. No influence of the localised heating on the quality of the bond (mechanical stability up to 290 N) was observed. Additionally, the temperature in the centre of the device was kept at least 120°C lower than in the joining area (up to 350°C).

Bonding times as short as a single second have been achieved; however, these resulted in a considerably reduced mechanical stability of the seal suggesting insufficient cure of the polymer layer. There is a trade-off between bonding speed and mechanical stability.

Further development of this process to wafer-level packaging (section 4.3), typically used for conventional bonding techniques, was investigated. The term wafer-level packaging describes bonding processes where the entire wafer is covered with structures to be bonded. In this work the feasibility of such a laser-based process is shown for more simple patterns of 5 or 9 samples on the same wafer which can be expanded easily to a full wafer-level.

The key issue in bonding processes, such as laser bonding, which are carried out in sequence rather than in parallel is that the bonding force must be applied individually for every single device to be bonded. For that purpose a precision glass sphere is centred over each sample to locally flex the cover glass slightly.

For a pattern of 5 samples (section 4.3.1) – arranged like the five on a throwing dice – successful bonding of all individual samples on the same wafer was achieved. No significant influence of the distance between the neighbouring samples on the bond quality was observed; even if the distance was reduced to a minimum leaving a gap only sufficient for the width of the dicing saw blade. Shear forces (up to 285 N) comparable to single chip packaging were achieved.

For a more densely packaged pattern of 9 (section 4.3.2) – array of 3 by 3 samples which resembles full wafer-level packaging – on average more than 80% yield of bonded structures was accomplished; comparable to other laser-based wafer-level packaging processes. Maximum shear forces of up to 150 N were achieved which is considerably lower than for the pattern of 5.

Despite the reduced mechanical stability of these packages this process benefits from the two main advantages of wafer-level packaging:

- considerable reduction in process time, i.e. production costs, and
- protection of the devices to be encapsulated prior to dicing.

For applications where high seal strengths and wafer-level packaging are required the pattern of 5 can be used given the benefits of parallel processing out-weigh the waste of material (un-used silicon areas) due to the reduced sample density.

Future work in this area should be aimed at refining the bonding setup with particular focus on applying the bonding force individually for every single device. Inspection of the setup had shown that the glass spheres were set at a slightly different height resulting in an uneven force distribution. Therefore it is this particular setup and not the actual bonding approach that is the limitation of this packaging process. Once this issue has been resolved bonding of all nine structures on the same wafer with high repeatability is to be expected and this bonding approach could be easily extended to full wafer-level packaging.

So far the optimum bonding parameters were obtained by trial and error due to a lack of an appropriate method to measure the temperature during the bonding process. As mentioned in chapter 6.1, the introduction of pyrometric control of the laser power, i.e. bonding temperature, would greatly facilitate the optimisation of the bonding parameters and a multiple laser beam approach would result in a considerable reduction of the overall process time.

In this work silicon to glass joining with a BCB adhesive layer was investigated. The same laser-based localised heating packaging technology could also be applied to different adhesive layers and silicon to silicon joining. If polymers were to be used which are absorptive at the wavelength of the laser directly – e.g. by doping with an appropriate dye, also bonding of glass to glass could be achieved.

6.3 Hermetic Glass Frit Packaging of LCC Packages

In chapter 5, hermetic packaging of LCC devices in air and vacuum has been demonstrated using a novel laser-based glass frit packaging process where the heat is restricted greatly to the joining area only. The temperature in the centre of the device is kept at least 230°C below the temperature in the joining region (375°C or 440°C) enabling the use of temperature sensitive materials within the package. The development of a temperature monitoring method allowed for precise control of the bonding temperature, the key process parameter, resulting in process yields above 90%. Testing of the packaged devices showed that hermetic seals with excellent mechanical stability were achieved in a simple and robust process.

For glass frit packaging of LCC devices in air (see section 5.1) the glass frit material DM2700P/H848 from Diemat was used. Hermetic seals were achieved in as short as 75 s in this laser-based process. By active cooling of the substrate the temperature in the centre of the device is kept below 140°C despite a temperature of 375°C in the joining area.

Leak testing showed that hermetic seals were achieved in a high yield process (>90%). Shear forces as high as 855 N were required to split these packages. Additional temperature cycling and acceleration testing showed that the LCC packages even pass a major part of the qualification process required in military and space grade products. All these tests were carried out according to MIL-STD-883G by certified test laboratories as often required in commercial applications.

In comparison to conventional furnace-based processes a considerable reduction of the bonding time and a greatly reduced thermal strain on the device to be encapsulated were achieved without affecting the quality of the seal.

A further development of this process to vacuum packaging was demonstrated in section 5.2. For these experiments the vacuum compatible glass frit paste 5115HT1 from AGC was used. The vacuum process required a thin PTFE sheet as interface material between the substrate and the heat sink to ensure a constant, repeatable thermal transfer. A reliable process (yield rate ~95%) was developed where the temperature in the centre of the device was kept below 250°C by active cooling despite a required process temperature of 440°C. By introduction of localised cooling and a special cooling sandwich structure the heat flow within the sample was tailored to reduce the temperature further below 200°C.

A further advantage of the laser-based process opposed to conventional furnace heating is that a reduction of the overall process time for a single bonding cycle by more than 7× (7 min instead of 50 min) was achieved.

Shear force and hermeticity testing did not show any influence of the reduced process time on the quality of the seal. Shear forces in excess of 1 kN (limit of the test

machine) were obtained. Inside the cavity of the vacuum packaged LCC devices a moderate vacuum of around 5 mbar was achieved as confirmed by residual gas analysis.

Successful packaging of miniature pressure gauges, which can only withstand a maximum temperature of 300°C, underlined the advantage this laser-based localised heating glass frit packaging process in vacuum in comparison to conventional techniques. A global temperature of 440°C applied to the entire package would have resulted in thermal destruction of the sensor.

The laser-based glass frit packaging processes in air and vacuum demonstrated in this thesis feature a yield rate above 90%. For commercial applications an even higher rate is desirable; future investigations should be aimed at this goal. Imperfect deposition of the glass frit material in the sealing area, in particular for the Diemat material where a screen-printing process was used, affects the hermeticity of the seal. A further refinement of this process should result in a higher yield.

Additionally, online process control of the laser power (see chapter 6.1) should be considered for precise control of the bonding temperature to avoid failure of the seal due to over-heating of the glass frit material or insufficient reflow.

Some further research areas which have been identified for future investigations are:

- further reduction of the temperature in the centre of the device by enhanced thermal management through localised cooling and specially engineered interface materials,
- application of this novel bonding technique to other (off-the-shelf) packages (e.g. all-ceramic packages, CQFP), and
- the use of getter materials within the package to achieve higher levels of vacuum.

Finally, a further development of this process to multiple chip packaging, as demonstrated for the silicon to glass joining process, should be investigated.

To draw a final conclusion, in the course of this PhD it was demonstrated that by using a laser-based process and by further tailoring the heat flow by thermal management,

packaging processes for micro-devices were achieved where the temperature in the centre of the device was greatly reduced in comparison to the sealing area. These packaging processes are of great potential for the encapsulation of temperature sensitive materials and devices, which is a common problem in device manufacture in microsystems technologies. As example applications two processes were investigated: (i) for applications requiring hermetic sealing glass frit packaging of a chip carrier package was demonstrated, and (ii) for MEMS-type application near hermetic sealing of silicon to glass with an adhesive layer. The custom-made bonding setup has shown great flexibility and the capability to provide for the requirements of different bonding processes. It is an important step towards a generic packaging process for micro-devices, which has the potential to significantly reduce the high cost of packaging as a percentage of the overall device costs.

Further to the future work which was already pointed out at the end of the previous sections a more theoretical analysis of the described work should be taken into consideration. Modelling of the bonding process using Finite Element Analysis could be used to get a more thorough understanding of the heat flow, stress distribution (thermal and residual) within the sample and damage thresholds. This requires calculation of the beam absorption on the silicon surface and the energy transmission at the bond interfaces. The modelling results could also be used for the systematic design of the localised cooling and force application opposed to the experimental approach described in this thesis. Furthermore, the method “Design of Experiments” could be considered for the optimisation of the laser processing parameters to highlight the interrelation of the various parameters, e.g. laser power, spot size of the laser, bonding time and force.

References

[1] Lorenz, N., M.D. Smith, and D.P. Hand, *Wafer-level packaging of silicon to glass with a BCB intermediate layer using localised laser heating.* Microelectronics Reliability, 2011. **In Press, Corrected Proof**.

[2] Lorenz, N. and et al., *Hermetic glass frit packaging in air and vacuum with localized laser joining.* Journal of Micromechanics and Microengineering, 2011. **21**(4): p. 045039.

[3] Niklaus, F., G. Stemme, J.Q. Lu, and R.J. Gutmann, *Adhesive wafer bonding.* Journal of Applied Physics, 2006. **99**(3).

[4] Dressendorfer, P.V., D.A. Peterson, and C.A. Reber, *MEMS packaging - Current issues and approaches*, in *2000 HDInternational Conference on High-Density Interconnect and Systems Packaging*. 2000, SPIE-Int Society Optical Engineering: Bellingham. p. 208-213.

[5] Yufeng, Z., T. Xiaoyun, C. Weiping, Z. Guowei, and L. Xiaowei. *Study of MEMS Packaging Technology*. in *6th International Conference on Electronic Packaging Technology*. 2005. Harbin, China.

[6] Chen, M.X., L.L. Yuan, and S. Liu, *Research on low-temperature anodic bonding using induction heating.* Sensors and Actuators A: Physical, 2007. **133**(1): p. 266-269.

[7] Reichl, H. and V. Grosser, *Overview and development trends in the field of MEMS packaging*, in *14th IEEE International Conference on Micro Electro Mechanical Systems, Technical Digest*. 2001, IEEE: New York. p. 1-5.

[8] Gilleo, K., *MEMS Packaging Issues and Materials.* Advancing Microelectronics, 2000. **27**(6): p. 9-15.

[9] Madou, M.J., *Fundamentals of Microfabrication - The Science of Miniaturization*. 2nd ed. 2002, Florida, USA: CRC PRESS.

[10] Sun, L., A. Malshe, S. Cunningham, and A. Morris, *Investigation of localized laser bonding process for ceramic MEMS packaging*, in *56th Electronic Components & Technology Conference 2006, Vol 1 and 2, Proceedings*. 2006, IEEE: New York. p. 1740-1744.

[11] Lin, L.W., *MEMS post-packaging by localized heating and bonding.* IEEE Transactions on Advanced Packaging, 2000. **23**(4): p. 608-616.

[12] Garcia-Blanco, S., P. Topart, K. Le Foulgoc, J.-S. Caron, Y. Desroches, C. Alain, F. Chateauneuf, and H. Jerominek. *Hybrid wafer-level vacuum hermetic micropackaging technology for MOEMS-MEMS.* in *Reliability, Packaging, Testing, and Characterization of MEMS/MOEMS and Nanodevices VIII*. 2009. San Jose, CA, USA: SPIE.

[13] Lasky, J.B., *Wafer bonding for silicon-on-insulator technologies.* Applied Physics Letters, 1986. **48**(1): p. 78-80.

[14] Shimbo, M., K. Furukawa, K. Fukuda, and K. Tanzawa, *Silicon-to-silicon direct bonding method.* Journal of Applied Physics, 1986. **60**(8): p. 2987-2989.

[15] Gösele, U., Q.Y. Tong, A. Schumacher, G. Kräuter, M. Reiche, A. Plößl, P. Kopperschmidt, T.H. Lee, and W.J. Kim, *Wafer bonding for microsystems technologies.* Sensors and Actuators A: Physical, 1999. **74**(1-3): p. 161-168.

[16] Harendt, C. and et al., *Silicon fusion bonding and its characterization.* Journal of Micromechanics and Microengineering, 1992. **2**(3): p. 113.

[17] Klaassen, E.H., K. Petersen, J.M. Noworolski, J. Logan, N.I. Maluf, J. Brown, C. Storment, W. McCulley, and G.T.A. Kovacs, *Silicon fusion bonding and deep reactive ion etching: a new technology for microstructures.* Sensors and Actuators A: Physical, 1996. **52**(1-3): p. 132-139.

[18] Kräuter, G., A. Schumacher, and U. Gösele, *Low temperature silicon direct bonding for application in micromechanics: bonding energies for different combinations of oxides.* Sensors and Actuators A: Physical, 1998. **70**(3): p. 271-275.
[19] Barth, P.W., *Silicon fusion bonding for fabrication of sensors, actuators and microstructures.* Sensors and Actuators A: Physical, 1990. **23**(1-3): p. 919-926.
[20] Wei, J., *Wafer bonding techniques for microsystem packaging.* Journal of Physics: Conference Series, 2006. **34**(1): p. 943.
[21] Wallis, G. and D.I. Pomerantz, *Field Assisted Glass-Metal Sealing.* Journal of Applied Physics, 1969. **40**(10): p. 3946-3949.
[22] Lee, T.M.H., I.M. Hsing, and C.Y.N. Liaw, *An improved anodic bonding process using pulsed voltage technique.* Journal of Microelectromechanical Systems, 2000. **9**(4): p. 469-473.
[23] Rogers, T. and J. Kowal, *Selection of glass, anodic bonding conditions and material compatibility for silicon-glass capacitive sensors.* Sensors and Actuators A: Physical, 1995. **46**(1-3): p. 113-120.
[24] Schmidt, M.A., *Wafer-to-wafer bonding for microstructure formation.* Proceedings of the IEEE, 1998. **86**(8): p. 1575-1585.
[25] Wei, J. and et al., *Low temperature wafer anodic bonding.* Journal of Micromechanics and Microengineering, 2003. **13**(2): p. 217.
[26] Younger, P.R., *Hermetic glass sealing by electrostatic bonding.* Journal of Non-Crystalline Solids, 1980. **38-39**(Part 2): p. 909-914.
[27] Yu, P., C. Pan, and J. Xue, *The anodic bonding between K4 glass and Si.* Materials Letters, 2005. **59**(19-20): p. 2492-2495.
[28] Lin, Y.C., M. Baum, M. Haubold, J. Fromel, M. Wiemer, T. Gessner, and M. Esashi. *Development and evaluation of AuSi eutectic wafer bonding*. in *The 15th International Conference on Solid-State Sensors, Actuators and Microsystems, TRANSDUCERS 2009.* 2009. Denver, US.
[29] Wolffenbuttel, R.F. and K.D. Wise, *Low-temperature silicon wafer-to-wafer bonding using gold at eutectic temperature.* Sensors and Actuators A: Physical, 1994. **43**(1-3): p. 223-229.
[30] Khalil, N. *Micropackaging Technologies for Integrated Microsystems: Applications to MEMS and MOEMS*. 2003: SPIE.
[31] Tan, A.W.Y. and F.E.H. Tay, *Localized laser assisted eutectic bonding of quartz and silicon by Nd : YAG pulsed-laser.* Sensors and Actuators A: Physical, 2005. **120**(2): p. 550-561.
[32] Wolffenbuttel, R.F., *Low-temperature intermediate Au-Si wafer bonding; eutectic or silicide bond.* Sensors and Actuators A: Physical, 1997. **62**(1-3): p. 680-686.
[33] Wang, Q., S.-H. Choa, W. Kim, J. Hwang, S. Ham, and C. Moon, *Application of Au-Sn eutectic bonding in hermetic radio-frequency microelectromechanical system wafer level packaging.* Journal of Electronic Materials, 2006. **35**(3): p. 425-432.
[34] Kim, W., Q. Wang, K. Jung, J. Hwang, and C. Moon. *Application of Au-Sn eutectic bonding in hermetic RF MEMS wafer level packaging*. in *9th International Symposium on Advanced Packaging Materials: Processes, Properties and Interfaces*. 2004. Atlanta, Georgia, US.
[35] Tiensuu, A.L., J.A. Schweitz, and S. Johansson. *In situ investigation of precise high strength micro assembly using Au-Si eutectic bonding*. in *The 8th International Conference on Solid-State Sensors and Actuators and Eurosensors IX, TRANSDUCERS '95*. 1995.

[36] Lee, C., W.-F. Huang, and J.-S. Shie, *Wafer bonding by low-temperature soldering.* Sensors and Actuators A: Physical, 2000. **85**(1-3): p. 330-334.
[37] Ham, S.J., B.G. Jeong, J.H. Lim, K.D. Jung, K.D. Baek, W.B. Kim, and C.Y. Moon, *Characterization and reliability verification of wafer-level hermetic package with nano-liter cavity for RF-MEMS applications*, in *Proceedings of 57th Electronic Components & Technology Conference*. 2007, IEEE: New York. p. 1127-1134.
[38] Sohn, Y.C., Q. Wang, S.J. Ham, B.G. Jeong, K.D. Jung, M.S. Choi, W.B. Kim, and C.Y. Moon, *Wafer-level low temperature bonding with Au-In system*, in *Proceedings of 57th Electronic Components & Technology Conference*. 2007, IEEE: New York. p. 633-637.
[39] Chong, S.C., X.L. Zhang, S. Mohanraj, C.S. Premachandran, and N. Ranganathan. *Effect of passivation on frit glass bonding method for wafer level hermetic sealing on MEMS devices*. in *Proceedings of 5th Electronics Packaging Technology Conference*. 2003. New York: IEEE.
[40] Dresbach, C., A. Krombbolz, M. Ebert, and J. Bagdahn, *Mechanical properties of glass frit bonded micro packages.* Microsystem Technologies, 2006. **12**(5): p. 473-480.
[41] Ebert, M. and J. Bagdahn, *Determination of residual stress in glass frit bonded MEMS by Finite Element Analysis*, in *Thermal and Mechanical Simulation and Experiments in Microelectronics and Microsystems*, L.J. Ernst, et al., Editors. 2004, IEEE: New York. p. 407-412.
[42] Fujii, M., I. Kimura, T. Satoh, and K. Imanaka. *RF MEMS Switch with Wafer Level Package Utilizing Frit Glass Bonding*. in *32nd European Microwave Conference*. 2002. Milan, Italy.
[43] Knechtel, R., *Glass frit bonding: an universal technology for wafer level encapsulation and packaging.* Microsystem Technologies, 2005. **12**(1-2): p. 63-68.
[44] Knechtel, R., M. Wiemer, and J. Fromel, *Wafer level encapsulation of microsystems using glass frit bonding.* Microsystem Technologies, 2006. **12**(5): p. 468-472.
[45] Petzold, M., C. Dresbach, M. Ebert, J. Bagdahn, M. Wiemer, K. Glien, J. Graf, R. Muller-Fiedler, and H. Hofer, *Fracture mechanical life-time investigation of glass frit-bonded MEMS sensors*, in *2006 Proceedings 10th Intersociety Conference on Thermal and Thermomechanical Phenomena in Electronics Systems, Vols 1 and 2*. 2006, IEEE: New York. p. 1343-1348.
[46] Seki, T. *Recent progress in packaging of RF MEMS*. in *IEEE Compound Semiconductor Integrated Circuit Symposium*. 2004. Monterey, US.
[47] Sparks, D., S. Massoud-Ansari, and N. Najafi, *Long-term evaluation of hermetically glass frit sealed silicon to Pyrex wafers with feedthroughs.* Journal of Micromechanics and Microengineering, 2005. **15**(8): p. 1560-1564.
[48] Sparks, D., S. Massoud-Ansari, and N. Najafi, *Reliable vacuum packaging using NanoGetters (TM) and glass frit bonding*, in *Reliability, Testing and Characterization of MEMS/MOEMS III*, D.M. Tanner and R. Ramesham, Editors. 2004, SPIE-Int Society Optical Engineering: Bellingham. p. 70-78.
[49] Sparks, D.R., S. Massoud-Ansari, and N. Najafi, *Chip-level vacuum packaging of micromachines using NanoGetters.* IEEE Transactions on Advanced Packaging, 2003. **26**(3): p. 277-282.
[50] Audet, S.A. and K.M. Edenfeld. *Integrated sensor wafer-level packaging*. in *The 9th International Conference on Solid-State Sensors and Actuators, TRANSDUCERS '97*. 1997. Chicago, US.
[51] *Email correspondence with Asahi Glass Company*.

[52] http://www.diemat.com/docs/products/glass/pdf/DM2700P-H848%202011-06-02.pdf.
[53] Sparks, D.R. and et al., *An all-glass chip-scale MEMS package with variable cavity pressure.* Journal of Micromechanics and Microengineering, 2006. **16**(11): p. 2488.
[54] Olowinsky, A. and H. Kind. *Laser glass frit bonding for hermetic sealing of glass substrates and sensors*. in *Proceedings of LPM2010 - the 11th International Symposium on Laser Precision Microfabrication*. 2010. Stuttgart, Germany.
[55] Choi, Y.S., J.S. Park, H.D. Park, Y.H. Song, J.S. Jung, and S.G. Kang, *Effects of temperatures on microstructures and bonding strengths of Si-Si bonding using bisbenzocyclobutene.* Sensors and Actuators A: Physical, 2003. **108**(1-3): p. 201-205.
[56] Jourdain, A., P. De Moor, K. Baert, I. De Wolf, and H.A.C. Tilmans, *Mechanical and electrical characterization of BCB as a bond and seal material for cavities housing (RF-)MEMS devices.* Journal of Micromechanics and Microengineering, 2005. **15**(7): p. S89-S96.
[57] Jourdain, A., P. De Moor, S. Pamdighantam, and H.A.C. Tilmans, *Investigation of the hermeticity of BCB-sealed cavities for housing (RF-)MEMS devices*, in *Fifteenth IEEE International Conference on Micro Electro Mechinical Systems, Technical Digest*. 2002, IEEE: New York. p. 677-680.
[58] Jourdain, A., H. Ziad, P. De Moor, and H.A.C. Tilmans, *Wafer-scale 0-level packaging of (RF-)MEMS devices using BCB*, in *DTIP 2003: Design, Test, Integration and Packaging of MEMS/MOEMS 2003*, K. Bergman, et al., Editors. 2003, IEEE: New York. p. 239-244.
[59] Kim, Y.K., E.K. Kim, S.W. Kim, and B.K. Ju, *Low temperature epoxy bonding for wafer level MEMS packaging.* Sensors and Actuators A: Physical, 2008. **143**(2): p. 323-328.
[60] Liming, Y. and et al., *Adhesive bonding with SU-8 at wafer level for microfluidic devices.* Journal of Physics: Conference Series, 2006. **34**(1): p. 776.
[61] Lou, X., Z.H. Li, and Y.F. Jin, *Plastic-silicon bonding for MEMS packaging application*, in *Proceedings of 7th International Conference on Electronics Packaging Technology (ICEPT)*, B. Kenyun, Editor. 2006, IEEE: New York. p. 524-526.
[62] Na, K.H., I.H. Kim, E.S. Lee, H.C. Kim, Y.H. Lee, and K. Chun, *Wafer level package using polymer bonding of thick SU-8 photoresist*, in *Proceedings of International Conference on MEMS, Nano and Smart Systems*, W. Badawy and A. Salem, Editors. 2006, IEEE: New York. p. 31-34.
[63] Niklaus, F., P. Enoksson, E. Kalvesten, and G. Stemme, *Low-temperature full wafer adhesive bonding.* Journal of Micromechanics and Microengineering, 2001. **11**(2): p. 100-107.
[64] Noh, H.S., K.S. Moon, A. Cannon, P.J. Hesketh, and C.P. Wong, *Wafer bonding using microwave heating of parylene for MEMS packaging*, in *54th Electronic Components & Technology Conference, Vols 1 and 2, Proceedings*. 2004, IEEE: New York. p. 924-930.
[65] Oberhammer, J., E. Niklaus, and G. Stemme, *Selective wafer-level adhesive bonding with benzocyclobutene for fabrication of cavities.* Sensors and Actuators A: Physical, 2003. **105**(3): p. 297-304.
[66] Oberhammer, J., F. Niklaus, and G. Stemme, *Sealing of adhesive bonded devices on wafer level.* Sensors and Actuators A: Physical, 2004. **110**(1-3): p. 407-412.

[67] Oberhammer, J. and G. Stemme, *BCB contact printing for patterned adhesive full-wafer bonded 0-level packages.* Journal of Microelectromechanical Systems, 2005. **14**(2): p. 419-425.
[68] Pan, C.T., P.J. Cheng, M.F. Chen, and C.K. Yen, *Intermediate wafer level bonding and interface behavior.* Microelectronics and Reliability, 2004. **45**(3-4): p. 657-663.
[69] Pan, C.T. and et al., *A low-temperature wafer bonding technique using patternable materials.* Journal of Micromechanics and Microengineering, 2002. **12**(5): p. 611.
[70] Polyakov, A., M. Bartek, and J.N. Burghartz, *Area-Selective Adhesive Bonding Using Photosensitive BCB for WL CSP Applications.* Journal of Electronic Packaging, 2005. **127**(1): p. 7-11.
[71] Seok, S., N. Rolland, and P.A. Rolland, *Design, fabrication, and measurement of benzocyclobutene polymer zero-level packaging for millimeter-wave applications.* IEEE Transactions on Microwave Theory and Techniques, 2007. **55**(5): p. 1040-1045.
[72] Seok, S., N. Rolland, and P.A. Rolland, *Mechanical and electrical characterization of Benzocyclobutene membrane packaging*, in *57th Electronic Components & Technology Conference, Proceedings*. 2007, IEEE: New York. p. 1685-1689.
[73] Seok, S., N. Rolland, and P.A. Rolland, *A new BCB film zero-level packaging for RF devices*, in *2006 European Microwave Conference, Vols 1-4*. 2006, IEEE: New York. p. 13-16.
[74] Tai, A., H. Karagozoglu, and K.L. Chuan, *Organic sealant materials for quasi-hermetic sealing of MEMS sensor packages*, in *EPTC 2006: 8th Electronic Packaging Technology Conference, Vols 1 and 2*, J.H.L. Pang, et al., Editors. 2006, IEEE: New York. p. 462-471.
[75] Tian, J. and M. Bartek. *Low Temperature Wafer-Level Packaging of RF-MEMS using SU-8 Printing*. in *STW Annual Workshop on Semiconductor Advances for Future Electronics and Sensors (SAFE 2005)*. 2005. Veldhoven, the Netherlands.
[76] Tilmans, H.A.C., H. Ziad, H. Jansen, O. Di Monaco, A. Jourdain, W. De Raedt, E. Rottenberg, E. De Backer, A. Decaussemaeker, and K. Baert. *Wafer-level packaged RF-MEMS switches fabricated in a CMOS fab*. in *Technical Digest on International Electron Devices Meeting (IEDM)*. 2001. Washington, DC, USA.
[77] Wiemer, M., C. Jia, M. Toepper, and K. Hauck. *Wafer Bonding with BCB and SU-8 for MEMS Packaging*. in *1st Electronics Systemintegration Technology Conference*. 2006. Dresden, Germany.
[78] Budraa, N.K., H.W. Jackson, M. Barmatz, W.T. Pike, and J.D. Mai, *Low pressure and low temperature hermetic wafer bonding using microwave heating*, in *Technical Digest on 12th IEEE International Conference on Micro Electro Mechanical Systems (MEMS '99)*. 1999, IEEE: New York. p. 490-492.
[79] Noh, H.S., K.S. Moon, A. Cannon, P.J. Hesketh, and C.P. Wong, *Wafer bonding using microwave heating of parylene intermediate layers.* Journal of Micromechanics and Microengineering, 2004. **14**(4): p. 625-631.
[80] Chen, M., X. Yi, L. Yua, Z. Gan, and S. Liu. *Rapid and Selective Induction Heating for Sensor Packaging*. in *6th International Conference on Electronic Packaging Technology*. 2005.
[81] Hu, C.C., S.Y. Wen, C.P. Hsu, C.W. Chang, C.T. Shig, and H.W. Lee, *Solder bonding with a buffer layer for MOEMS packaging using induction heating.* Microsystem Technologies, 2006. **12**(10-11): p. 1011-1014.

[82] Yang, H.A., M.C. Wu, and W.L. Fang, *Localized induction heating solder bonding for wafer level MEMS packaging*, in *Technical Digest on 17th IEEE International Conference on Micro Electro Mechanical Systems (MEMS 2004)*. 2004, IEEE: New York. p. 729-732.
[83] Yang, H.A., M.C. Wu, and W.L. Fang, *Localized induction heating solder bonding for wafer level MEMS packaging.* Journal of Micromechanics and Microengineering, 2005. **15**(2): p. 394-399.
[84] Cheng, Y.T., W.T. Hsu, K. Najafi, C.T.C. Nguyen, and L.W. Lin, *Vacuum packaging technology using localized aluminum/silicon-to-glass bonding.* Journal of Microelectromechanical Systems, 2002. **11**(5): p. 556-565.
[85] Cheng, Y.T., L.W. Lin, and K. Najafi, *Localized silicon fusion and eutectic bonding for MEMS fabrication and packaging.* Journal of Microelectromechanical Systems, 2000. **9**(1): p. 3-8.
[86] Economikos, L. and E. al., *Hermetic sealing of a substrate of high thermal conductivity using an interposer of low thermal conductivity*. 1999: USA.
[87] Hand, D.P., *Personal Communication*. 2011.
[88] Slee, R.K. and E. al., *Advanced parallel seam-sealing system*. 1990: USA.
[89] Susumu, A., O. Kouichi, F. Masaki, and T. Toshiaki, *Newly Developed Micro-Parallel Seam Joining Equipment and its Applications : Micro-Parallel Seam Joining and Development of Joining Equipment (4th Report).* Transactions of the Japan Welding Society, 1990. **21**(2): p. 95-102.
[90] Wang, W. and D. Fries. *FEA modeling of a wafer level seam sealing approach for MEMS packaging*. in *International ANSYS Conference*. 2004: www.ansys.com.
[91] Bosse, L., A. Schildecker, A. Gillner, and R. Poprawe, *High quality laser beam soldering.* Microsystem Technologies, 2002. **7**(5-6): p. 215-219.
[92] Chaminade, C., A. Olowinsky, and H. Kind. *Laser-based glass soldering for MEMS packaging*. in *ICALEO 2007 Congress Proceedings*. 2007. Orlando, FL, USA.
[93] Gillner, A., J. Holtkamp, C. Hartmann, A. Olowinsky, J. Gedicke, K. Klages, L. Bosse, and A. Bayer, *Laser applications in microtechnology.* Journal of Materials Processing Technology, 2005. **167**(2-3): p. 494-498.
[94] Gillner, A., M. Wild, and R. Poprawe, *Laser bonding of micro optical components*, in *Laser Micromachining for Optoelectronic Device Fabrication*, A. Ostendorf, Editor. 2003, SPIE-Int Society Optical Engineering: Bellingham. p. 112-120.
[95] Haberstroh, E., W.M. Hoffmann, R. Poprawe, and F. Sari, *3 Laser transmission joining in microtechnology.* Microsystem Technologies, 2006. **12**(7): p. 632-639.
[96] Joseph, P.J., P. Monajemi, F. Ayazi, and P.A. Kohl, *Wafer-level packaging of micromechanical resonators.* IEEE Transactions on Advanced Packaging, 2007. **30**(1): p. 19-26.
[97] Luo, C. and L.W. Lin, *The application of nanosecond-pulsed laser welding technology in MEMS packaging with a shadow mask.* Sensors and Actuators A: Physical, 2002. **97-8**: p. 398-404.
[98] Mescheder, U.M., M. Alavi, K. Hiltmann, C. Lietzau, C. Nachtigall, and H. Sandmaier, *Local laser bonding for low temperature budget.* Sensors and Actuators A: Physical, 2002. **97-8**: p. 422-427.
[99] Mohan, A., C.B. O'Neal, A.P. Malshe, and R.B. Foster, *A wafer-level packaging approach for MEMS & related microsystems using selective laser-assisted bonding (LAB).* Proceedings of 55th Electronic Components & Technology Conference, 2005. **1&2**: p. 1099-1102.

[100] Sun, L., A.P. Malshe, S. Cunningham, and A. Morris, *Localized CO2 laser bonding process for MEMS packaging.* Transactions of Nonferrous Metals Society of China, 2006. **16**: p. S577-S581.
[101] Tan, A.W.Y., F.E.H. Tay, and J. Zhang, *Characterization of localized laser assisted eutectic bonds.* Sensors and Actuators A: Physical, 2006. **125**(2): p. 573-585.
[102] Tao, Y., A.P. Malshe, and W.D. Brown, *Selective bonding and encapsulation for wafer-level vacuum packaging of MEMS and related micro systems.* Microelectronics Reliability, 2004. **44**(2): p. 251-258.
[103] Tao, Y., A.P. Malshe, W.D. Brown, D.R. DeReus, and S. Cunningham, *Laser-assisted sealing and testing for ceramic packaging of MEMS devices.* IEEE Transactions on Advanced Packaging, 2003. **26**(3): p. 283-288.
[104] Theppakuttai, S., D.B. Shao, and S.C. Chen, *Localized laser transmission bonding for microsystem fabrication and packaging.* Journal of Manufacturing Processes, 2004. **6**(1): p. 1-8.
[105] Wild, M.J., A. Gillner, and R. Poprawe, *Advances in silicon to glass bonding with laser.* MEMS Design, Fabrication, Characterization, and Packaging, 2001. **4407**: p. 135-141.
[106] Wild, M.J., A. Gillner, and R. Poprawe, *Locally selective bonding of silicon and glass with laser.* Sensors and Actuators A: Physical, 2001. **93**(1): p. 63-69.
[107] Bardin, F., S. Kloss, C.H. Wang, A.J. Moore, A. Jourdain, I. De Wolf, and D.P. Hand, *Laser bonding of glass to silicon using polymer for microsystems packaging.* Journal of Microelectromechanical Systems, 2007. **16**(3): p. 571-580.
[108] Garrou, P.E., R.H. Heistand, M.G. Dibbs, T.A. Mainal, C.E. Mohler, T.M. Stokich, P.H. Townsend, G.M. Adema, M.J. Berry, and I. Turlik, *Rapid Thermal Curing of BCB Dielectric.* IEEE Transactions on Components Hybrids and Manufacturing Technology, 1993. **16**(1): p. 46-52.
[109] http://www.dow.com/cyclotene/solution/trans.htm.
[110] http://www.dow.com/cyclotene/solution/4000hot.htm.
[111] Liu, Y.F., J. Zeng, and C.H. Wang, *Accurate Temperature Monitoring in Laser-Assisted Polymer Bonding for MEMS Packaging Using an Embedded Microsensor Array.* Journal of Microelectromechanical Systems, 2010. **19**(4): p. 903-910.
[112] Liu, Y.F., J. Zeng, and C.H. Wang, *Temperature monitoring in laser assisted polymer bonding for MEMS packaging using a thin film sensor array*, in *Proceedings of IEEE Sensors Applications Symposium (SAS 2009)*. 2009, IEEE: New York. p. 52-55.
[113] Wang, C., J. Zeng, and Y. Liu. *Recent advances in laser assisted polymer intermediate layer bonding for MEMS packaging*. in *International Conference on Electronic Packaging Technology & High Density Packaging (ICEPT-HDP '09)*. 2009. Beijing, China.
[114] Wu, Q., N. Lorenz, K.M. Cannon, and D.P. Hand, *Glass frit as a hermetic joining layer in laser based joining of miniature devices.* IEEE Transactions on Components and Packaging Technologies, 2010. **33**(2): p. 470-477.
[115] DEPARTMENT OF DEFENSE, U.S., *MIL-STD-883G*. 2006: Defense Supply Center Columbus.
[116] Kloss, S., *Design and test of a setup for laserassisted bonding of MEMS*. 2006, Heriot-Watt University.
[117] http://www.virginiasemi.com/pdf/Optical%20Properties%20of%20Silicon71502.pdf, *Optical properties of silicon*.

[118] Wu, Q., N. Lorenz, and D.P. Hand, *Localised laser joining of glass to silicon with BCB intermediate layer*. Microsystem Technologies, 2009. **15**(7): p. 1051-1057.
[119] http://www.uqgoptics.com/materials_optical_borosilicateBorofloat.aspx.
[120] http://www.ma-info.de/html/download_en.html.
[121] Dow Chemicals, *Processing Prodecures for CYCLOTENE 4000 Series Photo BCB Resins - DS2100 Puddle Develop Process*. CYCLOTENE 4000 Series Advanced Electronic Resins (Photo BCB), Feb. 2005.
[122] http://www.ino.ca/Micro-pirani-pressure-microsensor.pdf.
[123] Sisto, M.M., S. Garcia-Blanco, L. Le Noc, B. Tremblay, Y. Desroches, J.-S. Caron, F. Provencal, and F. Picard. *Pressure sensing in vacuum hermetic micropackaging for MOEMS-MEMS*. in *Reliability, Packaging, Testing, and Characterization of MEMS/MOEMS and Nanodevices IX*. 2010. San Francisco, California, USA: SPIE.